FINAL ENGINEERING/PROJECT REPORT

FOR

SURFACE COMPOSITION MAPPING RADIOMETER INSTRUMENT·

Contract No. NAS 5-21112

Prepared by

ITT Aerospace/Optical Division
Fort Wayne, Indiana 46803

Prepared for

NATIONAL AERONAUTICS AND SPACE ADMINISTRATION
GODDARD SPACE FLIGHT CENTER
Greenbelt, Maryland 20771

FINAL ENGINEERING/PROJECT REPORT

FOR

SURFACE COMPOSITION MAPPING RADIOMETER INSTRUMENT

Contract No. NAS 5-21112

Prepared by

ITT Aerospace/Optical Division
Fort Wayne, Indiana 46803

Prepared for

NATIONAL AERONAUTICS AND SPACE ADMINISTRATION
GODDARD SPACE FLIGHT CENTER
Greenbelt, Maryland 20771

Contributors

R. Annable          H. Kalina
N. Franklin         D. Juarez
R. Harber           J. Stark

Approved

D. Juarez, Program Manager

# TABLE OF CONTENTS

TABLE OF CONTENTS (Cont.)

# LIST OF ILLUSTRATIONS

# LIST OF TABLES

## 1.0 INTRODUCTION

ITT Aerospace/Optical Division has completed NASA Contract NAS 5-21112 which was to provide a design study, to design, to develop, to fabricate and to test a three-channel scanning radiometer. The instrument was flown on the GSFC Nimbus 5 Satellite and measured infrared energy in the 8.3-9.3 micron, 10.2-11.2 micron and 0.8-1.1 micron spectral regions. Instrument parameters are shown in Fig. 1.0-1.

The scope of work includes:

a.   The design study, design, fabrication and assembly of an Engineering Model, a Prototype Model, and a Flight Model instrument.

b.   The generation of acceptance test procedures, ground support and test equipment.

c.   The qualification testing of the instrument.

d.   The field engineering as required for experiment-spacecraft integration, testing and launch support.

This report provides a description of the SCMR Flight Model instrument and contains theoretical discussions of the instrument subassemblies. Operational details of the mechanical and electrical portions of the instrument are included.

## TABLE 1.0-1

### NIMBUS "E"
### SURFACE COMPOSITION MAPPING RADIOMETER
### PARAMETERS

PRIMARY MODE - MEASUREMENT OF "RESTSTRAHLEN" EFFECT TO IDENTIFY SURFACE MINERAL COVER.

SECONDARY MODE - I.R. MAPPING OF EARTH SURFACE

SIZE ------------------------------------ 22.25" L x 9" W x 17.68" H

WEIGHT----------------------------------- 51 POUNDS

POWER------------------------------------ 16.4 WATTS

LINE RATE-------------------------------- 10 LINES/SEC.

VIDEO PASSBAND--------------------------- 50 KHz

INFRARED BANDWIDTH

    CHANNEL 1 ------------------------ 8.3 - 9.3 MICRONS

    CHANNEL 2 ------------------------ 10.2 - 11.2 MICRONS

VISIBLE BANDWIDTH------------------------ 0.8 - 1.1 MICRONS

INSTANTANEOUS FIELD OF VIEW-------- 0.6 MILLIRAD

GROUND RESOLUTION AT SUBSATELLITE
    POINT ---------------------------- 0.41 MILES

NOISE EQUIVALENT TEMP DIFFERENCE
    (NE T) (280$^{\circ}$K)------------------ 0.3$^{\circ}$K (GOAL)
    ------------------ 1.0$^{\circ}$K (REQUIRED)

PEAK SIGNAL/RMS NOISE RATIO-------- 52 DB

OPTICS SIZE------------------------------ 8 INCH

OPTICS SPEED----------------------------- f/.82

DETECTOR TEMPERATURE--------------- 115$^{\circ}$K

NUMBER OF COMMANDS------------------ 16

NUMBER OF TM POINTS----------------- 22

## 2.0    INSTRUMENT DESCRIPTION

The Nimbus E High Resolution Surface Composition Mapping Radiometer (SCMR) is a three channel radiometrically calibrated scanning radiometer. Two narrow IR spectral bands, 8.3 μm to 9.3 μm and 10.2 μm to 11.2 μm, are utilized to measure the thermal emission of igneous rocks which exhibit the reststrahlen effect. The third channel, 0.8 μm to 1.1 μm, is a near IR channel used for cloud mapping and albedo measurements. The SCMR also produces strip maps of the Earth and seas in all three channels simultaneously by rotation of the field of view in a plane normal to the spacecraft velocity vector. The multispectral data which is separated by dichroic beam splitters, is registered channel to channel within a single instantaneous field of view (0.6 milliradians).

Figure 2.0-1 indicates the absorbtion of ozone as measured by Chaney, et al[1] against a 290°K blackbody, together with the calculated spectrum for solid samples of granite and dunite both at 290°K, with emissivities determined from the results of Hovis and Callahan[2]. The relative spectral position of the two SCMR IR channels used to measure the reststrahlen are also indicated. The difference between the simultaneous radiance measurements made in the two narrow band IR channels is used to determine the relationship of acidic and ultra-basic compositions of the Earth's surface.

Physically, the SCMR is 22.25 inches long, 9.00 inches wide, and 17.68 inches high. The instrument weighs slightly more than 50 pounds and uses 15 watts of power in the normal operation mode. The SCMR consists of five basic modules. These are the Baseplate Unit, the Scanner Module, Optics Module, Radiant Cooler Module, and the Electronics Module (see Figure 2.0-2).

The Baseplate Unit is the basic structure to which the other modules are mechanically referenced and coupled. The momentum compensator and scan motor electronic drive circuits are contained within this structure. A reference blackbody which completely fills the optical field of view is mounted on the top side of the baseplate unit directly under the scan mirror. The blackbody is thermally coupled to the baseplate unit and its temperature, while monitored and telemetered, is not controlled.

---

1.      L.W. Chaney, S.R. Drayson and C. Young, Appl. Opt. 6,347 1967.

2.      W.A. Hovis, Jr.; L.R. Blaine and Wm. R. Callahan Appl. Opt. Vol. 7 1137 1968.
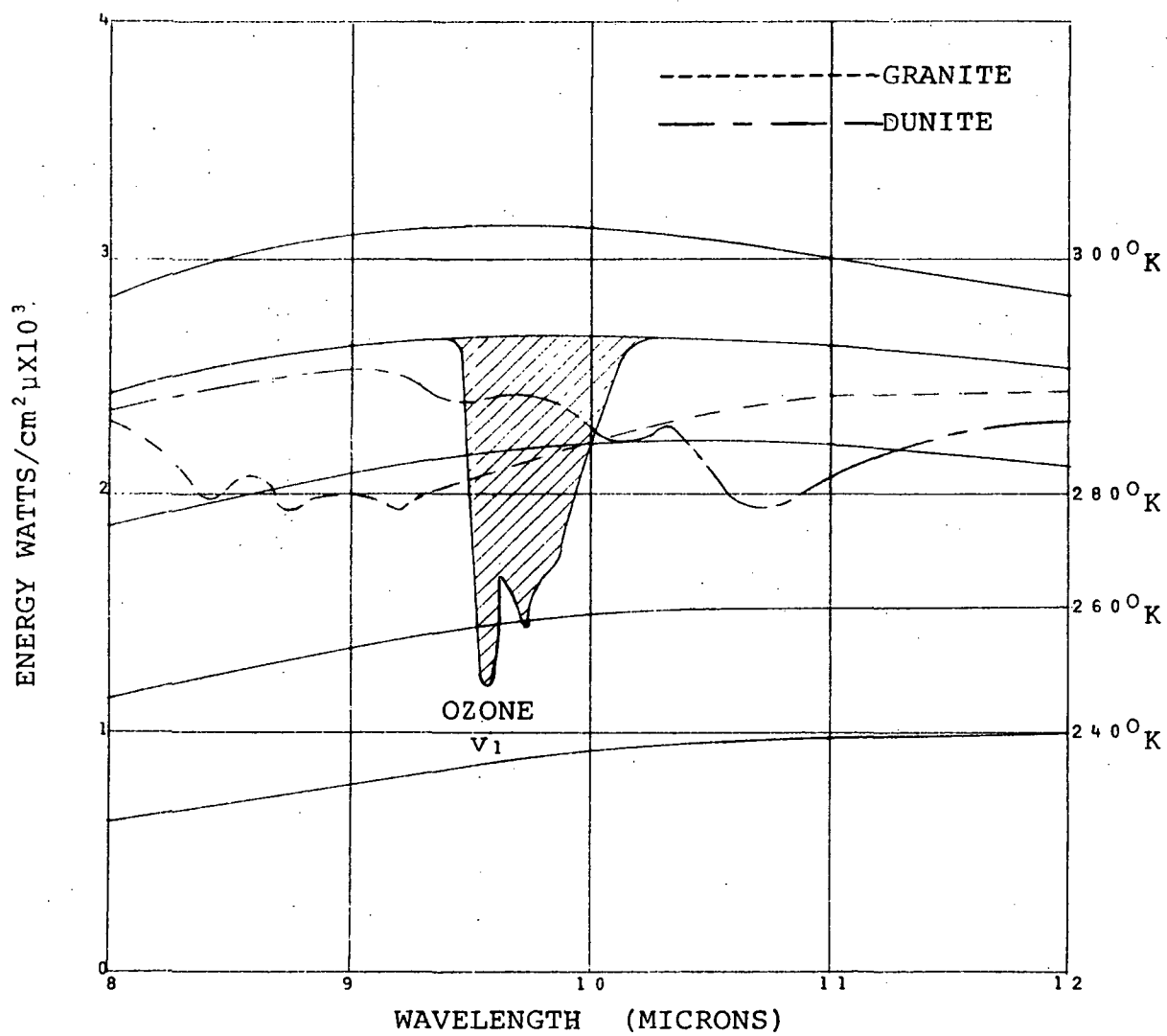
Figure 2.0-1

OZONE ABSORPTION AND CALCULATED RESTSTRAHLEN EFFECT

EARTH SHIELD

RADIANT COOLER

ELECTRONICS

SUN SHIELDS

SCAN MIRROR

SCAN MOTOR (600 RPM)

MOMENTUM COMPENSATOR

8" TELESCOPE

BASEPLATE UNIT
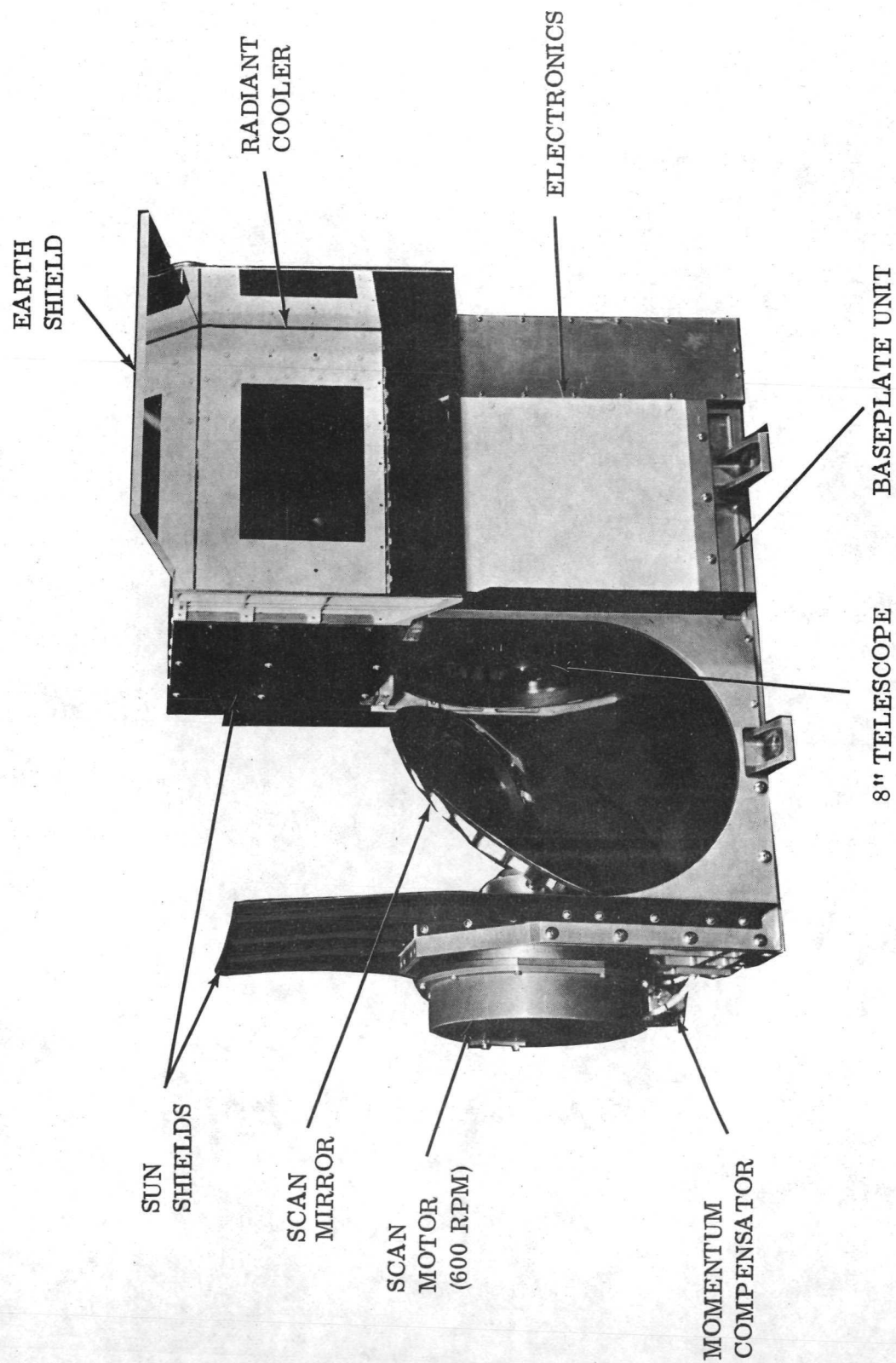
SATELLITE: NIMBUS 5

INFRARED CHANNELS:  8.3 – 9.3 MICRONS
                    10.2 – 11.2 MICRONS

RESOLUTION: 0.6 MILLIRADIANS

FIGURE 2.0-2  SCMR INSTRUMENT

The Scanner Module is comprised of the scanner mechanical housing, the eliptically shaped beryllium scan mirror, the hysteresis synchronous scan and momentum compensator motors, and a scan cavity sun shield.

The Optics Module consists of a modified 8 inch Dall-Kirkham operating afocally at a speed of f/.92. The beam diameter is reduced from 8 inches to 1 inch. Spectral separation is accomplished by two beam splitters. The near IR detector and associated preamplifier is contained within the optics module as are the beam splitter and focusing lens assembly.

The Radiant Cooler Assembly is comprised of a thermally isolated housing, a truncated pyramid cooling "cone" around which is an apron for radiation of heat to space. The cone walls are optically polished, hard coated, and finished with evaporated gold. The cone is thermally isolated from the housing and optical ports sealed off with irtran windows close off the cone from all but the optical radiative inputs. Located in the truncation plane and centered within the cooling "cone" is a radiative patch. Two mercury cadmium telluride (HgCdTe) detector packages are mounted on the patch which is thermally decoupled from the cooling cone. The radiant cooler is designed to cool the patch under normal operating conditions to $\simeq$ 105K. The actual operating temperature is regulated at 115K $\pm$ 0.1K giving a reserve capacity of about $10^{\circ}$K. Incorporated into the radiant cooler system are a number of features dedicated to the prevention of condensation of contaminants on the cooled areas. The features include a deployable Earth shield, cold traps, cone wall and patch heaters, and a dry Gas Patch Purge System. Operational use of the cooler requires the cooler be heated to $\simeq$ 300K in vacuum for a period of time sufficiently long enough to outgas water vapor and other contaminants which may be trapped within the instrument. The HgCdTe detector preamplifiers are also located on the radiant cooler housing.

The Electronics Module contains the signal processing circuits, electronic calibration and sync circuits, digital to analog telemetry conversion, and buffer interface circuitry. Normal operation requires approximately 16 watts of power. The electronic circuit boards are heat sinked to the electronics module frame which is thermally isolated from the baseplate unit. The power dissipated by the electronics is radiated to space by an attached radiating panel that extends in front of the optical module and has a view of space.

Electrical Interface

The electrical interface requirements, in addition to commands which are described in Section 7 of this report, are shown in Table 2.0-1 ELECTRICAL INTERFACE.

A power profile for operational modes and power required for decontamination modes are shown in Table 2.0-2. In the minimum operational mode all telemetry circuits are functional as well as the patch temperature control circuitry.

## TABLE 2.0-1

### ELECTRICAL INTERFACE

POWER REQUIREMENT

-24.5VDC (SEE FIG. 1.0-2.1 POWER PROFILE)

CLOCK REQUIREMENT

```
50 KHZ   5V.P.P.  SQUAREWAVE
10 KHZ   5V.P.P.  SQUAREWAVE
400 HZ   20V.P.P. TWO PHASE SQUAREWAVE
```

INTERFACE CONNECTORS

| CONNECTOR NO. | FUNCTION | CONNECTOR TYPE |
|---|---|---|
| J1 | VIDEO OUTPUT | DAM-15S |
| *J2 | TEST | DCM-37S |
| J3 | CLOCK | DBM-25P |
| J4 | COMMAND | DDJ-50P |
| J5 | ANALOG TELEMETRY | DBJ-25P |
| J6 | POWER | DEJ-9P |
| J7 | DIGITAL TELEMETRY | DAJ-15P |

*TEST ONLY - NO INTERFACE REQUIRED

TABLE 2.0-2

POWER PROFILE

OPERATIONAL MODES

MINIMUM - MOTOR ON/MOTOR LOW POWER                          =   6.25 WATTS

NOMINAL - MOTOR ON/MOTOR LOW POWER/ELECTRONICS ON  =  16.25 WATTS

MAXIMUM - MOTOR ON/MOTOR HIGH POWER/ELECTRONICS ON =  20.33 WATTS

DECONTAMINATION MODES

PATCH HEAT FULL TIME          =      0.245 WATTS

PURGE VALVE OPEN              =      0.80 WATTS

CONE HEAT ON                 =      3.0 WATTS

CONE COVER STORE/DEPLOY       =      14.7 WATTS
                                     (10-SECOND DURATION)

## Mechanical Interface

An outline drawing (ITT Dwg. #8113887) showing mechanical inter-
face of the SCMR instrument is included in this report as
Figure 2.0-3. The instrument is shown with outside dimensions
of 25.28 long x 11.5 wide x 17.68 high with the cover door closed.
The instrument weighs 51 lbs. The c.g. is located on the drawing.
Uncompensated angular momentum will not exceed .01 ft. 16 sec.
based upon tolerances of the rotating masses. A momentum com-
pensator is included in the instrument to reduce the uncompensated
portion to .01 or less.

The view angle for the scanner is shown in this figure. When the
instrument is mounted on the spacecraft, 145$^{\circ}$ of scanner angle
as shown must be unobstructed. In addition, the following areas
listed below must be left open.

1. Area surrounding daylight calibration assembly

2. Area in front of radiant cooler including viewing
   angle and path of cooler door deployment.

3. Radiating Panel for cooling electronics.

4. Radiating Panel for cooling radiant cooler housing

5. Access area for filling patch purge system

Means is provided for attachment of a thermal blanket to the
exterior of the instrument after installation of the spacecraft.
This blanket was supplied by the spacecraft contractor and not
by ITT.

Built into the instrument is a purge system for flushing the
volume around the radiant cover patch with ultra-dry nitrogen
while in orbit. This system may be exercised during pre-launch
test but should be recharged prior to launch. A transducer is
installed in the system for measuring gas supply pressure.

The instrument is designed with 4 mounting feet. Mounting bolts
are 3/8-16. The four mounting feet are to be in thermal contact
with the spacecraft. A compensation heater of 8 watts capacity
is attached to the base plate and motor housing.

The motor and momentum compensator operated continuously--even
during launch. For further details on the thermal interface,
refer to SCMR Thermal Design Status and Effects on S/C Interface
by F. Florio of GE (PIR # 1R44-NE-554).

PARTIAL VIEW A-A

FILL VALVE FOR PATCH PURGE SYSTEM (SEE DETAIL B)

RADIANT PANEL FOR COOLING RADIANT COOLER HOUSING

CONNECTOR LAYOUT SCALE 1/1

ALIGNMENT SURFACE

28° COOLER FOV

6 MILLIRADIANS FOV OF OPTICS

SUN SHIELD

49° COOLER FOV

DAYLIGHT CALIBRATION AREA MUST BE FREE OF OBSTRUCTIONS

RADIATING PANEL FOR COOLING ELECTRONICS

NAME TAG ATTACHED TO THIS SIDE

SHUTOFF TORQUE 25 IN. LBS

CAP ASSY AN929-2C

DETAIL B SCALE 2/1

THIS FOV MUST BE FREE OF OBSTRUCTIONS

14.5° SCANNER ANGLE

SCAN MIRROR-VIEWED FROM MOTOR END

.406 DIA MTG HOLES (4)

NOTES:
1. ALIGNMENT PAD 8116034 TO BE INSTALLED ON INSTRUMENT FOR ALIGNMENT WITH SPACECRAFT, IT SHOULD BE REMOVED PRIOR TO LAUNCH.
2. APPROXIMATE TOTAL WEIGHT = 51.0 POUNDS.
3. UNCOMPENSATED ANGULAR MOMENTUM WILL NOT EXCEED 0.01 FT. LB. SEC.
4. INDIVIDUAL MOUNTING FOOT AREA 1.56 IN², ALL 4 MOUNTING FEET TO BE IN THERMAL CONTACT WITH THE SPACECRAFT.
5. THE AREA SURROUNDING THE DAYLIGHT CALIBRATION ASSY MUST BE FREE OF ANY OBSTRUCTIONS WHICH WOULD IMPAIR ITS OPERATION.
6. PLANNED OUT GASSING PORTS
7. PRIOR TO LAUNCH CUT 4 RED LEADS OFF FLUSH WITH HEATERS ON COOLER DOOR.
8. PRIOR TO LAUNCH CUT 4 RED LEADS OFF FLUSH AT OR BELOW ON END PLATE FOR HEATERS IN COOLER ASSY.
9. THESE HEATERS ARE FOR SOLAR INPUT SIMULATION IN CHAMBER TEST ONLY.

ITT AEROSPACE/OPTICAL DIVISION
FORT WAYNE, INDIANA, U.S.A.
INTERNATIONAL TELEPHONE AND TELEGRAPH CORPORATION

OUTLINE
SURFACE COMPOSITION
MAPPING RADIOMETER

CONTRACT NO. NAS 5-21112

E 31550 8113887
SCALE 1/2

LIST OF MATERIALS OR PARTS LIST

# 3.0 INSTRUMENT FUNCTIONAL DESCRIPTION

## 3.1 Optics

Radiation from the Earth or the internal calibration black-
body is reflected from the continuously rotating scan mirror
into the 8 inch diameter collecting telescope as shown in
Figure 3.0-1. The modified Dall-Kirkham telescope is
operated afocally at a speed of f/.92. The secondary mirror
of the telescope collimates the optical beam into a smaller
diameter which is 1 inch. The first dichroic beam splitter
is thinly gold coated glass which transmits the near-infrared
radiation but reflects the 8 to 12 micron radiation. The
near infrared (0.8 to 1.1 m) beam passes through the dichroic
beam splitter and then through a long wavelength pass
(interference) filter and is then focused by use of a para-
bolic mirror onto a hybrid silicon detector/preamplifier
assembly. The parabolic mirror position is adjustable for
purposes of channel registration. The short wavelength beam
splitter is set at a $45^{\circ}$ angle to the collimated 1 inch beam
and folds the beam at $90^{\circ}$ to the telescope so that the long
wavelength radiation emerges through the side of the telescope
between the primary and secondary mirrors. The second IR
beam splitter is a multiple coated germanium substrate dichroic
again set at $45^{\circ}$ to the 1 inch collimated beam. This beam
splitter transmits >80% of the radiation between 8.3 and 9.3μm
and reflects 98% or more of the radiation between 10.2 and
11.2μm. The spectrally separated 1 inch diameter beams are
focused on their respective detectors by a large (1 inch)
germanium focusing lens and a germanium aplanat lens in each
leg. The two long wavelength IR beams also pass through an
Irtran optical port window that separates the interior of the
radiant cooling cone from the cooler housing and then through
the narrow spectral band pass filters which are located on the
radiant patch with the detectors. The final aplanats speed the
total system operating speed to f/0.82 enabling the 0.6 milli-
radian field of view to be focused on the 0.10 mm by 0.10 mm
detectors.

## IR Detectors

The IR detectors are located on a patch assembly shown in
Figure 3.0-2 as Item #1. The temperature of the patch assembly
is controlled by the electronics utilizing a sensing and
heating element located on the patch to minimize the detector
responsivity changes with temperature variations that would
occur due to heat load variations over an orbital period. The
temperature of the patch and the heat load variations are also
monitored and telemetered. Table 3.0-1 and 3.0-2 describes the
flight model IR detectors.

Bias for the detectors is provided by a regulated voltage source
generated by the detector pre-amplifiers. Figure 3.0-3 and
Figure 3.0-4 are graphs of D* vs bias current and responsivity as
a function of wavelength for the flight model detectors.
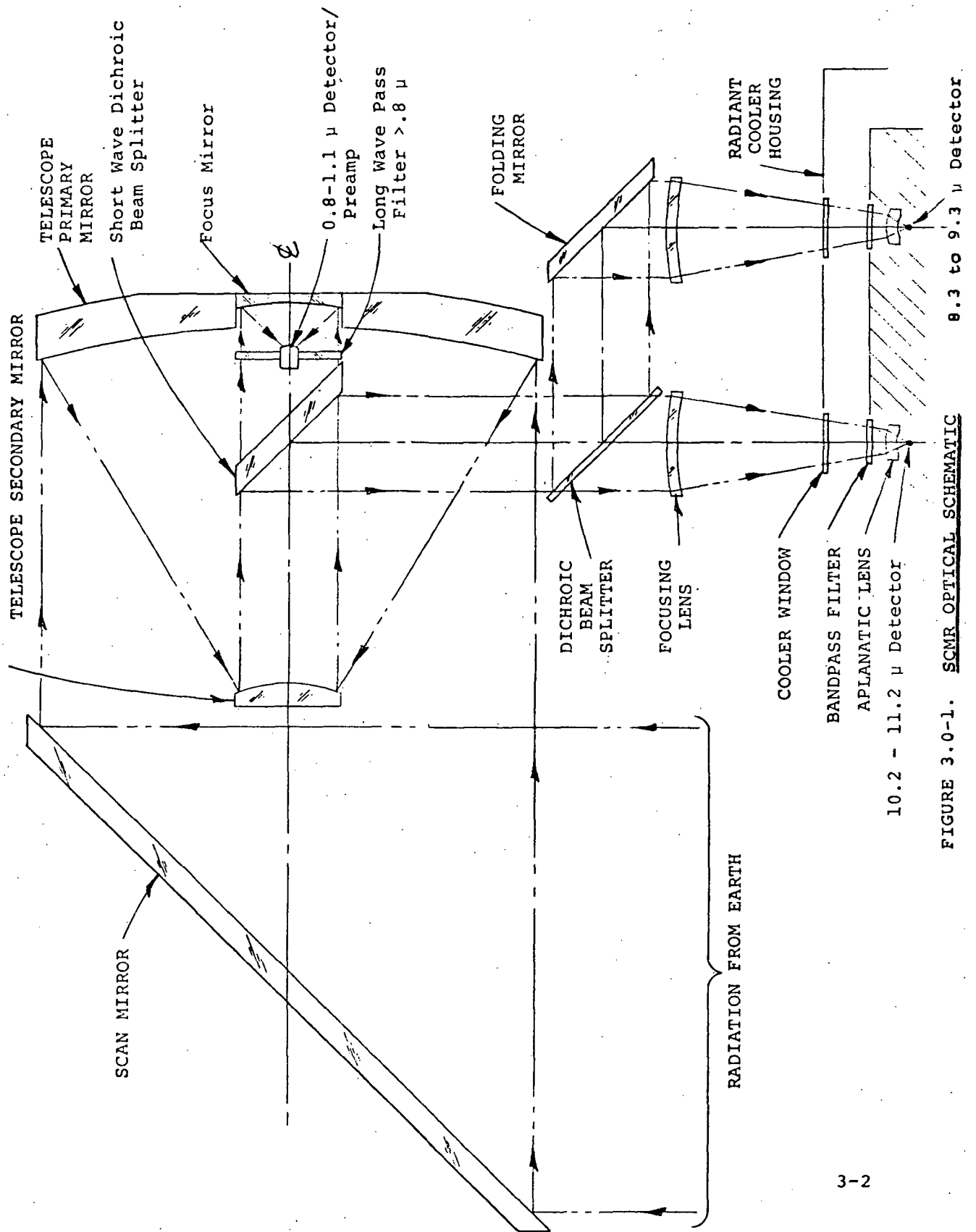
FIGURE 3.0-1. SCMR OPTICAL SCHEMATIC

FIGURE 3.0-2
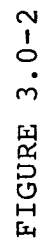
# TABLE 3.0-1

## FLIGHT MODEL SWL CHANNEL DETECTOR

### Description of Detector

| | |
|---|---|
| Type | Mercury Cadmium Telluride (Hg Cd Te) |
| Identification Number | DLK21E1 S/N Z1 |
| Detector Type | Photoconductive |
| Date of Manufacture | October 1970 |
| Window | Irtran II, AR Coated |
| Element Size | Length .097 mm |
| | Width .097 mm |
| Element Area | .0094 mm$^2$ |
| Maximum Bias Not to be Exceeded | 20.0 milliamps |
| Field of View | 80$^\circ$ |
| Element-Backside of Housing | .100 inches |

### Test Results at 100$^\circ$K

| | |
|---|---|
| Resistance at 100$^\circ$K | 17.5 ohms |
| Power at Optimum Bias | .280 m watts |
| Optimum Bias | 4.0 milliamps |
| Peak Spectral Response | 9.5 microns |
| $D^*_{bb}$ (500, 10KHz, 1) | $3.38 \times 10^{10}$ cm-Hz$^{\frac{1}{2}}$w$^{-1}$ |
| $D^*_\lambda$ (9.5$\mu$, 10KHz, 1) | $8.3 \times 10^{10}$ cm-Hz$^{\frac{1}{2}}$w$^{-1}$ |
| Responsivity ($R_\lambda$) | 22,100 volts/watt |

TABLE 3.0-2

## FLIGHT MODEL LWL CHANNEL DETECTOR

### Description of Detector

| | |
|---|---|
| Type | Mercury Cadmium Telluride (Hg Cd Te) |
| Identification Number | DLK 21 Fl Z2 |
| Detector Type | Photoconductive |
| Date of Manufacture | October 1970 |
| Window | Irtran II, AR Coated |
| Element Size | Length .093 mm |
| | Width .099 mm$^2$ |
| Element Area | .0092 mm$^2$ |
| Maximum Bias Not to be Exceeded | 20.0 milliamps |
| Field of View | 80$^{\circ}$ |
| Element-Backside of Housing | .100 inches |

### Test Results at 100$^{\circ}$K

| | |
|---|---|
| Resistance at 100$^{\circ}$K | 30 ohms |
| Power at Optimum Bias | .760 m watts |
| Optimum Bias | 5 milliamps |
| Peak Spectral Response | 11 microns |
| $D^{*}_{bb}$ (500, 10KHz, 1) | $2.67 \times 10^{10}$ cm-Hz$^{\frac{1}{2}}$w$^{-1}$ |
| $D^{*}_{\lambda}$ (11μ, 10KHz, 1) | $6.4 \times 10^{10}$ cm-Hz$^{\frac{1}{2}}$w$^{-1}$ |
| Responsivity ($R_{\lambda}$) | 65,170 volts/watt |

2.6  D* vs Bias at 100°K

$D^*_{BB}$ (500, 10 KHz, 1)  $\times 10^{10}$ cm-Hz$^{1/2}$ w

BIAS CURRENT (In Milliamps)

2.5 Relative Spectral Response  at 100°K

Relative Response

WAVELENGTH IN MICRONS
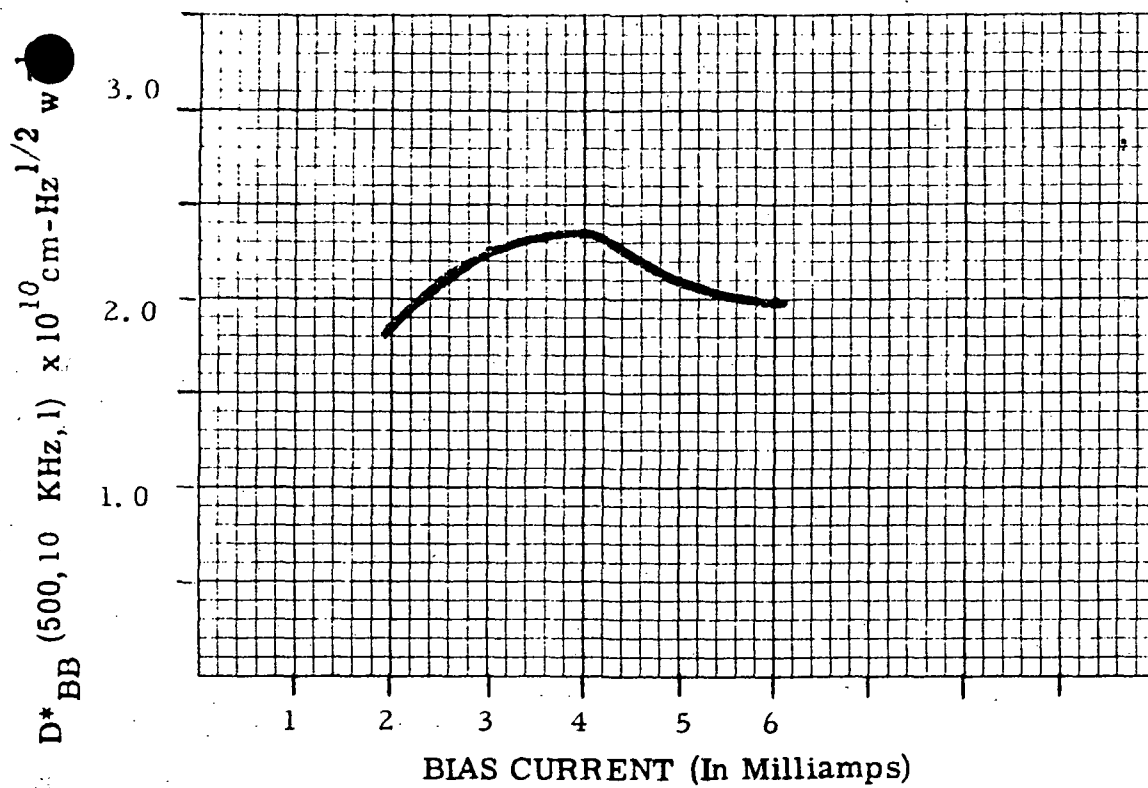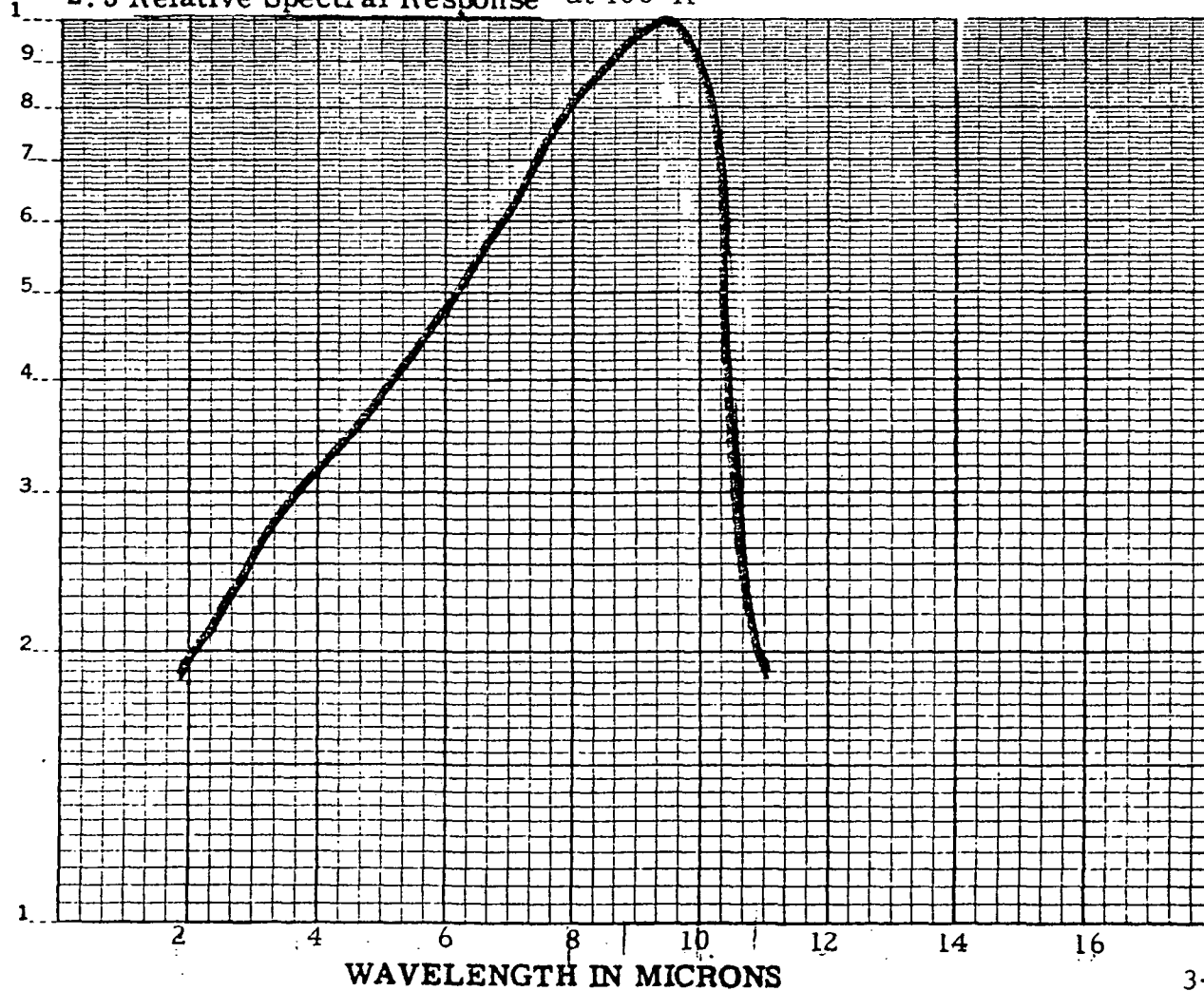
FIGURE 3.0-3  SWL DETECTOR D*, SPECTRAL RESPONSE

3-6

## 2.6  D* vs Bias    at 100°K

D*$_{BB}$ (500, 10 KHz, l) x 10$^{10}$ cm-Hz$^{1/2}$ w$^{-1}$

BIAS CURRENT (In Milliamps)

## 2.5 Relative Spectral Response    at 100°K

Relative Response

WAVELENGTH IN MICRONS
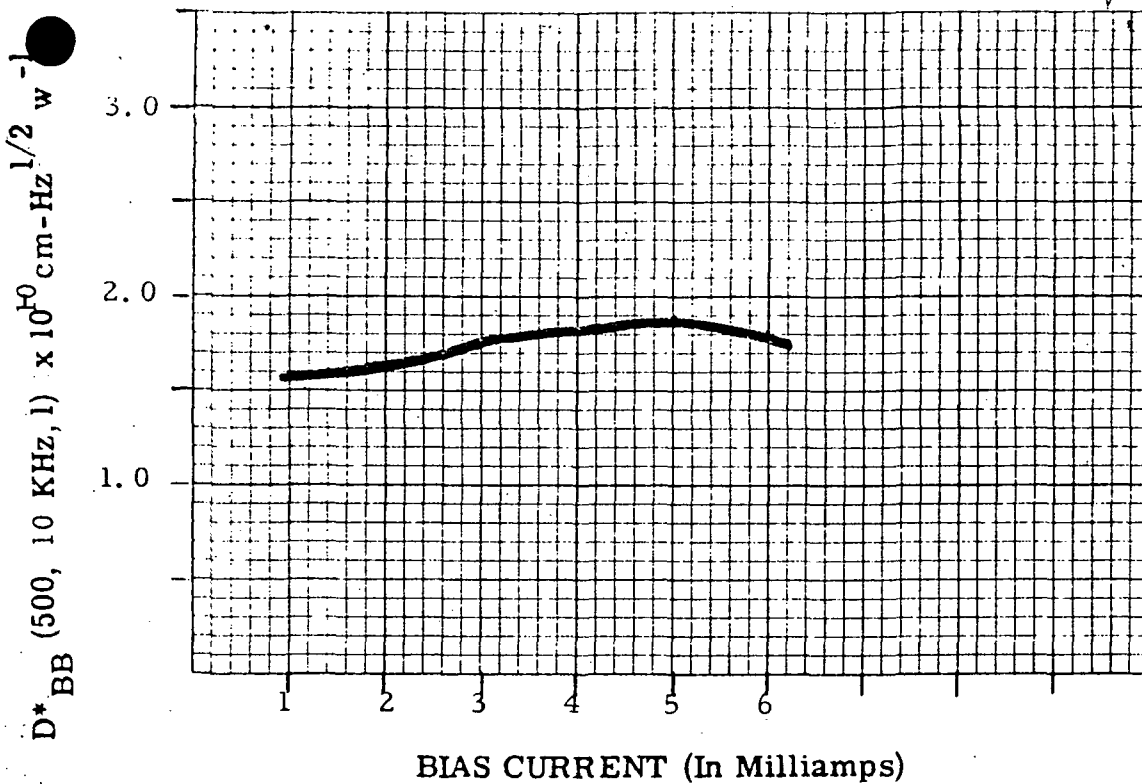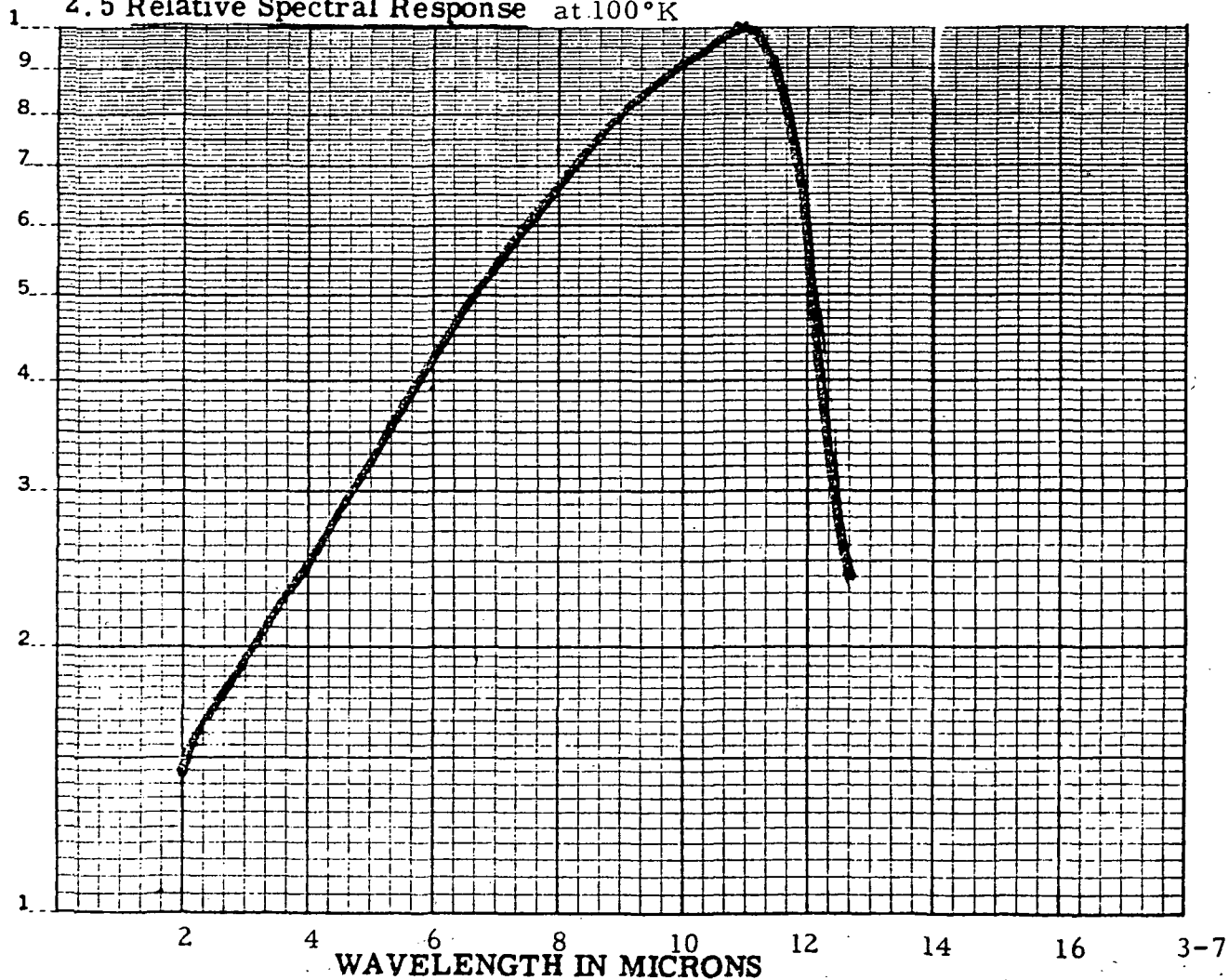
FIGURE 3.0-4 LWL Detector D*, SPECTRAL RESPONSE

3-7

## Visible Detector

The near IR Channel Detector (0.80 to 1.10 microns) is a silicon photodiode. The photodiode is packaged along with a preamplifier in a TO-5 package with a window. Guard ring construction is used to reduce leakage current and the unit is similar to the EG&G Type HAD-130.

The effective focal length of the near infrared channel is 11.17 inches so that a detector with a sensitive area of 0.0067" by 0.0067" is required to produce the IFOV of 0.6 m.r. by 0.6 m.r. This corresponds to an f-number of 1.39 for this channel. The parabolic focusing mirror which focuses the energy onto the silicon photodiode has a focal length of 1.39 inches and has an evaporated aluminum reflective coating with silicon monoxide protective overcoat. The near infrared filter transmission characteristics are given in Figure 5.6-9, p. 5-36; the coatings are proprietary to O.C.L.I. The beam-splitter which reflects the two far infrared channels but transmits the near infrared is a flat glass substrate with a thin layer of gold evaporated on one side; characteristics are given in Section 5.6.2, p. 5-26.

Measured data for Spectral Response, Noise, NEP and off-set voltage for the SCMR Flight Model Detector is shown in Tables 3.0-5 and 3.0-6.

## Signal Processing

Instrument signal processing of the IR data begins in the pre-amplifier assembly which provides voltage gain, injects the space clamp reference and injects a voltage calibration signal to provide a means to monitor the stability of the voltage gain of the amplifier stages. Restoration of the space clamp is accomplished once every rotation of the scanner and is held for the duration of the scan.

Signal processing is completed in the post amplifier assembly which provides additional gain, synchronization pulses, output calibration for monitoring the stability of the spacecraft data link and a low output impedance unity gain buffer to provide an analog signal at the video interface connector with a line structure as shown in Figure 7.1-2 of the Electrical system description.

## Visible Data Channel

Signal processing of the visible data begins in the visible pre-amplifier which is an integral part of the visible detector assembly. The detector assembly is illustrated in Figure 3.0-5. Signal processing is completed in the visible post-amplifier assembly in much the same manner as the IR data, the exception being that in place of Blackbody Temperature telemetry, an internal visible calibration target is inserted into the data line structure.

Visible analog data can be substituted for CH 1 SWL data of the video interface connector upon execution of ground command.

**EG&G**

SPECTRAL RESPONSE

| | | ATP. REF. |

| | | | ATP. REF. |
|---|---|---|---|
| **ID** | PART NUMBER: | | |
| | DEVICE SERIAL NUMBER: 11A (DIODE: 02111-1-517) | | 8.1.3.5. |
| | EG&G JOB NUMBER: 2-H78-01 | | |
| **CAL** | BARNES CHOPPER | Cal #: N/R | 8.1.3.4. |
| | | Cal Due Date: On request | |
| | PRECISION POWER SUPPLY | Cal #: N/A | |
| | | Cal Due Date: N/A | |
| | ~~PAR PHASE LOCK AMPLIFIER~~ QUAN TECH | Cal #: 1954 | |
| | | Cal Due Date: 2-26-72 | |
| | POWER SUPPLIES | Cal #: N/R | |
| | | Cal Due Date: N/R | |

| $\lambda$ ($\mu$) | $V_{pSTD}$ (mV) | $V_{psref}$ ( ↑ ) | $V_{pDUT}$ (mV) | $V_{pDref}$ ( ↑ ) | K | S @ $\lambda$ (a/w) | ATP. REF. |
|---|---|---|---|---|---|---|---|
| 0.4 | 0.051 | | 0.019 | | | 0.002 | |
| 0.45 | 0.078 | | 0.32 | | | 0.063 | |
| 0.5 | 0.29 | | 2.10 | | | 0.153 | |
| 0.55 | 0.24 | | 1.75 | | | 0.197 | |
| 0.6 | 0.40 | | 3.20 | | | 0.245 | 8.1.3.13 |
| 0.65 | 0.54 | | 4.60 | | | 0.288 | 8.1.3.14 |
| 0.7 | 0.67 | N/A | 5.50 | N/A | $3.44 \times 10^3$ | 0.319 | 8.1.3.19 |
| 0.75 | 0.75 | | 6.20 | | | 0.349 | 8.1.3.20 |
| 0.8 | 0.91 | | 7.60 | | | 0.386 | 8.1.3.24 |
| 0.85 | 1.30 | | 9.45 | | | 0.360 | |
| 0.9 | 1.11 | | 7.40 | | | → 0.356 ← | |
| 0.95 | 1.23 | | 6.55 | | | 0.298 | |
| 1.0 | 1.59 | | 5.90 | | | 0.188 | |
| 1.06 | 0.59 | | 1.81 | | | 0.064 | |
| 1.1 | 0.255 | | 0.73 | | | 0.018 | |

| **SIG.** | Test Executor: Ken Pearson | Test Engineer: HH 10/19/71 | 8.1.3.5. |
|---|---|---|---|
| | Date: 19 October 1971 | Temp: 23 °C | 8.1.3.3. |

TABLE 3.0-3  VISIBLE DETECTOR SPECTRAL RESPONSE

**EG&G**

| | NOISE, NEP, OFFSET VOLTAGE | ATP. REF. |

| ID | PART NUMBER: | 7.1.3.4. |
| | DEVICE SERIAL NUMBER: 11A (DIODE: 02111-1-517) | 9.1.3.4. |
| | EG&G JOB NUMBER: 2-H78-01 | |

| CAL | TEST FIXTURE | Cal # N/R | Due Date N/R | |
| | 5454 454 SCOPE | Cal # 948 | Due Date 12-1-71 | 7.1.3.4. |
| | HARRISON POWER SUPPLY | Cal # N/A | Due Date N/A | |
| | HP POWER SUPPLY | Cal # N/A | Due Date N/A | 9.1.3.4. |
| | WAVE ANALYZER | Cal # 7159 | Due Date 2-17-72 | |
| | KEITHLEY AMPLIFIER | Cal # 2351 | Due Date 2-25-72 | |

DATA — NOISE

| f(Hz) | $\Delta$ f(Hz) | $V_N$( $\mu v$ ) | Rf(M $\Omega$ ) | In | |
|-------|------|-----------|----------|------|----|
| 1 K | 10 | 0.58 | 2.0 | 0.29 pa | |
| 2 K | 10 | 0.62 | 2.0 | 0.31 pa | 9.1.3.11 |
| 4 K | 10 | 0.58 | 2.0 | 0.29 pa | |
| 7 K | 10 | 0.64 | 2.0 | 0.32 pa | |
| 10 K | 10 | 0.62 | 2.0 | 0.31 pa | |
| 20 K | 10 | 0.62 | 2.0 | 0.31 pa | |
| 50 K | 10 | 0.75 | 2.0 | 0.38 pa | |
| 100 K | 10 | 0.76 | 2.0 | 0.38 pa | |
| 4 K | 1 K | 5.4 | 2.0 | 2.7 pa * | |

NEP

$$NEP = \frac{I_n^*}{S.9.\mu} \times 7.0 \qquad NEP = \underline{5.31 \times 10^{-11} \ watts}$$

9.1.3.15

OFFSET

$$E_{OS} = \underline{- 0.002 \ volts}$$

(indicate polarity )

7.1.3.8.

| DT | DATE: 19 OCT 1971 | TEMP: 23°C | 7.1.3.3. 9.1.3.3. |
| SIG | *K. Pearson* TEST EXECUTOR: | TEST ENGINEER 10/19/71 | 7.1.3.4. 9.1.3.4. |

TABLE 3.0-4   VISIBLE DETECTOR NOISE, NEP, OFFSET VOLTAGE

SPACER

SILICON DETECTOR
(TO-5 PACKAGE)

ELEC. LEADS

MOUNT

1.125 DIA

45°

BEAMSPLITTER

1.489

FILTER

FOCUSING
MIRROR
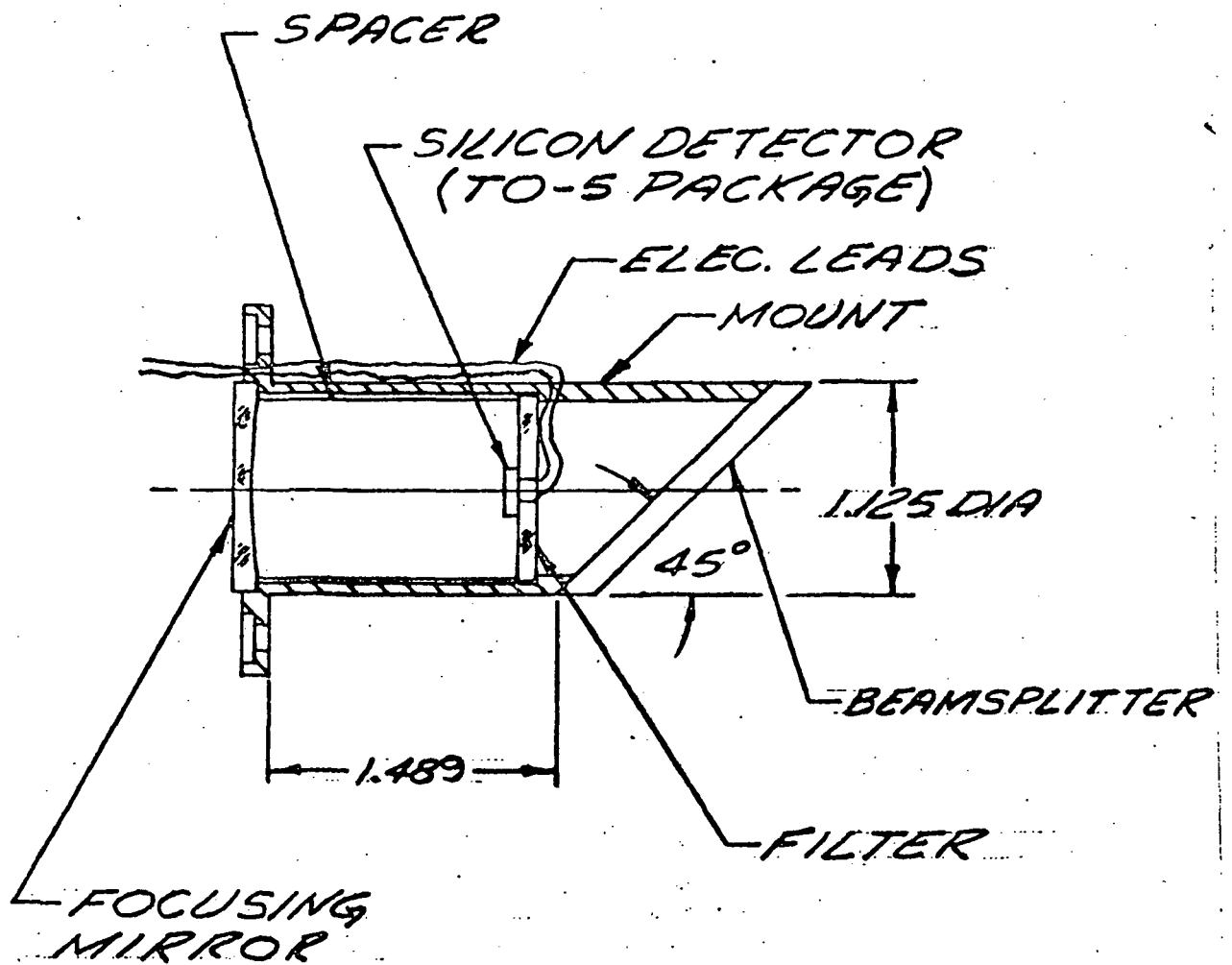
FIGURE 3.0.5

## 4.0 SCANNER DESCRIPTION

The SCMR Scanner is shown schematically in Figure 4.0-1. The scanner consists of a scan motor, shaft, bearings, mirror, balance weights, oil reservoir and housing.

The scan motor is an 80-pole hysteresis, synchronous motor which rotates at 10 Hz. The motor drives the scan mirror directly with no gear passes. It is a dual power level motor and develops 4.25 in. oz. torque at 24 Volts and 1.0 in. oz. torque at 15 Volts. Torque curves for the serial number 003 motor used in the SCMR Flight Model is shown in Figures 4.0-2 and 4.0-3.

Two different bearings are used in the scanner. A pre-loaded duplex set is used on the mirror end of the shaft for stability. On the motor end of the shaft, a single bearing is used. The single bearing is allowed to float on the shaft in order to compensate for differences in thermal expansion.

The SCMR Flight Motor Bearings are:

Duplex       8113937-2 Rev. B      Serial No. 006

Single       8113936-1 Rev. B      Serial No. 001A

Drawings of these bearings are shown in Figures 4.0-4 and 4.0-5, respectively. Both bearings were cleaned in hot chloroform and lubricated at GSFC in January of 1972. Data received from GSFC indicates that the S/N 006 bearing retained 0.0354 gms and .0343 gms of F-50 Versilube for the front and rear, respectively. The S/N 001A bearing retained .0193 gms of F-50.

Jitter tests were run at ITT using the two bearings in March 1972. Copies of the test printout are included in this report as Table 4.0-1.

The momentum compensator used on the SCMR Flight Model was S/N 002. This unit had been modified with the necessary design changes required to withstand vibration tests (see SCMR Quarterly Report 10 for the period 1 May 1972 to 1 August 1972).

ROTOR/SHAFT

STATOR

BALANCE WEIGHT

SINGLE BEARING

DUPLEX BEARING

SCAN MIRROR

OIL RESERVOIR

BALANCE WEIGHT

# SCMR SCAN MOTOR

4-2
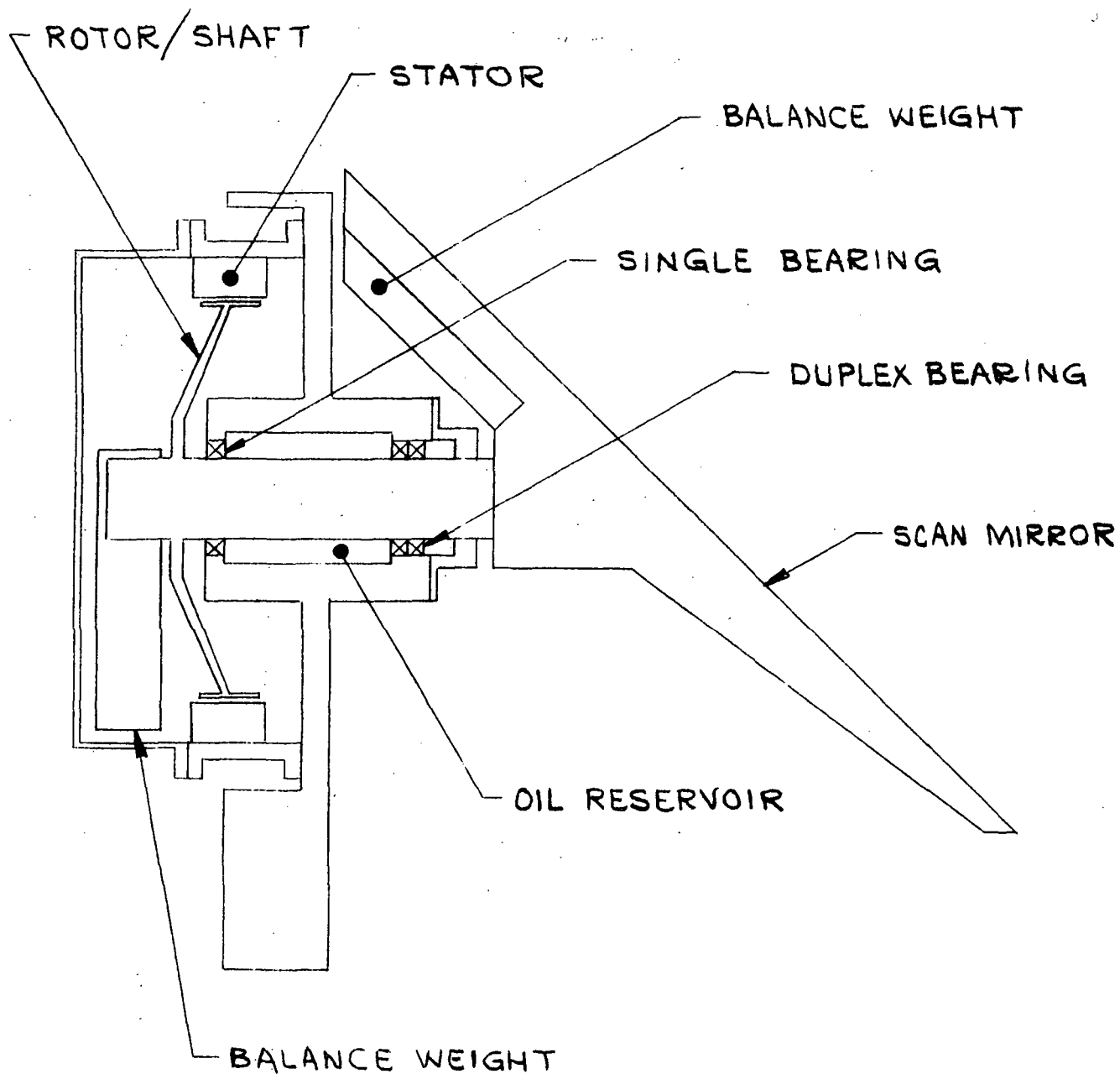
Figure 4.0-1

TORQUE VS. RPM
3 PHASE 4 POLE MOTOR
SER. NO. 003
DATE 6-11-71

TORQUE in/oz.

SPEED RPM

24.0V
22.0V
20.0V
18.0V
16.0V
14.0V

Figure 4.0-2

4-3
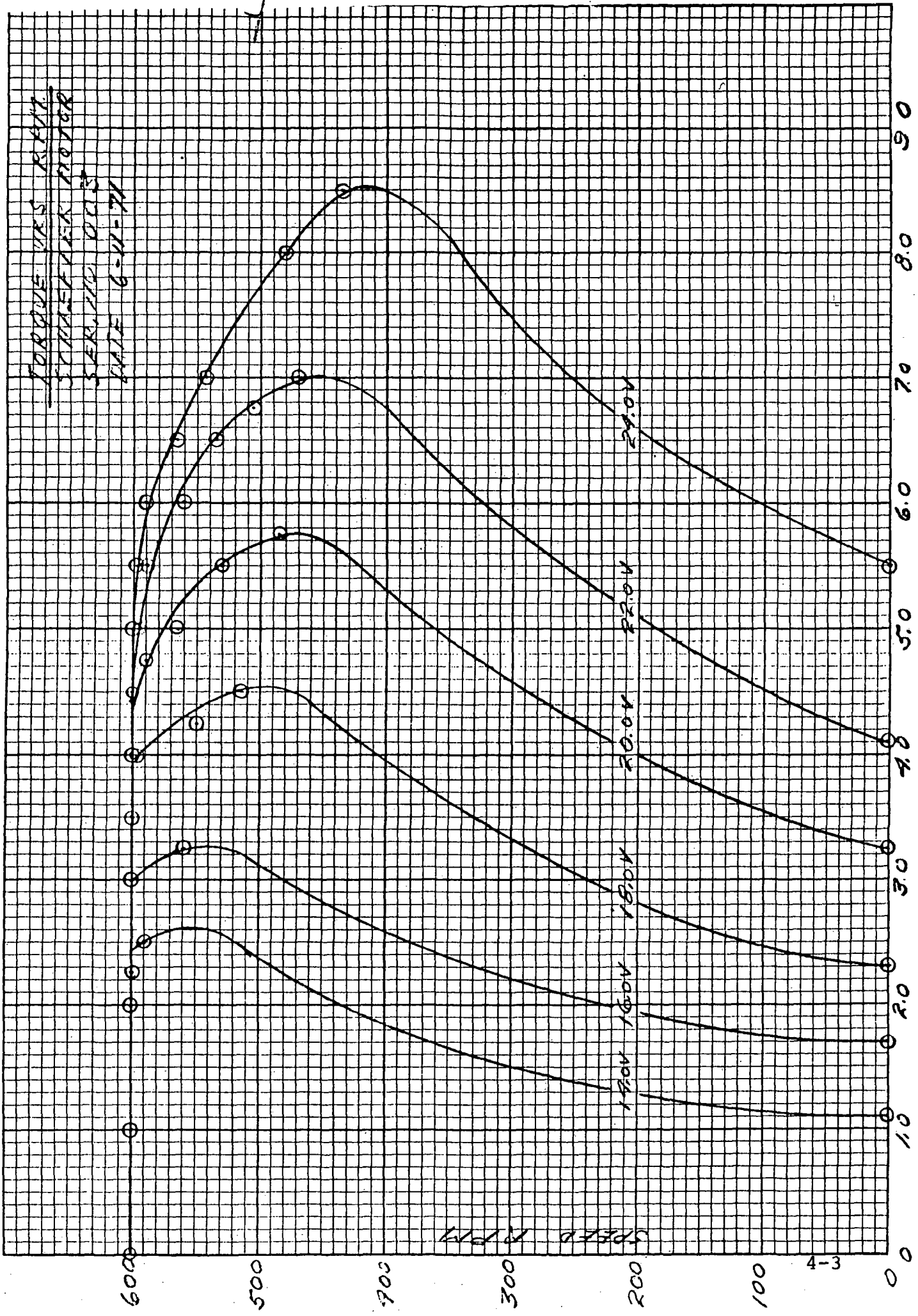
Figure 4.0-3

Figure 4.0-4
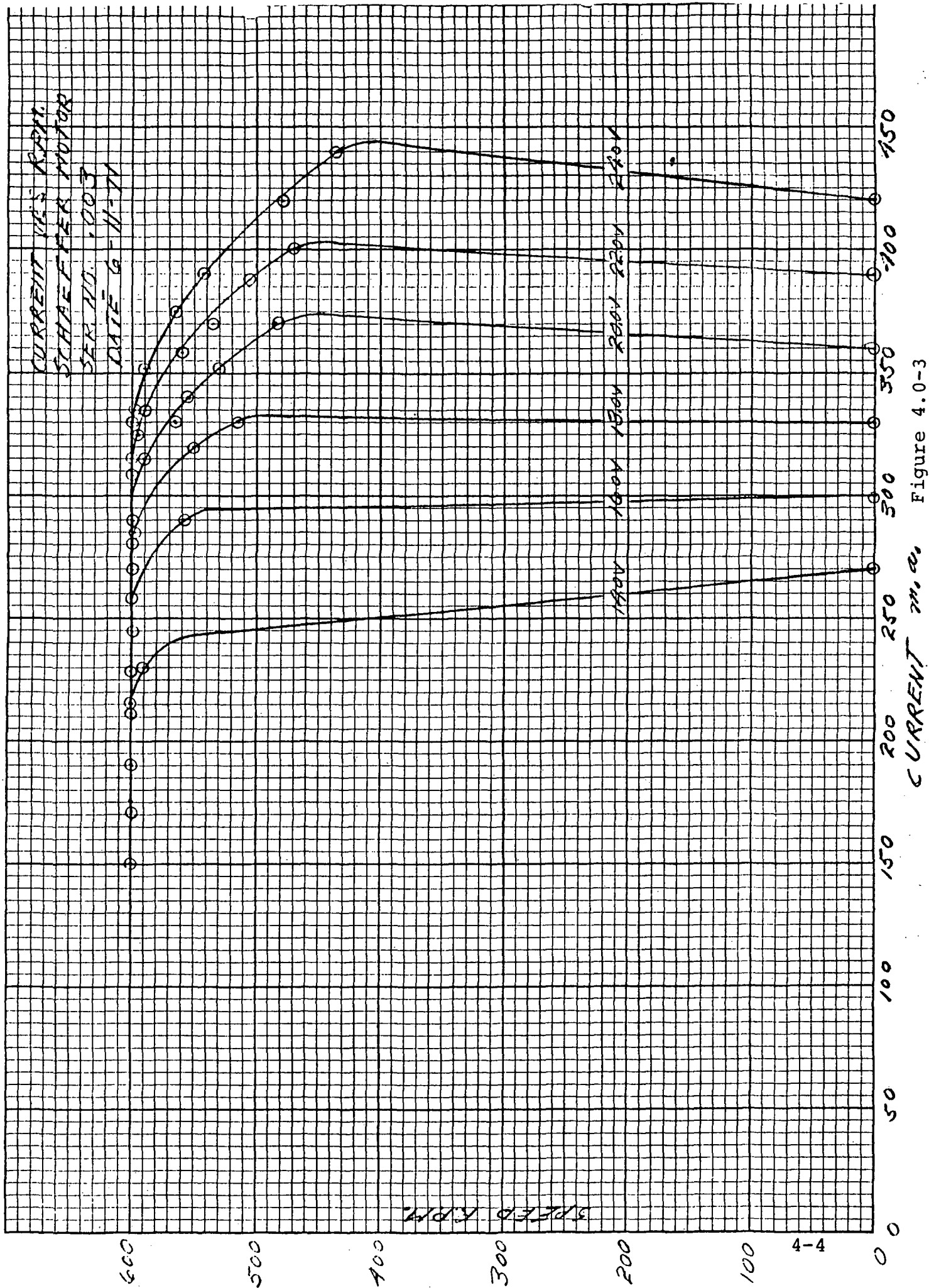
PT NO. | DESCRIPTION
-1 | ROUND BALL POCKETS IN RETAINER
-2 | SQUARE SHAPED BALL POCKETS IN RETAINER

NOTES:
1. DUPLEX PAIR: DB SET
2. PRELOAD: 1.5 TO 3.5 LBS
3. RETAINER: LINEN BASE PHENOLIC - CLEAN ULTRA SONICALLY WITH HOT CHLOROFORM
4. LUBRICATION: IMPREGNATE RETAINER WITH G.E. VERSILUBE F-50
5. WEIGHT OF BEARING BEFORE AND AFTER LUBRICATION MUST BE RECORDED SO THAT AMOUNT OF LUBRICANT CAN BE DETERMINED.
6. APPROVED SOURCE: SPLIT BALL BEARING INC., LEBANON, NEW HAMPSHIRE. BASIC PT. NO. 3TARI7-24.
7. BEARINGS MUST CONFORM TO SPEC. NASA NPC200-3.

REVISIONS

ZONE | LTR | DESCRIPTION | DATE | APPROVED
 | A | NOTE 3 RETAINER WAS RULON II. NOTE 4 LUBE WAS MMT PLUS 245X. ADDED ECN 6124D-3 | 5-4-70 | 
 | B | -2 WAS DIMOUT SHAPED BALL POCKETS ECN 6124D-5 | 9-43 | 
 | C | ADDED -1, 7 T SPEC O NOTE 3,4 ECN 6124D-31 | JAN 29 1971 | 
 | D | DELETED PT SPEC 8113937 RELOC NOTES 34 RELOC ECN 61240-36 NOTE GW45 ECN 6124D-129 | OCT 1, 1971 | 

NOMENCLATURE OR DESCRIPTION

ITT AEROSPACE/OPTICAL DIVISION
FORT WAYNE, INDIANA, U.S.A.
INTERNATIONAL TELEPHONE AND TELEGRAPH CORPORATION

BEARING, DUPLEX, SCAN SHAFT

SIZE B | CODE IDENT NO. 31550 | 8113937
SCALE — | SHEET 1

LIST OF MATERIALS OR PARTS LIST

G7 | G6 | G5 | G4 | G3 | G2 | G1 | ITEM NO. | SIZE | PART OR IDENTIFYING NO.
QUANTITY PER GROUP

CONTRACT NO. NAS5-21112
APPROVALS
DRAWN | 8-17-70
CHECKED
ENGR

UNLESS OTHERWISE SPECIFIED DIMENSIONS ARE IN INCHES AND INCLUDE CHEMICALLY APPLIED OR PLATED FINISHES
TOLERANCES
2 PLACE DECIMALS ±.02
3 PLACE DECIMALS ±.010
ANGLES ±½°
COML TOL TO STOCK SIZES
SHOP PRACTICE. 39.101 APPLIES

MATERIAL | FINISH

8113989 | 6124D
NEXT ASSEMBLY | USED ON
APPLICATION

"EXCEPT AS MAY BE OTHERWISE PROVIDED BY CONTRACT. THESE DRAWINGS AND SPECIFICATIONS ARE THE PROPERTY OF ITT AEROSPACE/OPTICAL DIVISION, ARE ISSUED IN STRICT CONFIDENCE, AND SHALL NOT BE REPRODUCED, OR COPIED, OR USED AS THE BASIS FOR THE MANUFACTURE OR SALE OF APPARATUS WITHOUT PERMISSION."

1.0625 +.0000 -.0002 DIA (REF)
1.5000 +.0000 -.0002 DIA (REF)
.250 +.005 -.005 (REF)
.500 +.000 -.010 (REF)

4-5

Figure 4.0-5

## TABLE 4.0-1   BEARING JITTER

TEST DATE    3-28-72

BEARING SER # 006
                001A


NUMBER OF SAMPLES = 100

PEAK/PEAK JITTER = 8μsec.

<u>LINE/LINE JITTERμsec # OF OCCURENCES</u>

    0 μsec...................34
    1 μsec...................48
    2 μsec...................<u> 8</u>
                          100

| | | |
|---|---|---|
| *999970 | 1000011 | *999991 |
| *999965 | 1000008 | *999976 |
| *999978 | *999995 | *999966 |
| *999982 | *999980 | *999949 |
| *999979 | *999970 | *999951 |
| *999978 | *999965 | *999960 |
| *999969 | *999962 | *999971 |
| *999969 | *999960 | *999985 |
| *999969 | *999982 | 1000003 |
| *999952 | *999985 | 1000005 |
| *999955 | *999987 | 1000008 |
| *999969 | *999991 | 1000003 |
| *999969 | *999982 | *999997 |
| *999980 | *999967 | *999986 |
| *999991 | *999962 | *999980 |
| 1000012 | *999955 | *999972 |
| 1000018 | *999949 | *999977 |
| 1000013 | *999967 | *999998 |
| 1000018 | *999967 | *999997 |
| *999997 | *999979 | 1000002 |
| *999905 | *999956 | 1000008 |
| *999978 | 1000003 | *999996 |
| *999972 | 1000005 | *999986 |
| *999977 | *999996 | *999971 |
| *999990 | *999987 | *999959 |
| *999993 | *999971 | *999953 |
| 1000000 | *999977 | *999966 |
| 1000008 | *999968 | *999969 |
| *999997 | *999967 | *999981 |
| *999962 | *999979 | 1000001 |
| *999970 | *999976 | 1000008 |
| *999957 | *999972 | 1000008 |
| *999952 | *999965 | 1000000 |
| *999967 | *999953 | *999986 |
| *999973 | *999937 | *999969 |
| *999982 | | |

## 5.0    OPTICS DESCRIPTION

The SCMR optical subsystem is best described in the Final Design Review report written by Ferson Optics and dated June 15, 1972.  This report is included in this report on the following pages (Section 5.6).

A schematic illustration of the optical layout is given in Figure 3.0-1 and a general description of the methods used to focus the optical beam and divide it into the three channels is given in Section 3.0.  The three spectral bands are 0.8 to 1.0 µm, 8.3 to 9.3 µm and 10.2 to 11.2 µm.

### 5.1    Technical Description

The optical system for the SCMR is catadioptric, collecting with an afocal reflecting telescope and focusing with refractive elements at the detectors.  To project the required 0.6 by 0.6 milliradian field of view on the 0.10 mm by 0.10 mm square detector, a focal length of 167 mm, or 6.562 inches, is required, indicating a total system operating at an effective f-number of f/0.82.

The collecting telescope is a modified Dall-Kirkham configuration operating afocally at a speed of f/0.92.  It reduces the beam diameter from 8 inches to 1 inch and folds the far infrared beam to the side with the flat, transparent gold beam splitter.  The Dall-Kirkham type was chosen because of theoretical performance over the limited field, ease of manufacture and testing, and cost.

After separation spectrally by the infrared dichroic beam-splitter outside the telescope, the 1 inch diameter beams are focused on their respective detectors.  Focusing was achieved by moving the larger germanium focusing lens in each leg.  The focusing lenses operate at about f/3.2.  After passing through a window and filter the beam is focused on the detector by a germanium aplanat operating through a thin window.

Reflecting optics were manufactured of CERVIT for thermal insensitivity.  Cooler windows were made of Irtran II and lenses and infrared dichroic of optical grade germanium, accurate to 1/10 wave at the wavelengths used.

Housing of the primary telescope is critical because of the f/numbers involved.  An invar tube was used to separate the primary and secondary mirrors.  More conventional materials were used to house the focusing optics because of relative insensitivity to temperature defocusing.

The beam transmitted through the transparent gold beam-splitter (between the primary and secondary telescope mirrors) then passed through an optical filter which transmitted energy only for wavelengths longer than 0.8 μm. A parabolic mirror then focused the energy onto the silicon detector which was insensitive to energy with wavelengths greater than about 1.0 μm.

## 5.2    Flight Model Changes

Several changes were made to the flight model optical sub-assembly in an attempt to increase the percentage of energy collected within one geometric IFOV (instantaneous field of view). These included:

1.   Rework of the telescope mounting interface with the instrument structure to eliminate distortions caused by the original mounting arrangement,

2.   Removal of the germanium wedges used in the 8.3 to 9.3 μm channel, and

3.   Repolish of the scan mirror to achieve a flatter re-flecting surface.

The telescope mount was changed to a three-point type arrangement so that no stresses would be introduced into the telescope mirrors or associated structure. This proved to be very worthwhile and much smaller blur spot images were observed when the telescope was firmly bolted into the instrument structure.

The germanium wedges used to register or align the two far infrared channels were removed because it was possible to direct the beam into the focusing germanium lenses at an angle consider-ably off of the optical axes of these lenses using the wedges. Instead, channel registration was accomplished by adjusting the position of the focus lens in an X-Y plane normal to the lens optical axis. Some vignetting could occur with this technique but at least the optical beam would be parallel to the optical axis as designed.

The scan mirrors were procured from Speedring Systems Div. of Schiller Industries. They reported that the scan mirrors could be polished flat within specification but that after setting for a day or two the flatness had changed so that it was not within specification. After several repolishes to restore the flatness, and subsequent changes to out-of-spec flatness, they reported that the stresses introduced by the balance weights attached to the mirror were slowly relieving and causing the mirror to distort. The flight model scan mirror was taken to Surfaces Finishes Inc., Addison, Ill. for repolish since they had been doing some nice polishing on metal parts for our radiant coolers. Surfaces Finishes was able to polish a flatter reflecting surface on the mirror than Speedring and it did not appear to change significantly with time.

In spite of the above changes, the performance of the
SCMR instrument (i.e. percentage signal from one geometric IFOV)
was approximately the same as that of the prototype model.  The
conclusion was that the optical performance was limited by the
basic optical design.  A review of the design was made by Ferson
Optics and is given in Section 5.6.  A calculation of expected
energy collection is given in Section 5.5.

5.3    Final Optical Design Review

As part of the rework of the flight model optics, Ferson
Optics performed a reanalysis of the design.  A copy of their
report is given on the following pages (Section 5.6).

5.4    Acceptance Test Procedure

A summary of the SCMR flight model optics tests is shown in
Table 5.4-1.

The Optical Subassembly test procedures and measured re-
sults are given on the following pages.

5.5    Field of View

The instrument specification states that 85% of the energy
within one geometric IFOV shall fall on the detector sensitive
surface.  For measurement purposes this was taken to mean that
the signal from the preamplifier (i.e. before electronic filter-
ing) when scanning a hot aperture equal to one IFOV located in
the focal plane of a 9.0 inch clear aperture diameter collimator
should be 85% as large as the signal from an aperture at least
five times larger (linear dimension) than one IFOV.  This is a
very rigid test since such effects as detector time constant must
be insignificant.

It can be shown that on the basis of diffraction effects
only the signal from a one IFOV target will be approximately
87% (see ITT Technical Proposal for SCMR).  This leaves practically
no manufacturing errors for optical element fabrication or mounting
errors.  For a point source at infinity the energy in the central
diffraction disc (Airy circle) drops from 85% for a perfect op-
tical system to 68% for an optical system having a total "optical
path difference" of $\frac{1}{4} \lambda$, the latter representing a well corrected
and manufactured system (see Modern Optical Engineering by Warren
J. Smith, McGraw-Hill Book Co., p. 298, 1966).  Ferson Optical
Div. of Bausch and Lamb also estimated the expected energy in one
IFOV and state that 65% is a reasonable expectation (see next
section for their calculations).  Thus, the measured value of
about 65% seems to be the best that could have been expected.

# TABLE 5.4-1

SUMMARY OF SCMR FLIGHT MODEL OPTICS TESTS

| | |
|---|---|
| SERIAL NUMBER [1] | 2A |
| ACCEPTANCE TEST PROCEDURE [2] | #909390 |
| DATE TESTED | 6-22-72 |
| SIZE OF TEST SOURCE | 0.0014" DIA. |
| DIA. OF SOURCE WHEN IMAGED AT FOCUS OF TEST LENS (WITHOUT ABERRATIONS) | 0.00021" |
| PRIMARY MIRROR ALIGNMENT | <1 min. arc |
| DIA. OF OBSERVED BLUR SPOT | 0.0018" |
| ALLOWABLE MAX. DIA. OF BLUR SPOT | 0.0045" |
| PENTHOUSE BORESIGHT (MAX. ALLOWABLE 15 min.) | 2 min. arc |
| RADII OF GERMANIUM LENSES: | |
| PART NO. $909305R_1$ | 2.919" |
| PART NO. $909305R_2$ | 4.524" |
| PART NO. $909308R_1$ | 0.183" |
| PART NO. $909308R_2$ | 0.150" |
| SYSTEM FOCAL LENGTH | 6.535" |
| MECHANICAL DIMENSIONS | PER DWG. #8113881 |
| WEIGHT | 6.5 LBS. |

(1)    THE TELESCOPE HAD THE IMPROVED THREE POINT MOUNTING
       ARRANGEMENT.

(2)    A TEST COLLIMATOR WITH A 12" DIAMETER PRIMARY MIRROR
       AND 192" FOCAL LENGTH WAS USED IN PLACE OF THE 8"
       DIA., 84" F.L. MIRROR IN ORDER TO PROVIDE A SMALLER
       TEST SPOT OF LIGHT.

## 5.5.1  FOV Calculations by Ferson Optics

A series of diffraction response calculations were run and results at various wavelengths from 8.0 to 11.0 microns were plotted. From these point source results calculations were made to predict field of view response.

The system, with a clear aperture of 202.6 mm, has a focal length of 166.7 mm. The nominal 0.6 milliradian field of view subtends 0.100 mm, or 100 microns.

The optical subsystem consists of an afocal reflecting telescope, whose performance can be measured visually, and refracting optics opaque to visible radiation, which remain unknown until IR performance is measured.

The entire optical system theoretically is about ¼ λ at 10µ, and predicted performance shows several clear diffraction rings. Field images are essentially the same as axial over the small field. The general image has all of its energy in 40µ diameter and 70% within 18µ diameter at 10µ wavelength. The polychromatic nature of the radiation tends to smooth the diffraction rings into a triangular form of energy distribution.

Assume for estimation purposes that the theoretical image has an even distribution and a 40µ diameter. This will give the one-dimensional field of view a trapezoidal shape 0.140 mm wide at the base and 0.060 mm wide at the top. This would throw about 10% of the energy out of the 0.100 mm field. When projected on a square format, the percent response reduces to 80.5% due to losses in the other direction as well.

The introduction of errors in the reflecting telescope adds to the system final blur circle. Assume here a circular blur of 0.003 inch diameter as seen in the 3¼ inch test lens through the 8.0 power telescope. The angular blur is then

$$\frac{0.003 \text{ inch}}{3\frac{1}{4} \text{ inches}} \times 8 = 0.000115$$

This is equivalent to a 19µ blur in the final image plane. Assuming a 59µ blur at system focus this gives 72.7% response.

Adding degradation from the additional dichroics, folding mirrors, and germanium optics, a reasonable field of view response would seem to be in the order of 65%.

5.6    Final Design Review

FINAL DESIGN REVIEW
SCMR OPTICAL SUBSYSTEM
For

ITT/NASA

Prepared by

FERSON OPTICS DIVISION OF BAUSCH AND LOMB

Job Number 9539
June 15, 1972

## 1.0 SCMR OPTICAL SUBSYSTEM DESIGN PERFORMANCE PREDICTIONS

The optical design consists of an afocal reflecting Dall-Kirkham telescope of eight inch aperture operating at eight power feeding a visible channel and two infra-red channels. The IR channels are folded out by dichoric beamsplitters and focus on small detectors through germanium lenses.

To keep the detectors as small as possible the system operates at an effective focal length of 6.5 inches, about f/0.82. This is accomplished by aplanatic elements close to focus.

The afocal telescope design prediction is about .02 milliradians equivalent blur in object space. It is aligned at assembly to as close to parallel as the components permit, generally .002" blur at an equivalent 25" focal length, or .08 milliradians.

The germanium optics are designed with a slight residual spherical aberration, keeping curves and mounting sensitivities of the first germanium lens low. The aplanat adds very little aberration. Total system aberration prediction is about .0006" diameter blur from geometric aberrations, comparing with a diffraction size of .00062" at 8μ and .00078" diameter at 10μ. The system, then, if properly aligned, should give performance close to the diffraction limit. Chromatic aberration is negligible.

Assuming the system has a total blur diameter of .0006", optimistic because of diffraction effects, 90.9% of the energy from within the field of view falls on the detector. Using the more

reasonable diameter of .0008", equivalent to 10μ radiation, this decreases to about 88.7%. Obviously performance close to the diffraction limit is required. A geometric blur of .0008" diameter in the final image plane is well within manufacturing tolerances.

## 2.0 COOLER THERMAL EFFECTS

The optical elements in the detector vicinity are cooled to about 110°K during operation. Thermal runs were made to evaluate predicted performance, considering the changes in material index, mechanical spacing, thickness, and radii of curvature. Index shifts and linear coefficients of expansion were taken from "Properties of Infra-red Sensor Materials" by Caren, et al, MATERIAL RESEARCH AND STANDARDS, June 1971.

The chief effect of the thermal simulation was defocussing caused by curve and index shifts in the germanium aplanat. Left unfocussed, these generated a smooth defocus giving a .0030" diameter blur. To correct this the airspace between the focusing lens and aplanat was changed, .011" longer. With the refocus no detectable difference in performance between this condition and nominal design was noted. The effective focal length shifted .066 longer, or by about 1.0%. Chromatic, spherical and field aberrations were identical.

If the system were focussed with the aplanat at room temperature and used with it cooled, there would be a definite focus problem. The blur circle changes about .0001" diameter for every 10°K change in detector/aplanat temperature. If the bench cooler,

test chamber cooler, and actual projected temperature are within 30°K the blur will be less than half the diffraction limit. At present the cooled detector is used, indicating no real problem on SCMR.

A general result of this study indicates that precise measurement of IR focal positions using uncooled detectors in the optical laboratory is subject to error due to thermal defocussing when a cooled aplanat is used. The difference from nominal could be computed and used to refocus, or some focus adjustment should be retained on future similar systems.

## 3.0 TEST EQUIPMENT PERFORMANCE EFFECTS

If the system, with its focal length of 5.5 inches, is checked by a long focal length collimator, perhaps 190" EFL, the defects of the collimator are demagnified by the ratio of the focal lengths. If the 190" collimator has a .005" diameter blur, the equivalent blur in the IR focal plane is

$$.005" \times \frac{5.5}{190} = .00014"$$

This is about a quarter of the Airy disc diameter, making the test beam diffraction limited in the infra-red.

If the test collimator is misaligned and used off-axis, or the entrance beam is not parallel to the system axis, rather gross errors can occur. In this case, both channels should read equally bad, neglecting diffraction.

3

## 4.0 CHANGES IN FUTURE SYSTEMS

In order to improve system resolution in the future with a greater confidence factor in achieving design predictions, the following general recommendations are made:

4.1 Increase the envelope length available for the reflecting telescope. System difficulty, including correction of optical elements and sensitivity to mechanical errors, increases roughly as the inverse cube of the primary mirror f/number. In wide field systems like HIRS, theoretical performance at the field stop edge suffers badly as speed increases, by about the N.A. squared.

4.2 Increase the weight allowance of the optical subsystem and reduce informal pressures for ultra light weight. The rigidity of optical elements, especially mirrors and beamsplitters is a question of degree, with thicker elements being easier to figure to a good accuracy and being more likely to hold that accuracy in mounting. Cells, spacers, and retainers also resist torques and bending if heavier.

4.3 Design the system interface to a pseudo-kinematic configuration, adequately constraining the optical subsystem while not applying forces tending to misalign and skew. Provide complete enough interface drawings to avoid interference. Use a dummy interface during testing to simulate the actual integration.

4.4   Design adjustments in the optical system to have small
enough travel not to degrade the final image.  Provide
reference surfaces on the optical subsystem to align to
external sources and to check alignment during assembly.
IR components opaque in the visible should be removable
as a subassembly and the flange squareness checkable by
autocollimation.  If space permits, levelling screws or
shims can realign skewed components, in translation as
well as tilt.

4.5   At the primary assembly facility for the optical subsystem,
usually the optical vendor, facilities should be made
available for checking and aligning the system to the
final IR focus.  This can be done with room temperature
detectors and black body sources collimated by reflecting
optics.  Tests for squareness, alignment and system blur
can be made with graduated apertures.

NOMINAL SYSTEM

AXIAL FAN

8.8 μ

S FAN

FRAC OBJECT HEIGHT          0.0000

CHIEF RAY HEIGHT          0.0000

1 INCH =      0.001000

6
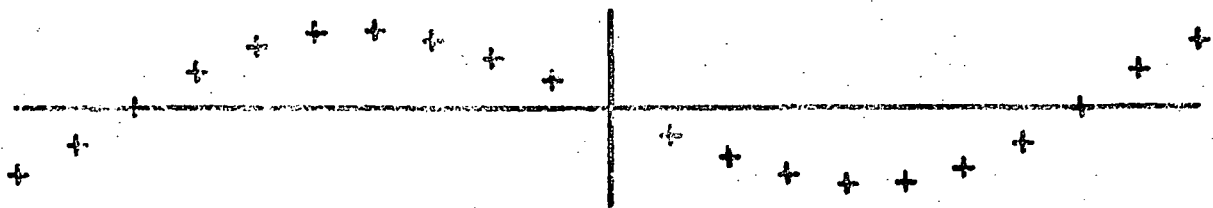
NOMINAL SYSTEM
SPOT DIAGRAM ON AXIS
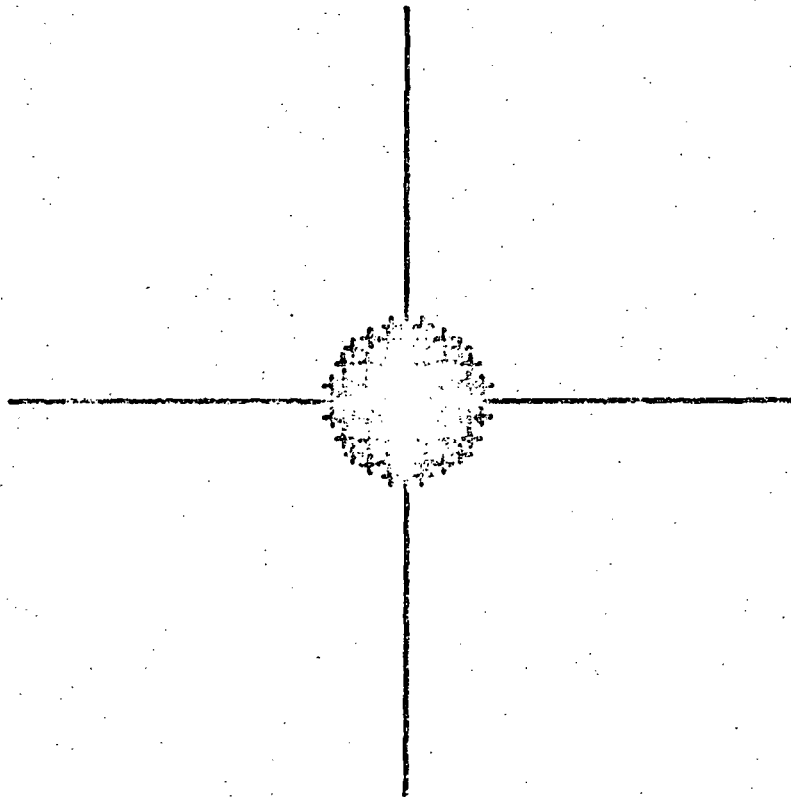
CHIEF RAY HEIGHT          0.0000

FOCUS SHIFT               0.000000

1 INCH =    0.001000

# NOMINAL SYSTEM
## FREQUENCY RESPONSE
### ON AXIS
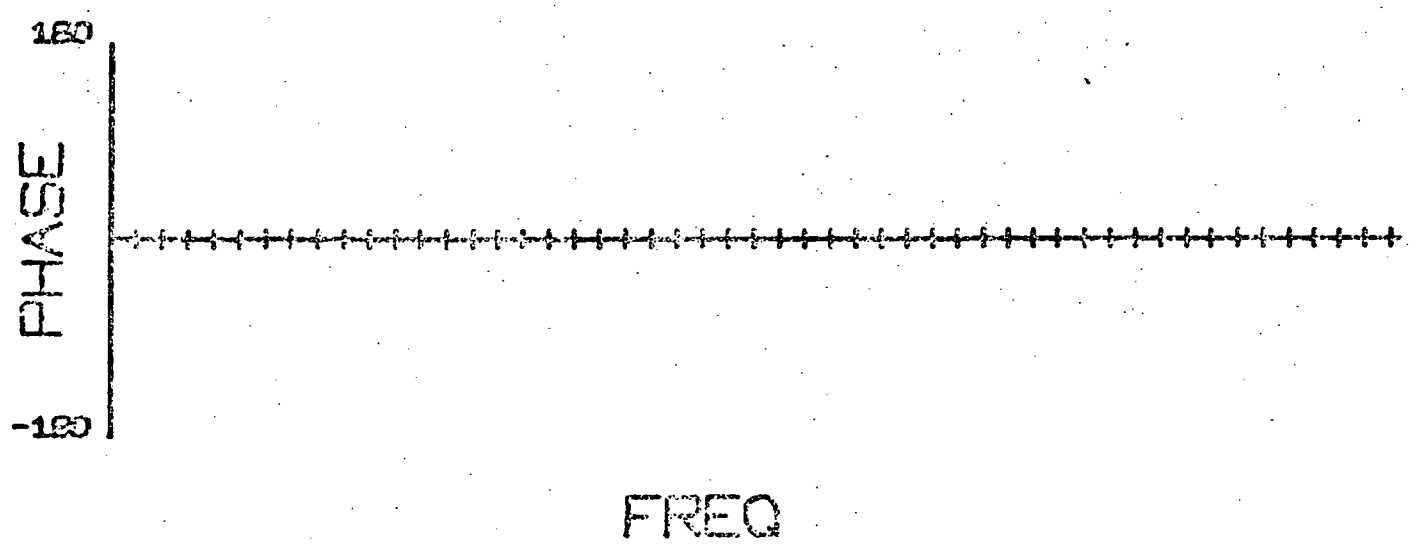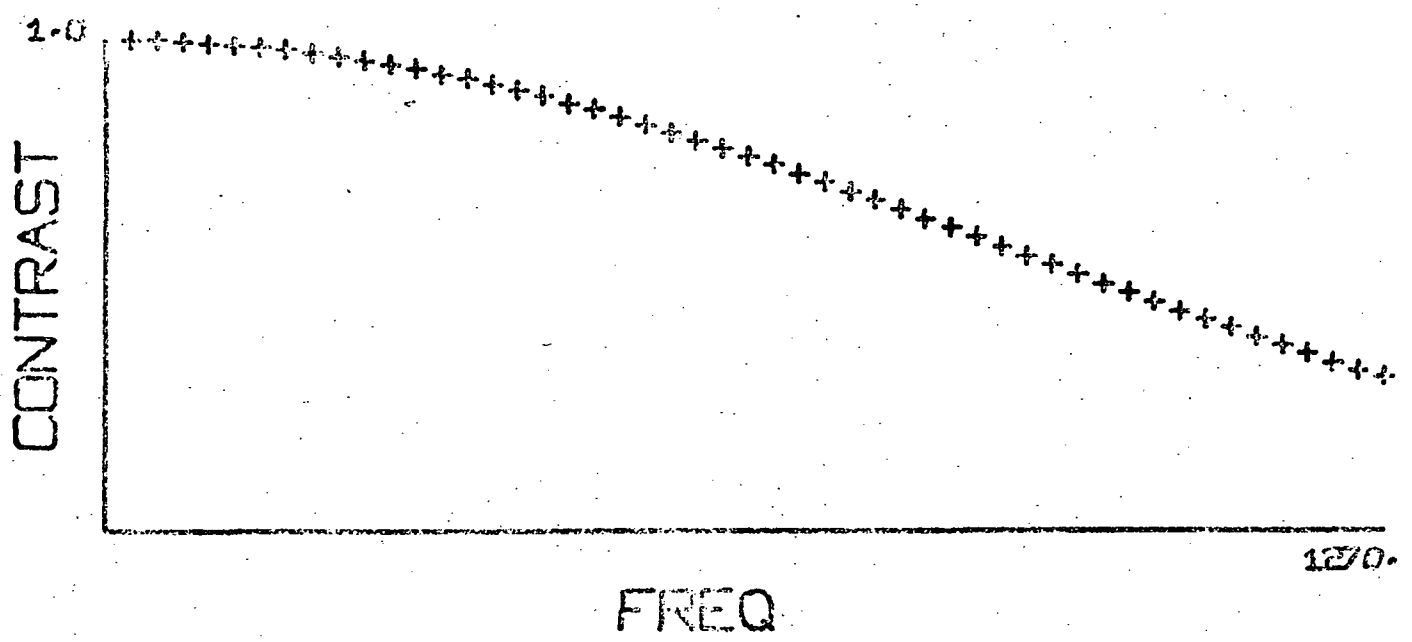


TARGET ORIENTATION        0.0

FOCUS SHIFT               0.000000

FRAC OBJECT HEIGHT        0.0000 12

8

5-14

NOMINAL SYSTEM

AXIAL FAN

8.3 μ
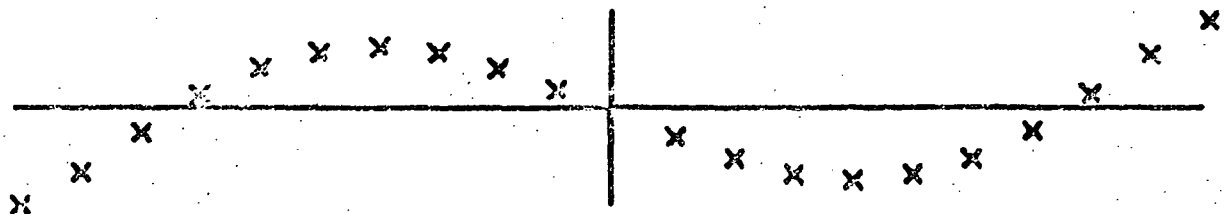


S FAN

FRAC OBJECT HEIGHT        0.0000

CHIEF RAY HEIGHT          0.0000

1 INCH =        0.001000

NOMINAL SYSTEM
AXIAL FAN
11 µ
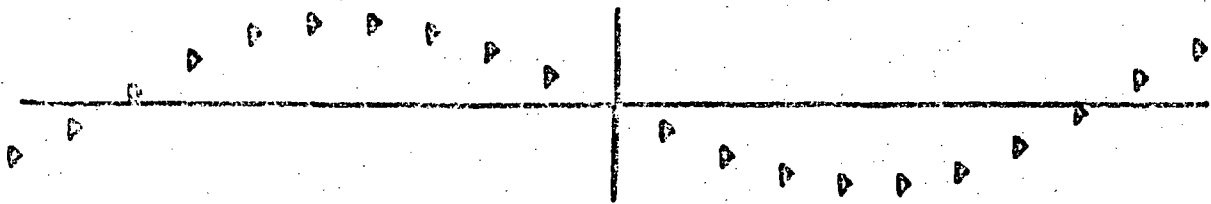


S FAN

FRAC OBJECT HEIGHT          0·0000

CHIEF RAY HEIGHT            0·0000

1 INCH =      0·001000

NOM SYSTEM WITH APLANAT ASSY AT $110^\circ$K
REFOCUSED .011 WITH FOCUSING LENS
AXIAL FAN
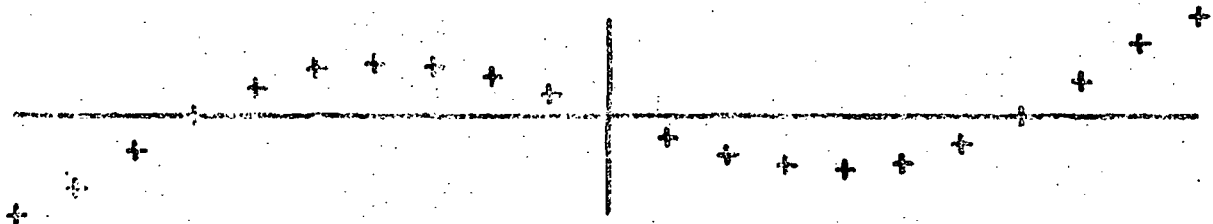
S FAN

FRAC OBJECT HEIGHT          0.0000

CHIEF RAY HEIGHT            0.0000

1 INCH =     0.001000

```
CALL PRT  0.0000000E 00  0.0000000E 00  0.0000000E 00  0.0000000E 00  0.0●●00E 00  0.0000000E 00
ITT SCVR 9093   System Description
STOP IS SURF  1
IMAGE IS 16.
PXRAY   0.4000000E 01  -0.3000000E 01  -0.3000000E 00  0.3000000E 06  0.3000000E-03  0.0000000E 00
WVLNS.  0.8800000E 01  0.8300000E 01  0.8300000E 01  0.1100000E 02

 1   0  CURVATURE DATA               0.0000000E 00   0.0000000E 00   0.0000000E 00   0.0000000E 00
 2   0  AXIAL SEPARATION             0.1000000E 10
 3   0  AIRSPACE

 1   1  CURVATURE DATA               0.0000000E 00   0.0000000E 00   0.0000000E 00
 2   1  AXIAL SEPARATION             0.5963756E 00
 3   1  AIRSPACE

 1   2  CURVATURE DATA              -0.7409000E-01  -0.1349709E 02  -0.8800000E 00
 2   2  AXIAL SEPARATION            -0.5875000E 01
 3   2  REFLECTING SURF.            -0.1000000E 01  -0.1000000E 01  -0.1000000E 01

 1   3  CURVATURE DATA              -0.5720000E 00  -0.1748251E 01   0.0000000E 00
 2   3  AXIAL SEPARATION             0.8470000E 01
 3   3  REFLECTING SURF.             0.1000000E 01   0.1000000E 01   0.1000000E 01

 1   4  CURVATURE DATA               0.0000000E 00   0.0000000E 00   0.0000000E 00
 2   4  AXIAL SEPARATION            -0.1750000E 01
 3   4  REFLECTING SURF.            -0.1000000E 01  -0.1000000E 01  -0.1000000E 01
 6   4  CURV OF REVOLUTION-TORIC     0.0000000E 00

 1   5  CURVATURE DATA               0.0000000E 00   0.0000000E 00   0.0000000E 00
 2   5  AXIAL SEPARATION             0.2000000E 01   0.1000000E 01
 3   5  REFLECTING SURF.             0.1000000E 01   0.1000000E 01

 1   6  RADIUS DATA                  0.3425835E 00   0.2919000E 01   0.0000000E 00
 2   6  AXIAL SEPARATION             0.1750000E 00
 3   6  INDICES                      0.4004100E 01   0.4004800E 01   0.4002600E 01

 1   7  RADIUS DATA                  0.2210433E 00   0.4524000E 01   0.0000000E 00
 2   7  AXIAL SEPARATION             0.6525729E 00
 3   7  AIRSPACE

 1   8  CURVATURE DATA               0.0000000E 00   0.0000000E 00   0.0000000E 00
 2   8  AXIAL SEPARATION             0.1000000E 01   0.2180000E 01   0.2130000E 01
 3   8  INDICES                      0.2155000E 01   0.2180000E 01   0.2130000E 01

 1   9  CURVATURE DATA               0.0000000E 00   0.0000000E 00   0.0000000E 00
 2   9  AXIAL SEPARATION             0.9420000E 00
 3   9  AIRSPACE

 1  10  CURVATURE DATA               0.0000000E 00   0.0000000E 00   0.0000000E 00
 2  10  AXIAL SEPARATION             0.4000000E-01   0.2180000E 01   0.2130000E 01
 3  10  PICKUP  8                    0.2155000E 01

 1  11  CURVATURE DATA               0.0000000E 00   0.0000000E 00   0.0000000E 00
 2  11  AXIAL SEPARATION             0.1000000E-01
 3  11  AIRSPACE

 1  12  RADIUS DATA                  0.5464480E-01   0.1830000E 00   0.0000000E 00
 2  12  AXIAL SEPARATION             0.8000000E-01
 3  12  PICKUP  6                    0.4004100E 01   0.4004800E 01   0.4002600E 01
```

5-18

```
1  13  RADIUS DATA              0.6666666E 01   0.1500000E 00   0.0000000E 00
2  13  AXIAL SEPARATION         0.7250000E-01
3  13  AIRSPACE

1  14  CURVATURE DATA           0.0000000E 00   0.0000000E 00   0.0000000E 00
2  14  AXIAL SEPARATION         0.4000000E-01
3  14  PICKUP  E                0.2155000E 01   0.2180000E 01   0.2130000E 01

1  15  CURVATURE DATA           0.0000000E 00   0.0000000E 00   0.0000000E 00
2  15  AXIAL SEPARATION         0.2600000E-01
3  15  AIRSPACE

1  16  CURVATURE DATA           0.0000000E 00   0.0000000E 00   0.0000000E 00
```

THIRD ORDER ABERRATIONS

```
PRX RAYS   -0.3000000E 06   0.4000000E-08   0.3000000E-03   0.4000000E 01   0.0000000E 00

FCLN,GSHT,BKFC,OVLN   0.6551656E 01   0.1861433E-02   0.2600000E-01   0.5779448E 01
REN,TEN,TEX           0.4000000E 01   0.0000000E 00   0.6642051E-01
SPHR,COMA,DIST        0.2867018E-02   0.9147276E-03   0.1089169E-02
TANG,SAGT,PETZ        0.7493329E-04   0.2483227E-04  -0.2182393E-06
PA,PL,SA,SL           0.1923357E-03   0.1246791E-04   0.1277932E-03   0.8438980E-05
```

FIFTH ORDER ABERRATIONS

```
PRX RAYS   -0.3000000E 06   0.4000000E-08   0.3000000E-03   0.4000000E 01   0.0000000E 00
FCLN,GSHT,BKFC,OVLN   0.6551656E 01   0.1861433E-02   0.2600000E-01   0.5779448E 01
REN,TEN,TEX           0.4000000E 01   0.0000000E 00   0.6642051E-01
      0.2867018E-02   0.9147276E-03   0.7493329E-04  0.2483227E-04  -0.2182393E-06   0.1089169E-02
     -0.6450222E-03  -0.3199596E-03   0.2314743E-06  0.4953586E-07   0.4176253E-08   0.2472667E-05
     -0.2605435E-03   0.5096809E-05   0.5931693E-04  0.1109805E-04
PA,PL,SA,SL           0.1923357E-03   0.1246791E-04   0.1277932E-03   0.8438980E-05
```

SAGITTAL FAN ON AXIS 8.8

BEAM HEIGHT =0.06000060802000.0600000E 00 0.0000000E 00 0.0000000E 00 0.0000000E 00 -0.4000000E 00 0.0000000E 00

| | | | | | | |
|---|---|---|---|---|---|---|
| 1P | 0.0000000E 00 | 0.0000000E 00 | 0.0000000E 00 | -0.4000000E 00 | 0.0000000E 00 | -0.4000000E-08 |
| 1 15 | -0.3377165 -03 | 0.0000000E 00 | 0.2693051 -01 | 0.0000000E 00 | 0.6746136 -08 | 0.0000000E 00 |
| 2P | 0.0000000E 00 | 0.0000000E 00 | 0.0000000E 00 | -0.3600000E 01 | 0.0000000E 00 | -0.3600000E-08 |
| 2 16 | -0.1877524 -03 | 0.0000000E 00 | 0.2408657 -01 | 0.0000000E 00 | 0.6005445 -08 | 0.0000000E 00 |
| 5P | 0.0000000E 00 | 0.0000000E 00 | 0.0000000E 00 | -0.3200000E 01 | 0.0000000E 00 | -0.3200000E-08 |
| 3 16 | 0.2179225 -05 | 0.0000000E 00 | 0.2128895 -01 | 0.0000000E 00 | 0.5266305 -08 | 0.0000000E 00 |
| 4P | 0.0000000E 00 | 0.0000000E 00 | 0.0000000E 00 | -0.2800000E 01 | 0.0000000E 00 | -0.2800000E-08 |
| 4 16 | -0.1770121 -03 | 0.0000000E 00 | 0.1853421 -01 | 0.0000000E 00 | 0.4541555 -05 | 0.0000000E 00 |
| 5P | 0.0000000E 00 | 0.0000000E 00 | 0.0000000E 00 | -0.2400000E 01 | 0.0000000E 00 | -0.2400000E-05 |
| 5 16 | 0.1304015 -03 | 0.0000000E 00 | 0.1581772 -01 | 0.0000000E 00 | 0.3337487 -00 | 0.0000000E 00 |
| 6P | 0.0000000E 00 | 0.0000000E 00 | 0.0000000E 00 | -0.2000000E 01 | 0.0000000E 00 | -0.2000000E-08 |
| 6 16 | 0.3771641 -03 | 0.0000000E 00 | 0.1313369 -01 | 0.0000000E 00 | 0.3155954 -08 | 0.0000000E 00 |
| 7P | 0.0000000E 00 | 0.0000000E 00 | 0.0000000E 00 | -0.1600000E 01 | 0.0000000E 00 | -0.1600000E-08 |
| 7 16 | 0.2875672 -03 | 0.0000000E 00 | 0.1047623 -01 | 0.0000000E 00 | 0.2495925 -08 | 0.0000000E 00 |
| 8P | 0.0000000E 00 | 0.0000000E 00 | 0.0000000E 00 | -0.1200000E 01 | 0.0000000E 00 | -0.1200000E-08 |
| 8 16 | 0.2432880 -03 | 0.0000000E 00 | 0.7839541 -02 | 0.0000000E 00 | 0.1354566 -09 | 0.0000000E 00 |
| 9P | 0.0000000E 00 | 0.0000000E 00 | 0.0000000E 00 | -0.8000000E 00 | 0.0000000E 00 | -0.8000000E-09 |
| 9 16 | 0.2547441 -03 | 0.0000000E 00 | 0.5218081 -02 | 0.0000000E 00 | 0.1227925 -00 | 0.0000000E 00 |
| 10P | 0.0000000E 00 | 0.0000000E 00 | 0.0000000E 00 | -0.4000000E 00 | 0.0000000E 00 | -0.4000000E-09 |
| 10 16 | 0.1352941 -03 | 0.0000000E 00 | 0.2606591 -02 | 0.0000000E 00 | 0.6113943 -09 | 0.0000000E 00 |
| 11P | 0.0000000E 00 | 0.0000000E 00 | 0.0000000E 00 | 0.3999999E 00 | 0.0000000E 00 | 0.3999999E-09 |
| 11 16 | -0.1552941 -03 | 0.0000000E 00 | -0.2606591 -02 | 0.0000000E 00 | -0.6113943 -01 | 0.0000000E 00 |
| 12P | 0.0000000E 00 | 0.0000000E 00 | 0.0000000E 00 | 0.7999999E 00 | 0.0000000E 00 | 0.7999999E-09 |
| 12 16 | -0.2547441 -03 | 0.0000000E 00 | -0.5218081 -02 | 0.0000000E 00 | -0.1227925 -03 | 0.0000000E 00 |
| 13P | 0.0000000E 00 | 0.0000000E 00 | 0.0000000E 00 | 0.1199999E 01 | 0.0000000E 00 | 0.1199999E-03 |
| 13 16 | -0.3432880 -03 | 0.0000000E 00 | -0.7839541 -02 | 0.0000000E 00 | -0.1854566 -00 | 0.0000000E 00 |
| 14P | 0.0000000E 00 | 0.0000000E 00 | 0.0000000E 00 | 0.1599999E 01 | 0.0000000E 00 | 0.1599999E-08 |
| 14 16 | -0.2875659 -03 | 0.0000000E 00 | -0.1047623 -01 | 0.0000000E 00 | -0.2495927 -08 | 0.0000000E 00 |
| 15P | 0.0000000E 00 | 0.0000000E 00 | 0.0000000E 00 | 0.1999999E 01 | 0.0000000E 00 | 0.1999999E-08 |
| 15 16 | -0.3771650 -03 | 0.0000000E 00 | -0.1313369 -01 | 0.0000000E 00 | -0.3155954 -08 | 0.0000000E 00 |
| 16P | 0.0000000E 00 | 0.0000000E 00 | 0.0000000E 00 | 0.2399999E 01 | 0.0000000E 00 | 0.2399999E-08 |
| 16 16 | -0.3064020 -03 | 0.0000000E 00 | -0.1581772 -01 | 0.0000000E 00 | -0.3837483 -08 | 0.0000000E 00 |
| 17P | 0.0000000E 00 | 0.0000000E 00 | 0.0000000E 00 | 0.2799999E 01 | 0.0000000E 00 | 0.2799999E-08 |
| 17 16 | -0.1770110 -03 | 0.0000000E 00 | -0.1853421 -01 | 0.0000000E 00 | -0.4541555 -08 | 0.0000000E 00 |
| 18P | 0.0000000E 00 | 0.0000000E 00 | 0.0000000E 00 | 0.3199999E 01 | 0.0000000E 00 | 0.3199999E-08 |
| 18 16 | -0.2183063 -05 | 0.0000000E 00 | -0.2128895 -01 | 0.0000000E 00 | -0.5266303 -08 | 0.0000000E 00 |
| 19P | 0.0000000E 00 | 0.0000000E 00 | 0.0000000E 00 | 0.3599999E 01 | 0.0000000E 00 | 0.3599999E-08 |
| 19 16 | 0.1877557 -03 | 0.0000000E 00 | -0.2408656 -01 | 0.0000000E 00 | -0.6005446 -08 | 0.0000000E 00 |
| 20P | 0.0000000E 00 | 0.0000000E 00 | 0.0000000E 00 | 0.3999999E 01 | 0.0000000E 00 | 0.3999999E-08 |
| 20 15 | 0.3377212 -03 | 0.0000000E 00 | -0.2693051 -01 | 0.0000000E 00 | -0.6746137 -08 | 0.0000000E 00 |

5-20

CALL FRQ     0.2540000E 02   0.0000000E 00   0.0000000E 00   0.0000000E 00   0.0000000E 00

| NO. | CBJ HT | CHF RAY | FOCUS SHFT | ORIENTATION | CUT-OFF |
|---|---|---|---|---|---|
| 1 | 0.0000000E 00 | 0.0000000E 00 | 0.0000000E 00 | 0.0000000E 00 | 0.0000000E 00 | 0.1270000E 04 |

| NO. | FREQUENCY | CONTRAST | PHASE ANGLE |
|---|---|---|---|
| 1. | 0.2540000 02 | 0.9995710 00 | -0.1247706 -07 |
| 2. | 0.5080000 02 | 0.9982852 00 | -0.2500901 -07 |
| 3. | 0.7620000 02 | 0.9961452 00 | -0.3786071 -07 |
| 4. | 0.1016000 03 | 0.9931556 00 | -0.5027435 -07 |
| 5. | 0.1270000 03 | 0.9893227 00 | -0.6279453 -07 |
| 6. | 0.1524000 03 | 0.9846546 00 | -0.7568775 -07 |
| 7. | 0.1778000 03 | 0.9791612 00 | -0.8829071 -07 |
| 8. | 0.2032000 03 | 0.9725541 00 | -0.1007186 -05 |
| 9. | 0.2286000 03 | 0.9657467 00 | -0.1140502 -05 |
| 10. | 0.2540000 03 | 0.9575539 00 | -0.1267410 -05 |
| 11. | 0.2794000 03 | 0.9491924 00 | -0.1399754 -05 |
| 12. | 0.3048000 03 | 0.9397503 00 | -0.1535762 -06 |
| 13. | 0.3302000 03 | 0.9296375 00 | -0.1672848 -06 |
| 14. | 0.3556000 03 | 0.9187851 00 | -0.1811522 -06 |
| 15. | 0.3810000 03 | 0.9072458 00 | -0.1944844 -05 |
| 16. | 0.4064000 03 | 0.8950455 00 | -0.2093234 -05 |
| 17. | 0.4317999 03 | 0.8822059 00 | -0.2251285 -05 |
| 18. | 0.4572000 03 | 0.8687533 00 | -0.2405107 -05 |
| 19. | 0.4826000 03 | 0.8547196 00 | -0.2564297 -05 |
| 20. | 0.5080000 03 | 0.8401315 00 | -0.2734530 -05 |
| 21. | 0.5334000 03 | 0.8250191 00 | -0.2915993 -06 |
| 22. | 0.5588000 03 | 0.8094131 00 | -0.3102698 -05 |
| 23. | 0.5842000 03 | 0.7933452 00 | -0.3300410 -05 |
| 24. | 0.6096000 03 | 0.7768479 00 | -0.3502867 -06 |
| 25. | 0.6350000 03 | 0.7599545 00 | -0.3719703 -06 |
| 26. | 0.6604000 03 | 0.7426988 00 | -0.3946452 -05 |
| 27. | 0.6858000 03 | 0.7251151 00 | -0.4195463 -06 |
| 28. | 0.7112000 03 | 0.7072382 00 | -0.4451155 -05 |
| 29. | 0.7366000 03 | 0.6891033 00 | -0.4745931 -05 |
| 30. | 0.7620000 03 | 0.6707458 00 | -0.5047775 -06 |
| 31. | 0.7874000 03 | 0.6522014 00 | -0.5355360 -05 |
| 32. | 0.8128000 03 | 0.6335057 00 | -0.5704241 -05 |
| 33. | 0.8382000 03 | 0.6146944 00 | -0.6073222 -05 |
| 34. | 0.8636000 03 | 0.5958031 00 | -0.6466367 -06 |
| 35. | 0.8890000 03 | 0.5768673 00 | -0.6885791 -06 |
| 36. | 0.9144000 03 | 0.5579221 00 | -0.7318863 -06 |
| 37. | 0.9397999 03 | 0.5390025 00 | -0.7818106 -06 |
| 38. | 0.9652000 03 | 0.5201427 00 | -0.8325995 -06 |
| 39. | 0.9905999 03 | 0.5013767 00 | -0.8870442 -06 |
| 40. | 0.1016000 04 | 0.4827377 00 | -0.9489284 -05 |
| 41. | 0.1041400 04 | 0.4642583 00 | -0.1013039 -05 |
| 42. | 0.1066800 04 | 0.4459705 00 | -0.1085740 -05 |
| 43. | 0.1092200 04 | 0.4279051 00 | -0.1163403 -05 |
| 44. | 0.1117600 04 | 0.4100924 00 | -0.1247143 -05 |
| 45. | 0.1143000 04 | 0.3925616 00 | -0.1338236 -05 |
| 46. | 0.1168400 04 | 0.3753407 00 | -0.1436658 -05 |
| 47. | 0.1193800 04 | 0.3584558 00 | -0.1544544 -05 |
| 48. | 0.1219200 04 | 0.3419357 00 | -0.1661541 -05 |
| 49. | 0.1244600 04 | 0.3258022 00 | -0.1789030 -05 |
| 50. | 0.1270000 04 | 0.3100797 00 | -0.1925453 -05 |

18

CHIEF RAY, EVERY SURFACE
CALL RAYP, 0.18000000E 01 0.00000000E 00 0.00000000E 00 0.00000000E 00 0.00000000E 00 0.00000000E 00

| IP | | | | | | | |
|----|----|----|----|----|----|----|----|
| 1 | 0.00000000 00 | -0.30000000 06 | 0.00000000 00 | 0.00000000 00 | 0.00000000 00 | 0.00000000 00 | 0.00000000E 00 0.3000000E-03 |
| 1 1 | 0.00000000 00 | 0.00000000 00 | 0.00000000 00 | 0.00000000 00 | 0.0000000 00 | 0.3000000 -03 | |
| 1 2 | 0.00000000 00 | 0.1789126 -03 | -0.1185301 -03 | 0.00000000 00 | -0.2734687 -03 | |
| 1 3 | 0.00000000 00 | 0.1785659 -02 | -0.9119337 -05 | 0.00000000 00 | -0.2316287 -02 | |
| 1 4 | 0.00000000 00 | 0.2140461 -01 | 0.00000000 00 | 0.00000000 00 | -0.2316287 -02 | |
| 1 5 | 0.00000000 00 | 0.2545611 -01 | 0.00000000 00 | 0.00000000 00 | 0.2316287 -02 | |
| 1 6 | 0.00000000 00 | 0.3009105 -01 | 0.1551036 -03 | 0.00000000 00 | -0.7156012 -02 | |
| 1 7 | 0.00000000 00 | 0.2583920 -01 | 0.9192174 -04 | 0.00000000 00 | -0.9502785 -02 | |
| 1 8 | 0.00000000 00 | 0.2073625 -01 | 0.00000000 00 | 0.00000000 00 | -0.4409459 -02 | |
| 1 9 | 0.00000000 00 | 0.2029730 -01 | 0.00000000 00 | 0.00000000 00 | -0.9502765 -02 | |
| 1 10 | 0.00000000 00 | 0.1134568 -01 | 0.00000000 00 | 0.00000000 00 | -0.4409489 -02 | |
| 1 11 | 0.00000000 00 | 0.1116930 -01 | 0.00000000 00 | 0.00000000 00 | -0.9502786 -02 | |
| 1 12 | 0.00000000 00 | 0.1107109 -01 | 0.3351950 -03 | 0.00000000 00 | -0.4783134 -01 | |
| 1 13 | 0.00000000 00 | 0.7252224 -02 | 0.1754134 -03 | 0.00000000 00 | -0.4610689 -01 | |
| 1 14 | 0.00000000 00 | 0.3917418 -02 | 0.00000000 00 | 0.00000000 00 | -0.2137641 -01 | |
| 1 15 | 0.00000000 00 | 0.3062281 -02 | 0.00000000 00 | 0.00000000 00 | -0.4610889 -01 | |
| 1 16 | 0.00000000 00 | 0.1863450 -02 | 0.00000000 00 | 0.00000000 00 | -0.2953456 -06 | 0.0000000 00 -0.4610889 -01 |

MARGINAL AXIAL RAY EVERY SURFACE
CALL RAYP   0.0000000E 00   0.1000000E 00   0.0000000E 00

| IP | | 0.0000000E 00 | 0.0000000E 00 | 0.0000000E 01 | 0.0000000E 00 | 0.4000000E 01 | 0.0000000E 00 | 0.4000000E-08 | 0.0000000E 00 |
|---|---|---|---|---|---|---|---|---|---|
| 1 | 1 | 0.4000000 01 | 0.0000000 00 | 0.0000000 00 | 0.4000000 00 | 0.0000000E 01 | 0.0000000 00 | | |
| 1 | 2 | 0.4000000 01 | 0.0000000 00 | 0.0000000 00 | 0.6539128 -08 | 0.0000000 00 | | | |
| 1 | 3 | 0.4992669 00 | 0.0000000 00 | -0.5942900 00 | 0.1035728 -03 | 0.0000000 00 | | | |
| 1 | 4 | 0.5001517 00 | 0.0000000 00 | -0.7236651 -01 | 0.1035729 -03 | 0.0000000 00 | | | |
| 1 | 5 | 0.5003329 00 | 0.0000000 00 | 0.0000000 00 | 0.1035728 -03 | 0.0000000 00 | | | |
| 1 | 6 | 0.5005445 00 | 0.0000000 00 | 0.4323342 -01 | 0.1301937 00 | 0.0000000 00 | | | |
| 1 | 7 | 0.4500642 00 | 0.0000000 00 | 0.2554311 -01 | 0.2016113 00 | 0.0000000 00 | | | |
| 1 | 8 | 0.3131502 00 | 0.0000000 00 | 0.0000000 00 | 0.9218650 -01 | 0.0000000 00 | | | |
| 1 | 9 | 0.3035415 00 | 0.0000000 00 | 0.0000000 00 | 0.2018113 00 | 0.0000000 00 | | | |
| 1 | 10 | 0.1138352 00 | 0.0000000 00 | 0.0000000 00 | 0.9218650 -01 | 0.0000000 00 | | | |
| 1 | 11 | 0.1101478 00 | 0.0000000 00 | 0.0000000 00 | 0.2019113 -01 | 0.0000000 00 | | | |
| 1 | 12 | 0.1016775 00 | 0.0000000 00 | 0.3098335 -01 | 0.5263329 00 | 0.0000000 00 | | | |
| 1 | 13 | 0.6692059 -01 | 0.0000000 00 | 0.1575053 -01 | 0.6746136 00 | 0.0000000 00 | | | |
| 1 | 14 | 0.2542649 -01 | 0.0000000 00 | 0.0000000 00 | 0.2627206 00 | 0.0000000 00 | | | |
| 1 | 15 | 0.1787757 -01 | 0.0000000 00 | 0.0000000 00 | 0.6746135 00 | 0.0000000 00 | | | |
| 1 | 16 | 0.3377166 -03 | 0.0000000 00 | 0.0000000 00 | 0.2693051 -01 | 0.0000000 00 | -0.6746136 00 | 0.0000000 00 | |

SAGITTAL FAN ON AXIS   8.3μ
REF. HEIGHT = 0.0000000E 00

| | | | | | | |
|---|---|---|---|---|---|---|
| 1S | 0.0000000E 00 | 0.0000000E 00 | -0.4000000E 01 | 0.0000000E 00 | -0.4000000E-08 | 0.0000000E 00 |
| 1 16 | -0.4671816E-03 | 0.0000000E 00 | 0.2692203E 01 | 0.0000000E 00 | 0.6751328E 00 | 0.0000000E 00 |
| 2S | 0.0000000E 00 | 0.0000000E 00 | -0.3600000E 01 | 0.0000000E 00 | -0.3600000E-08 | 0.0000000E 00 |
| 2 16 | -0.3044498E-03 | 0.0000000E 00 | 0.2298774E 01 | 0.0000000E 00 | 0.6009967E 00 | 0.0000000E 00 |
| 3S | 0.0000000E 00 | 0.0000000E 00 | -0.3200000E 01 | 0.0000000E 00 | -0.3200000E-08 | 0.0000000E 00 |
| 3 16 | -0.1013252E-03 | 0.0000000E 00 | 0.2120038E 01 | 0.0000000E 00 | 0.5270024E 00 | 0.0000000E 00 |
| 4S | 0.0000000E 00 | 0.0000000E 00 | -0.2800000E 01 | 0.0000000E 00 | -0.2800000E-08 | 0.0000000E 00 |
| 4 16 | 0.8685502E-04 | 0.0000000E 00 | 0.1845654E 01 | 0.0000000E 00 | -0.4544644E 00 | 0.0000000E 00 |
| 5S | 0.0000000E 00 | 0.0000000E 00 | -0.2400000E 01 | 0.0000000E 00 | -0.2400000E-08 | 0.0000000E 00 |
| 5 16 | 0.2295718E-03 | 0.0000000E 00 | 0.1575110E 01 | 0.0000000E 00 | -0.3840014E 00 | 0.0000000E 00 |
| 6S | 0.0000000E 00 | 0.0000000E 00 | -0.2000000E 01 | 0.0000000E 00 | -0.2000000E-03 | 0.0000000E 00 |
| 6 16 | 0.3135350E-03 | 0.0000000E 00 | 0.1307823E 01 | 0.0000000E 00 | 0.3157976E 00 | 0.0000000E 00 |
| 7S | 0.0000000E 00 | 0.0000000E 00 | -0.1600000E 01 | 0.0000000E 00 | -0.1600000E-09 | 0.0000000E 00 |
| 7 16 | 0.3369673E-03 | 0.0000000E 00 | 0.1043195E 01 | 0.0000000E 00 | 0.2497439E 00 | 0.0000000E 00 |
| 8S | 0.0000000E 00 | 0.0000000E 00 | -0.1200000E 01 | 0.0000000E 00 | -0.1200000E-08 | 0.0000000E 00 |
| 8 16 | 0.3055314E-03 | 0.0000000E 00 | 0.7903400E 00 | 0.0000000E 00 | 0.1855708E 00 | 0.0000000E 00 |
| 9S | 0.0000000E 00 | 0.0000000E 00 | -0.8000000E 00 | 0.0000000E 00 | -0.8000000E-09 | 0.0000000E 00 |
| 9 16 | 0.2296718E-03 | 0.0000000E 00 | 0.5196028E 00 | 0.0000000E 00 | 0.1228672E 00 | 0.0000000E 00 |
| 10S | 0.0000000E 00 | 0.0000000E 00 | -0.4000000E 00 | 0.0000000E 00 | -0.4000000E-09 | 0.0000000E 00 |
| 10 16 | 0.1227866E-03 | 0.0000000E 00 | 0.2595552E 00 | 0.0000000E 00 | 0.6117636E 00 | 0.0000000E 00 |
| 11S | 0.0000000E 00 | 0.0000000E 00 | 0.4000000E 00 | 0.0000000E 00 | 0.3999999E-09 | 0.0000000E 00 |
| 11 16 | -0.1227386E-03 | 0.0000000E 00 | -0.2595558E 00 | 0.0000000E 00 | -0.6117635E 00 | 0.0000000E 00 |
| 12S | 0.0000000E 00 | 0.0000000E 00 | 0.7999999E 00 | 0.0000000E 00 | -0.7999995E-09 | 0.0000000E 00 |
| 12 16 | -0.2296710E-03 | 0.0000000E 00 | -0.5196027E 00 | 0.0000000E 00 | -0.1228672E 00 | 0.0000000E 00 |
| 13S | 0.0000000E 00 | 0.0000000E 00 | 0.1199999E 01 | 0.0000000E 00 | -0.1199999E-08 | 0.0000000E 00 |
| 13 16 | -0.3055620E-03 | 0.0000000E 00 | -0.7893699E 00 | 0.0000000E 00 | -0.1855708E 00 | 0.0000000E 00 |
| 14S | 0.0000000E 00 | 0.0000000E 00 | 0.1599999E 01 | 0.0000000E 00 | -0.1599999E-08 | 0.0000000E 00 |
| 14 16 | -0.3369625E-03 | 0.0000000E 00 | -0.1043195E 01 | 0.0000000E 00 | -0.2497491E 00 | 0.0000000E 00 |
| 15S | 0.0000000E 00 | 0.0000000E 00 | 0.1999999E 01 | 0.0000000E 00 | -0.1999999E-08 | 0.0000000E 00 |
| 15 16 | -0.3135391E-03 | 0.0000000E 00 | -0.1307823E 01 | 0.0000000E 00 | -0.3157975E 00 | 0.0000000E 00 |
| 16S | 0.0000000E 00 | 0.0000000E 00 | 0.2399999E 01 | 0.0000000E 00 | -0.2399999E-08 | 0.0000000E 00 |
| 16 16 | -0.2295746E-03 | 0.0000000E 00 | -0.1575111E 01 | 0.0000000E 00 | -0.3840014E 00 | 0.0000000E 00 |
| 17S | 0.0000000E 00 | 0.0000000E 00 | 0.2799999E 01 | 0.0000000E 00 | -0.2799999E-08 | 0.0000000E 00 |
| 17 16 | -0.8695060E-04 | 0.0000000E 00 | -0.1845654E 01 | 0.0000000E 00 | -0.4544644E 00 | 0.0000000E 00 |
| 18S | 0.0000000E 00 | 0.0000000E 00 | 0.3199999E 01 | 0.0000000E 00 | -0.3199999E-08 | 0.0000000E 00 |
| 18 16 | 0.1013214E-03 | 0.0000000E 00 | -0.2120038E 01 | 0.0000000E 00 | 0.3199999E 00 | 0.0000000E 00 |
| 19S | 0.0000000E 00 | 0.0000000E 00 | 0.3599999E 01 | 0.0000000E 00 | -0.3599999E-08 | 0.0000000E 00 |
| 19 16 | 0.3044501E-03 | 0.0000000E 00 | -0.2398774E 01 | 0.0000000E 00 | -0.6009857E 00 | 0.0000000E 00 |
| 20S | 0.0000000E 00 | 0.0000000E 00 | 0.3999999E 01 | 0.0000000E 00 | -0.3999999E-08 | 0.0000000E 00 |
| 20 16 | 0.4671862E-03 | 0.0000000E 00 | -0.2682203E 01 | 0.0000000E 00 | -0.6751329E 00 | 0.0000000E 00 |

21

SHUTTLE FAN ON AXIS FLOW
CALL SFNT  0.1000000E-02  0.0000000E 00
REF. HEIGHT = 0.0000000E 00

| | | | | | | |
|---|---|---|---|---|---|---|
| 1T | 0.0000000E 00 | 0.0000000E 00 | -0.4000000E 00 | 0.0000000E 00 | -0.4000000E-08 | 0.0000000E 00 |
| 1 16 | -0.2795421E-03 | 0.0000000E 00 | 0.2697540E-01 | 0.0000000E 00 | 0.6742849 | 0.0000000E 00 |
| 2T | 0.0000000E 00 | 0.0000000E 00 | -0.3600000E 00 | 0.0000000E 00 | -0.3600000E-08 | 0.0000000E 00 |
| 2 16 | -0.1332133E-03 | 0.0000000E 00 | 0.2412932E 00 | 0.0000000E 00 | 0.6002530 | 0.0000000E 00 |
| 3T | 0.0000000E 00 | 0.0000000E 00 | -0.3200000E 00 | 0.0000000E 00 | -0.3200000E-09 | 0.0000000E 00 |
| 3 16 | -0.5217192E-04 | 0.0000000E 00 | 0.2132856E 00 | 0.0000000E 00 | 0.5263759 | 0.0000000E 00 |
| 4T | 0.0000000E 00 | 0.0000000E 00 | -0.2800000E 00 | 0.0000000E 00 | -0.2800000E-05 | 0.0000000E 00 |
| 4 16 | 0.2217656E-03 | 0.0000000E 00 | 0.1857013E 00 | 0.0000000E 00 | 0.4539370 | 0.0000000E 00 |
| 5T | 0.0000000E 00 | 0.0000000E 00 | -0.2400000E 00 | 0.0000000E 00 | -0.2400000E-03 | 0.0000000E 00 |
| 5 16 | 0.3455547E-03 | 0.0000000E 00 | 0.1584928E 00 | 0.0000000E 00 | 0.3835650 | 0.0000000E 00 |
| 6T | 0.0000000E 00 | 0.0000000E 00 | -0.2000000E 00 | 0.0000000E 00 | -0.2000000E-08 | 0.0000000E 00 |
| 6 16 | 0.4100122E-03 | 0.0000000E 00 | 0.1316045E 00 | 0.0000000E 00 | 0.3154451 | 0.0000000E 00 |
| 7T | 0.0000000E 00 | 0.0000000E 00 | -0.1600000E 00 | 0.0000000E 00 | -0.1600000E-08 | 0.0000000E 00 |
| 7 16 | 0.4440674E-03 | 0.0000000E 00 | 0.1049792E 00 | 0.0000000E 00 | 0.2494742 | 0.0000000E 00 |
| 8T | 0.0000000E 00 | 0.0000000E 00 | -0.1200000E 00 | 0.0000000E 00 | -0.1200000E-08 | 0.0000000E 00 |
| 8 16 | 0.3632422E-03 | 0.0000000E 00 | 0.7855953E-02 | 0.0000000E 00 | 0.1853690 | 0.0000000E 00 |
| 9T | 0.0000000E 00 | 0.0000000E 00 | -0.8000000E 00 | 0.0000000E 00 | -0.8000000E-09 | 0.0000000E 00 |
| 9 16 | 0.2630844E-03 | 0.0000000E 00 | 0.5229083E 00 | 0.0000000E 00 | 0.1227346 | 0.0000000E 00 |
| 10 16 | 0.1415747E-03 | 0.0000000E 00 | -0.4000000E 00 | 0.0000000E 00 | 0.6111068E-01 | 0.0000000E 00 |
| 11T | 0.0000000E 00 | 0.0000000E 00 | 0.2412100E-02 | 0.0000000E 00 | 0.6111058E-01 | 0.0000000E 00 |
| 11 16 | -0.1415746E-03 | 0.0000000E 00 | 0.2612100E-02 | 0.0000000E 00 | 0.7999999E-09 | 0.0000000E 00 |
| 12T | 0.0000000E 00 | 0.0000000E 00 | -0.3999999E 00 | 0.0000000E 00 | -0.1227346E-08 | 0.0000000E 00 |
| 12 16 | -0.2630935E-03 | 0.0000000E 00 | 0.5229082E 00 | 0.0000000E 00 | 0.1199999E-05 | 0.0000000E 00 |
| 13T | 0.0000000E 00 | 0.0000000E 00 | 0.7855952E-02 | 0.0000000E 00 | 0.1653690 | 0.0000000E 00 |
| 13 16 | -0.3632397E-03 | 0.0000000E 00 | 0.1599999E 00 | 0.0000000E 00 | -0.1999999E-05 | 0.0000000E 00 |
| 14 16 | -0.4140384E-03 | 0.0000000E 00 | -0.1049792E 00 | 0.0000000E 00 | -0.2494743 | 0.0000000E 00 |
| 15T | 0.0000000E 00 | 0.0000000E 00 | 0.1999999E 00 | 0.0000000E 00 | 0.1999999E-08 | 0.0000000E 00 |
| 15 16 | -0.4100145E-03 | 0.0000000E 00 | -0.1316045E 00 | 0.0000000E 00 | -0.3154450 | 0.0000000E 00 |
| 16 16 | -0.3455845E-03 | 0.0000000E 00 | 0.2399999E 00 | 0.0000000E 00 | 0.2399999E-08 | 0.0000000E 00 |
| 17 16 | -0.2217654E-03 | 0.0000000E 00 | -0.1584928E 00 | 0.0000000E 00 | -0.3835650 | 0.0000000E 00 |
| 17 16 | 0.2799999E 00 | 0.0000000E 00 | 0.1857013E 00 | 0.0000000E 00 | 0.2799999E-08 | 0.0000000E 00 |
| 18T | 0.0000000E 00 | 0.0000000E 00 | 0.3199999E 00 | 0.0000000E 00 | 0.4539370 | 0.0000000E 00 |
| 18 16 | -0.5218257E-04 | 0.0000000E 00 | -0.2132856E 00 | 0.0000000E 00 | -0.5263758 | 0.0000000E 00 |
| 19 16 | 0.1532200E-03 | 0.0000000E 00 | 0.3599999E 00 | 0.0000000E 00 | 0.3599999E-08 | 0.0000000E 00 |
| 20T | 0.0000000E 00 | 0.0000000E 00 | -0.2412632E 00 | 0.0000000E 00 | -0.6002531 | 0.0000000E 00 |
| 20 16 | 0.2795464E-03 | 0.0000000E 00 | -0.2697540E-01 | 0.0000000E 00 | -0.6742850 | 0.0000000E 00 |

### 5.6.1 Scan Mirror

As noted in Section 5.2 the scan mirror supplied by Speed-ring was repolished by Surface Finishes Inc. The flatness of the mirror is illustrated by the fringe pattern which occurs when the scan mirror reflecting surface is placed in contact with a pre-cision optical flat and suitably illuminated; the fringe pattern is shown in Figure 5.6-1. The mirror was then aluminized by D.L. Clausing Co., Skokie, Ill.

### 5.6.2 Near Infrared Channel Beamsplitter

The transmission and reflectance characteristics of the beamsplitter used to reflect the two long wavelength infrared channels and transmit the near infrared channel are given in Figure 5.6-2 and Figure 5.6-3.

### 5.6.3 Infrared Dichroic

This dichroic reflected energy in the 8.3 to 9.3 μm band and transmitted in the 10.2 to 11.2 μm band. Figures 5.6-4 and 5.6-5 show that the reflectance is very high, averaging about 98%, with the transmittance averaging about 82% in the band. The dichroic was of the "balanced stress" design which means that the substrate material (germanium) was coated on both sides to equal the multilayer coating stresses and keep the part optically flat after coating. Tests on the "penthouse" assembly attached to the side of the telescope and containing the dichroic showed that the dichroic remained optically flat (within requirements). The parallelism of the two sides of the dichroic were within 0.7 milli-radian compared to the beam spread of 4.8 milliradians so that even a reflection from the second surface should not have caused sig-nificant optical degradation.

### 5.6.4 Bandpass Filters (LW Infrared Channels)

Transmission curves for the two longwavelength channels are given in Figures 5.6-6 and 5.6-7. These curves were measured by the manufacturer, OCLI, with the filters cooled to 100 Kelvin. The shift with wavelength is linear with temperature. At 25°C, the short wavelength cutoff of the 10.2 to 11.2 μm filter was at 10.33 μm (50% point) which gives a shift of (10.33 - 10.11 μm)÷ 200 K or 0.0011 μm/K shift. At 115 Kelvin the 50% T point would therefore be at 10.11 + 0.0011 (15) = 10.126 μm. The shift of the 8.3 to 9.3 μm filter is 0.0008 μm per Kelvin.

### 5.6.5 Cooler Windows

The transmission of the Irtran II windows used in the radi-ant cooler is given in Figure 5.6-8. The windows were antireflec-tion coated so that they would transmit either of the long wave infrared bands.

5-26
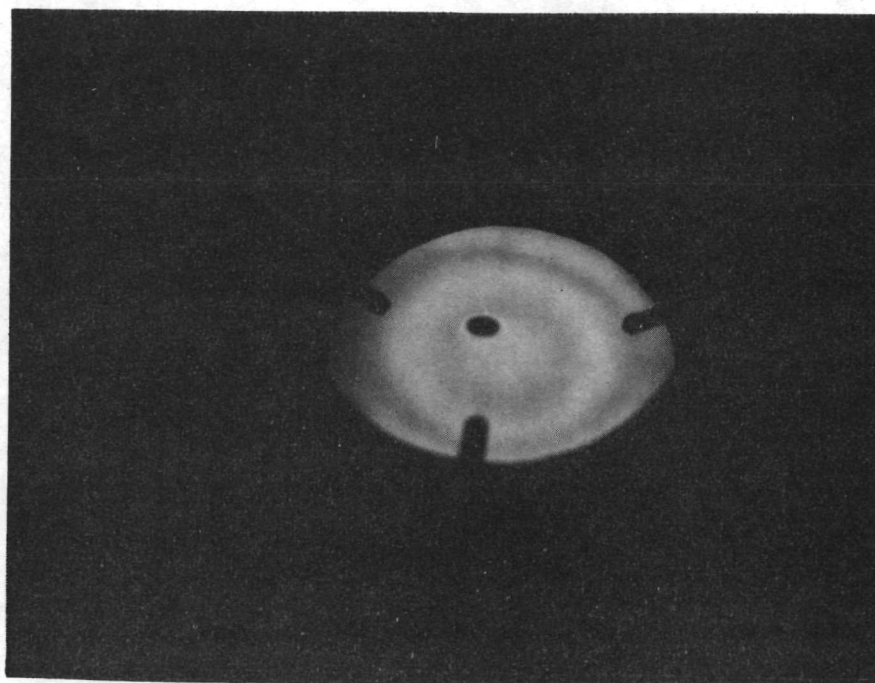
FIGURE 5.6-1    FLIGHT MODEL SCAN MIRROR

**OCLI** OPTICAL COATING LABORATORY, INC.

2789 Giffen Avenue
Santa Rosa, California
Telephone (707) 545-6440

SPECTRAL PERFORMANCE

| 14-9010-760 | GLASS | 0-100 |
| 6-P-7-1105-122 | WITNESS | PERCENT TRANS |
| | BECKMAN IR-4 | x PERCENT REFLECT. |
| | 2KSTO. SALT | |
| | 0.3u/min | ≈25°C | 45° |
| T.P.C. | 2 | B.E. | 6-7-71 |
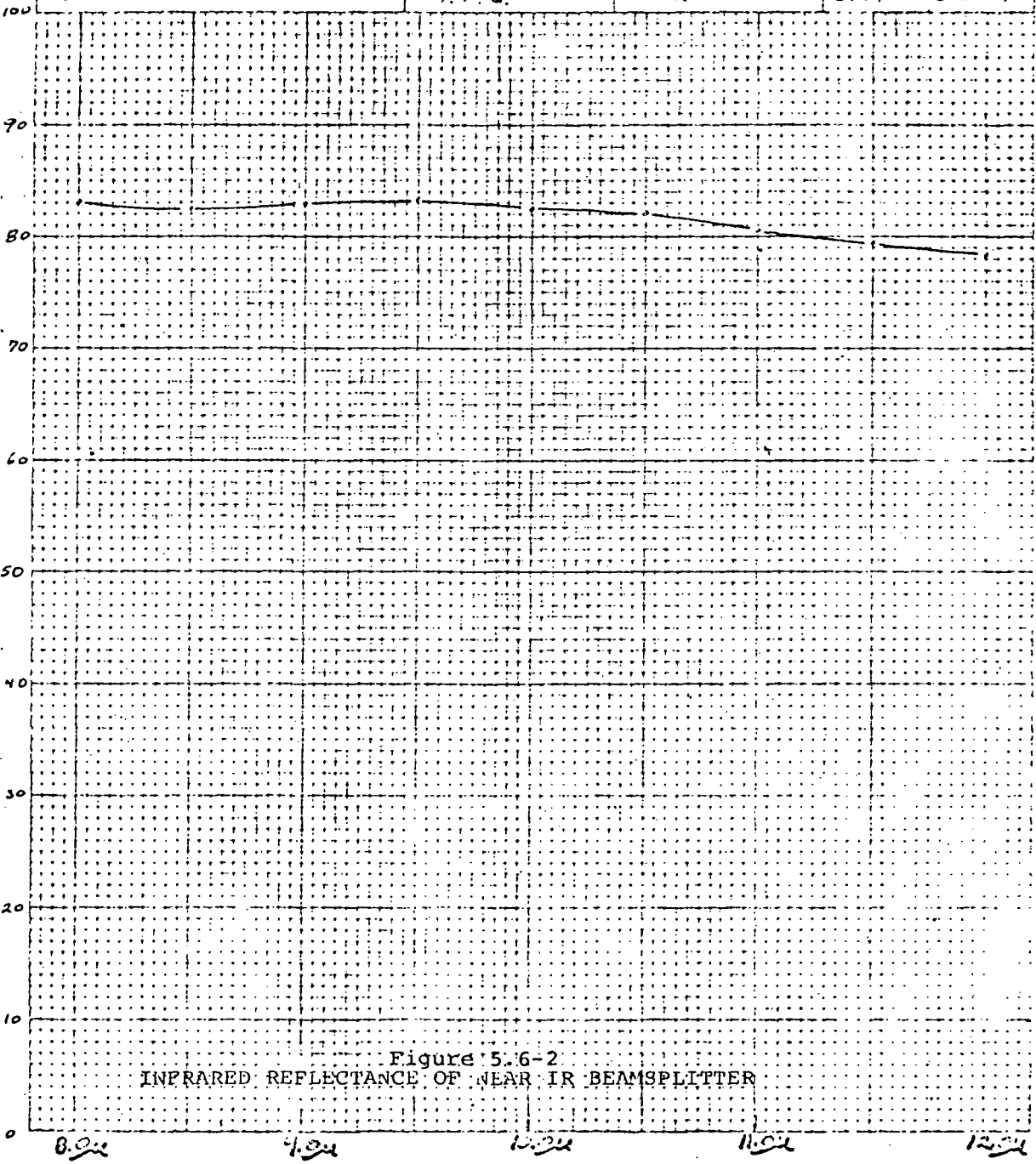


Figure 5.6-2
INFRARED REFLECTANCE OF NEAR IR BEAMSPLITTER
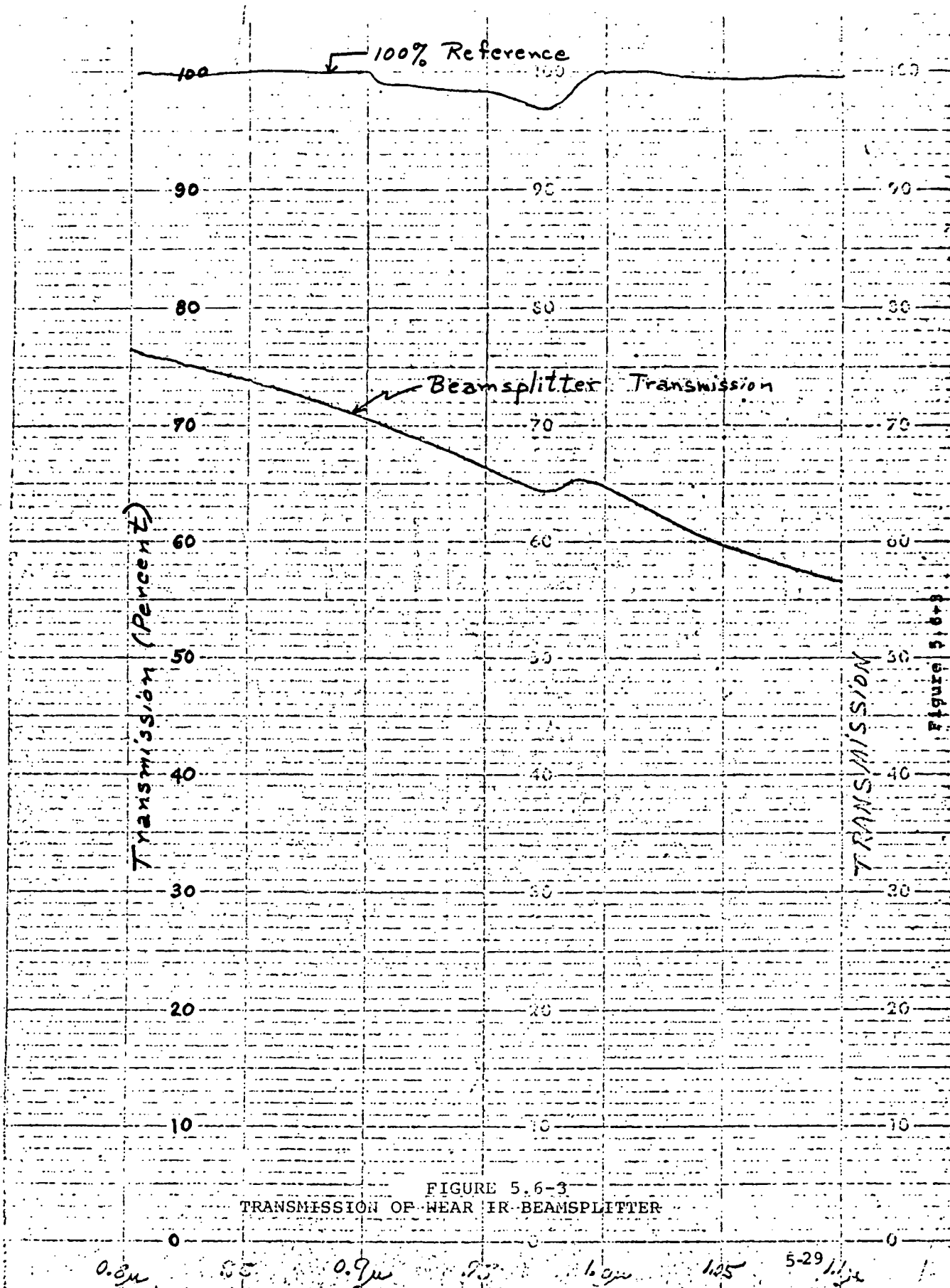
100% Reference

Beamsplitter Transmission

Transmission (Percent)

TRANSMISSION

FIGURE 5.6-3
TRANSMISSION OF NEAR IR BEAMSPLITTER

0.8μ          0.9μ          1.0μ     1.05     5-29 1.1μ

"Blocked Transmittance" Analysis

OPTICAL COATING
LABORATORY, INC.

Telephone (707) 545-6440

SPECTRAL PERFORMANCE

OCLI W/O
14-9057-760 GERMANIUM 45° ANGLE BLOCK & POLARIZER

6P-8-543-108 1.0" Ø WITNESS 0-100%

P/N 90934 IR-12 ☒

2.0 x STD. SLIT

S.N. → 1, 2, #3   20 CM¹/MIN.   ≈25°C   45°R

B/S   2.0   F.J.   6/18/71

% TRANSMITTANCE

10.2 μ

AVERAGE OF TWO
PLANES OF POLARIZATION

11.2 μ

100
90
80
70
60
50
40
30
20
10
0
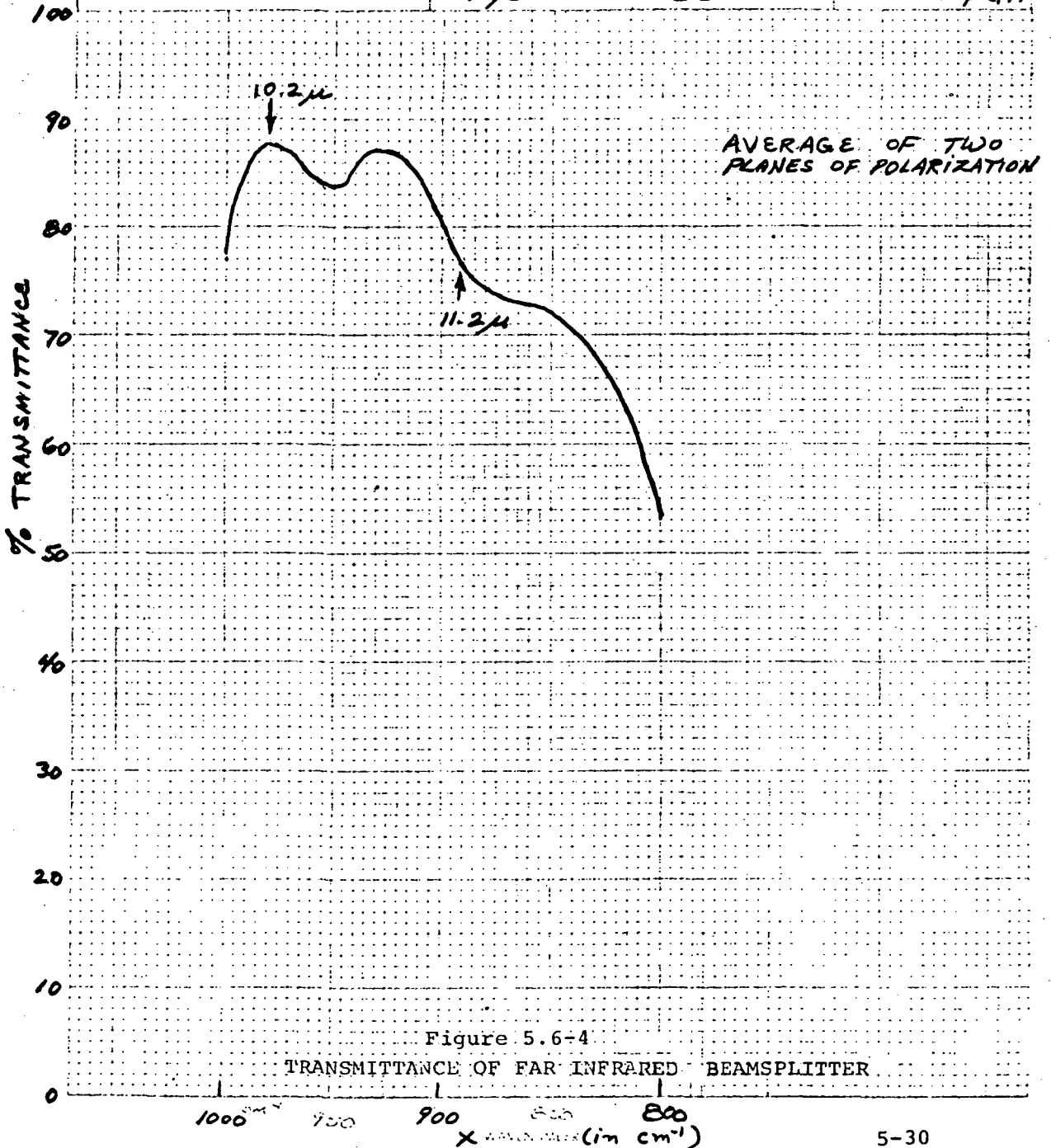
Figure 5.6-4

TRANSMITTANCE OF FAR INFRARED BEAMSPLITTER

1000   900   800

X   (in cm⁻¹)

5-30

"Black Tie" Project

OCLI W/O
14-9057-760 GERMANIUM

POLARIZER &
VARIABLE % FIXTURE

OPTICAL COATING
LABORATORY, INC.

6P8-543-10B
PN 8113926A
909304

CARY 90

o to 100.0%

X

SLIT: 6 cm⁻¹

SPECTRAL PERFORMANCE

S.N. 1, 2, & 3
B.S.

0.1 cm⁻¹/SEC  ≈25°C  45°
PERIOD: 10    RC   6/23/71

8.3µ

9.3µ

% REFLECTANCE

NOTE: Beam incident on the side opposite the system (yellow) dot.

Figure 5.6-5
REFLECTANCE OF FAR INFRARED BEAMSPLITTER

1250 CM-1        1200        1150        1100    1075

X                    (in cm⁻¹)
WAVELENGTH

5-31

FIGURE 5.6-6
TRANSMISSION OF 8.3-9.3µm BANDPASS FILTER

FIGURE 5.6-6
TRANSMISSION OF 8.3-9.3µm BANDPASS FILTER

SCANNED AT 100° Kelvin

1199.3 cm⁻¹
(8.35µ)

1081.0 cm⁻¹
(9.25µ)

1200.7 cm⁻¹
(8.33µ)

1075.7 cm⁻¹
(9.30µ)

SLOPE=1.46%

SLOPE=2.43%

TRANSMISSION ≤ 0.1%
AT 7.91µ AND BELOW.

TRANSMISSION ≤ 0.1%
AT 9.8µ AND ABOVE
TO 16.0µ

1215.5 cm⁻¹
(8.23µ)

1055.9 cm⁻¹
(9.47µ)

TRANSMISSION

PERCENT

1300    1200  λ(cm⁻¹) 1100    1000

DATA IDENTIFICATION

I.T.T. P/o # 3-922043
TYPE #1

SAMPLE IDENTIFICATION

S.F.
GERMANIUM

1.0" X 0.040"
WITNESS

INST. OPERATING PARAMETERS

☐ CARY 90    ☐ IR-12
☐ CARY 14    ☐ IR-4

TEST CONDITIONS

Date 11-6

FIGURE 5.6-6
TRANSMISSION OF 8.3-9.3μm BANDPASS FILTER

SCANNED AT 100° Kelvin

1199.3 cm⁻¹
(8.35μ)

1081.0 cm⁻¹
(9.25μ)

1200.7 cm⁻¹
(8.33μ)

1075.7 cm⁻¹
(9.30μ)

SLOPE=1.46%

SLOPE=2.43%

TRANSMISSION ≤ 0.1%
AT 7.91μ AND BELOW.

TRANSMISSION ≤ 0.1%
AT 9.8μ AND ABOVE
TO 16.0μ

1215.5 cm⁻¹
(8.23μ)

1055.9 cm⁻¹
(9.47μ)

1300    1200 ∂(cm⁻¹) 1100    1000

TRANSMISSION

PERCENT

100
90
80
70
60
50
40
30
20
10
5
0

DATA IDENTIFICATION

I.T.T P/S # 3-9 20043
TYPE #1

SAMPLE IDENTIFICATION
S.P.
GERMANIUM

10" x 0.040"
WITNESS

OPERATING PARAMETERS

CARY 90        IR-12
CARY 14        IR-9

TEST CONDITIONS

5-32

ALL POINTS TAKEN
ARE RATIOED TO
BACKGROUND

9875 cm⁻¹
(10.13μ)

910.7 cm⁻¹
(10.98μ)

AVE. IN-BAND TRANSMISSION
> 70%

989.6 cm⁻¹
(10.11μ)

901.0 cm⁻¹
(11.09μ)

SLOPE = 2.22%

SLOPE = 1.86%

0.1% Pt. @ 9.57μ

0.1% Pt. @ 11.67μ

1008.7 cm⁻¹
(9.91μ)

885.8 cm⁻¹
(11.29μ)
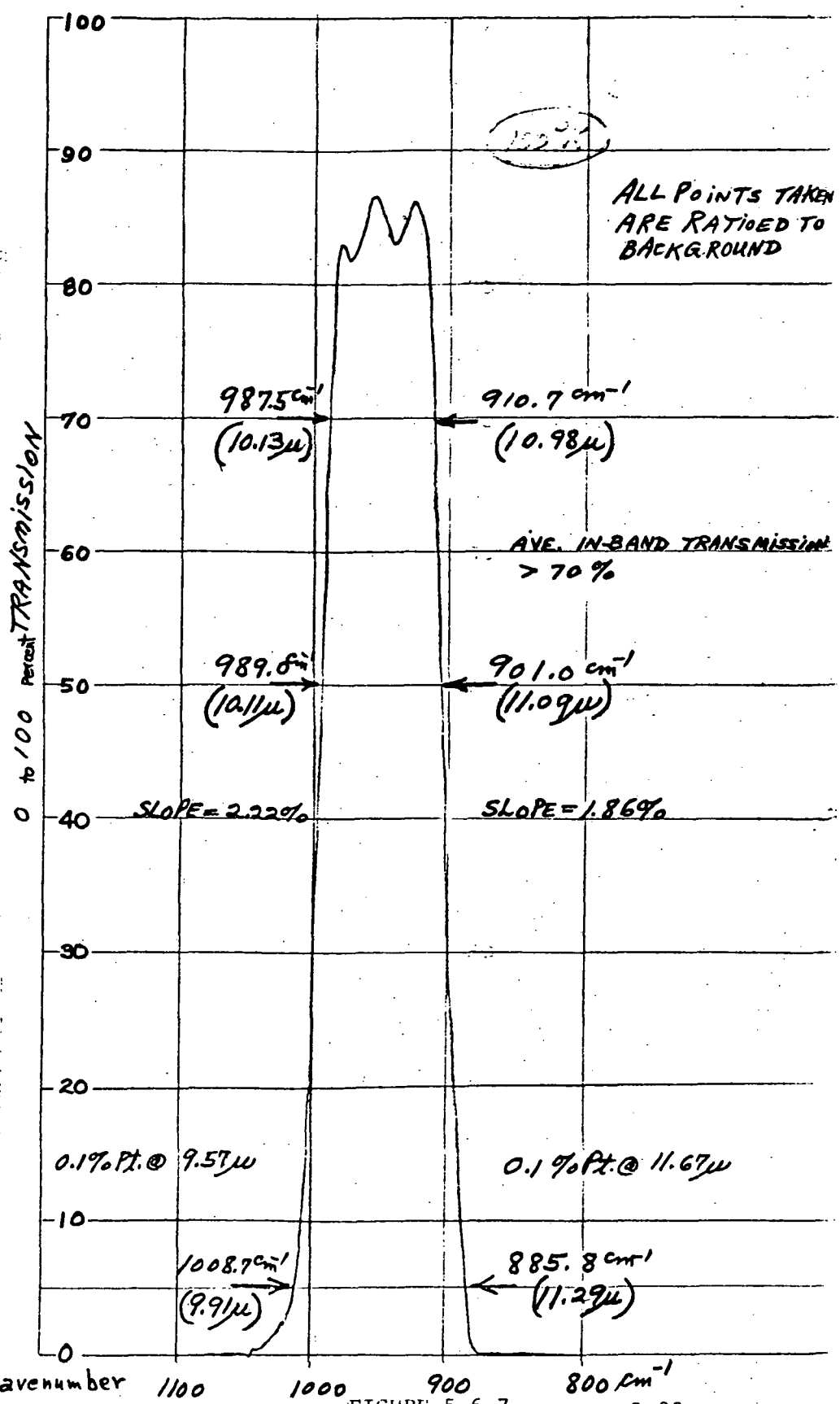
Wavenumber   1100      1000      900      800 cm⁻¹
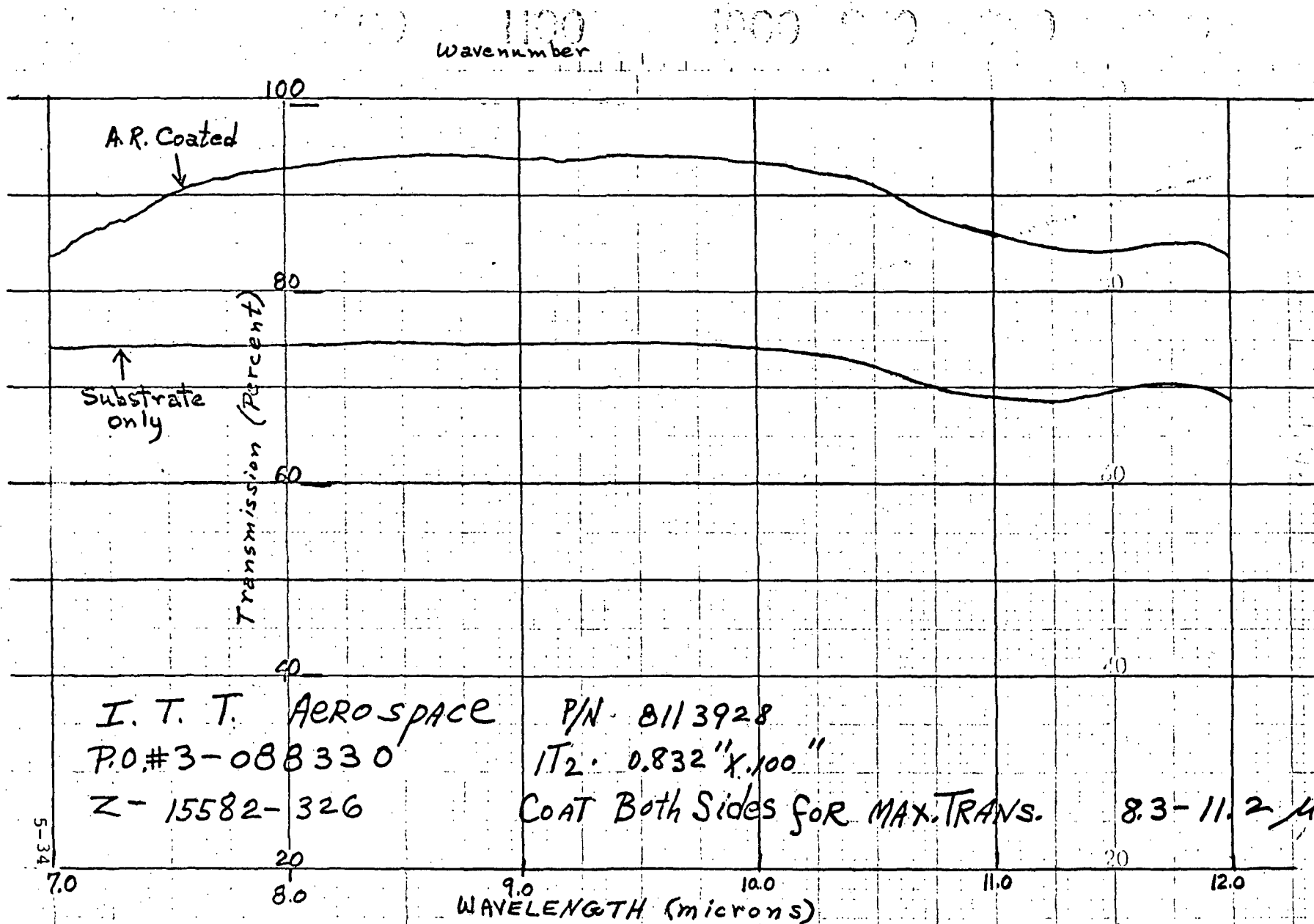
Percent TRANSMISSION    0 to 100

FIGURE 5.6-7

5-33

TRANSMISSION OF 10.2 - 11.2μm BANDPASS FILTER

Transmission of Antireflection Coated Irtran II Cooler Windows

Figure 5.6-8

## 5.6.6   Near Infrared Filter

The transmission of the near infrared filter, which is a long wave pass (LWP) filter, is given in Figure 5.6-9.

Transmission (Percent)

←814.6 mμ

←810.0 mμ

SLOPE = 2.38%

TRANSMISSION ≤ 0.1%
AT 764 mμ AND
BELOW TO 200 mμ.

TRANSMISSION OF
L.W.P. FILTER FOR
NEAR IR CHANNEL.

←795.7 mμ

Figure 5.6-9

WAVELENGTH (nanometers)

5-36
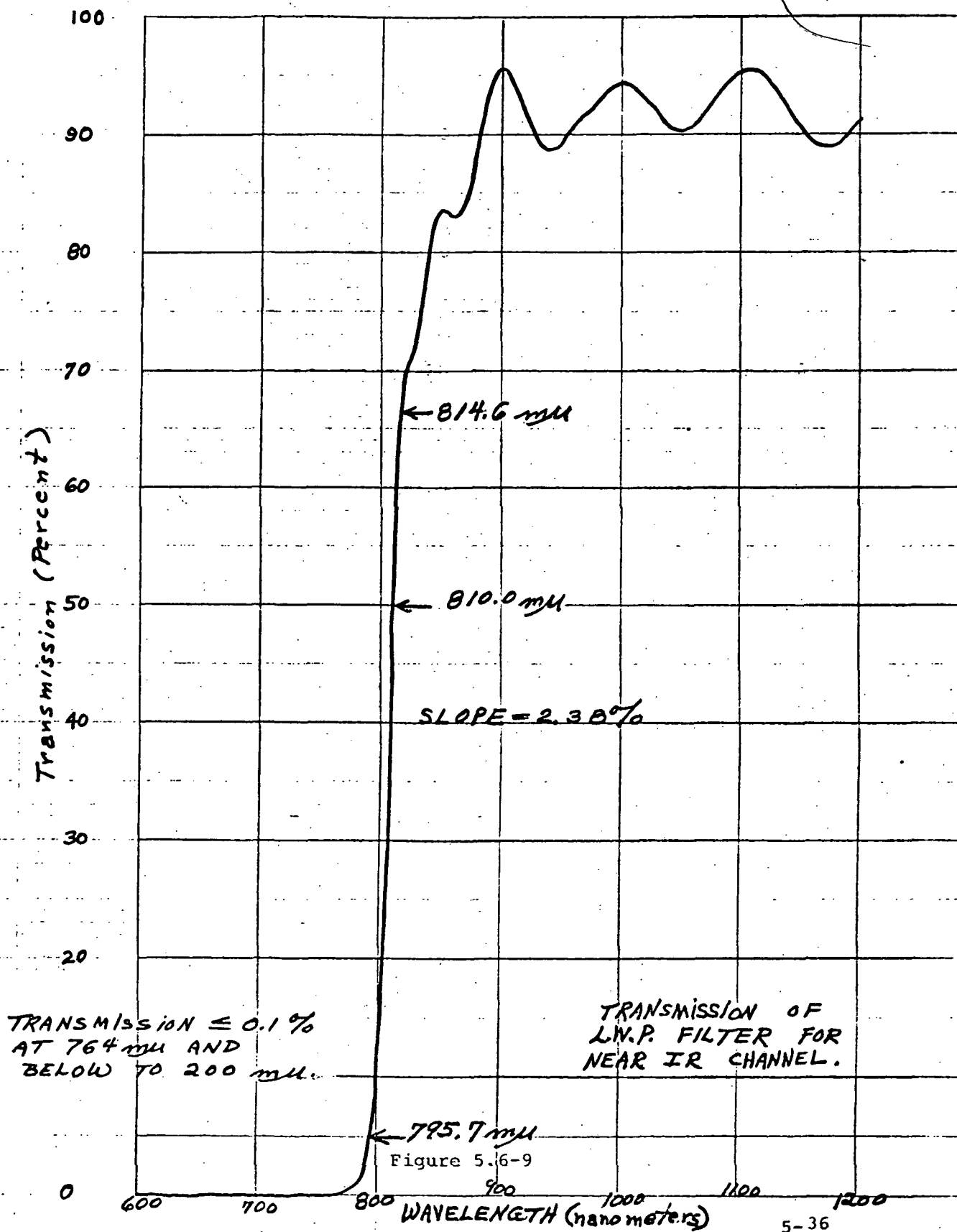
## 6.0   RADIANT COOLER DESIGN

The infrared detectors are cooled to the vicinity of 100K by means of a radiant cooler,  The conditions imposed by the spacecraft and its orbit in combination with additional mechanical and thermal constraints were used to establish a range of radiant cooler designs (Section 6.1).  Three examples from this range, including two modifications to one design (Section 6.2) were then analyzed in detail (Section 6.3).

The design of the radiant cooler used in the instrument is close to that of modification 2 to design IIIB.  The earth shield is modified to permit its use as a deployable cone mouth cover. The cover is used during launch to prevent the deposition of frost on the cone structure by delaying operation of the cooler until the bulk of spacecraft and instrument outgassing has taken place. It is also used to aid in the removal of frost accumulated after operation in orbit.

The patch has a view to cold space in the vertical plane of $28^o$ toward the earth (measure from the horizontal).  This permits operation at a minimum altitude of 925 km with a spacecraft wobble of $1^o$.  The view angle away from earth in the vertical plane is $48.8^o$ and in the horizontal plane, $\pm 52.0^o$.

## 6.1   Range of Designs

It is assumed that the radiant cooler has a rectangular geometry in which the patch normal (cone axis) is parallel to the orbit normal and the plane of the cone mouth is parallel to that of the patch.  To start with, a range of rectangular radiant cooler designs was subjected to a set of conditions or constraints.  The basic conditions are those inposed by the spacecraft and its orbit:

   a.   Minimum spacecraft altitude of 925 km.
   b.   Maximum orbit plane to earth-sun line angle of $12^o$.
   c.   Instrument temperature range of $25^o C \pm 25^o C$.

The specific requirements to be met by the radiant cooler design are:

   1.   Maximum view angle to cold space in the vertical plane through the centers of the patch and earth of $28^o$ toward the earth (includes $1^o$ for spacecraft wobble).
   2.   No direct sunlight in the cone mouth for sun angles from $0^o$ to $12^o$.
   3.   Maximum view angle to cold space in the vertical plane of $50^o$ away from the earth.
   4.   No more than one cone wall reflection to cold space for rays leaving the patch in the horizontal plane and away from earth in the vertical plane.

5. Minimum area at the patch opening (cone cross-section at the plane of the patch top) of 3.2 in$^2$.
6. Maximum cooler length of 10.6 inches.

The cooler is designed to operate at a minimum spacecraft altitude of 925 km; however, the thermal analysis was carried out at the nominal altitude of 1100 km.

Several initial designs of varying patch opening area and aspect ratio were studied; they are listed in Table 6.1-1.

Table 6.1-1

Range of Radiant Cooler Designs

Patch Opening

| Design | Width | Length | | |
|--------|-------|--------|-------|------|
|        |       | A      | B     | C    |
| I      | 0.80  | 4.00   | 4.375 |      |
| II     | 1.00  | 3.20   | 3.50  |      |
| III    | 1.20  | 2.66   | 2.92  | 3.17 |
| IV     | 1.40  | 2.28   | 2.50  |      |
| V      | 1.60  | 2.00   | 2.19  |      |
| Area of Opening (in$^2$) | | 3.2 | 3.5 | 3.8 |

All designs except IA, IB, and IIB met or very nearly met all the requirements. Designs IV and V were rejected because of their relatively large over-all vertical dimension and their reduced ratio of cone end area to cone mouth area. Designs IIA, IIIB, and IIIC were selected for detailed thermal analysis.

The exact geometry of radiant cooler design IIIB is shown in Figures 6.1-1, 6.1-2, and 6.1-3. The patch dimensions are those of the cone opening at the top of the patch and therefore include the cone-patch clearances. Similarly, the dimensions of the cone top (cone end and cone mouth) include the end-shield clearances.

To meet conditions (1) and (4), the upper vertical plane cone wall angle with respect to the patch normal (Figure 6.1-1) must be 31° or greater. The angle was set at the 31° minimum and various lower wall angles tried. At each lower wall angle, the cone length was adjusted to meet condition (1) and the design checked to see if it met condition (3). It was found that 10° is a good choice for the lower vertical cone wall angle. The
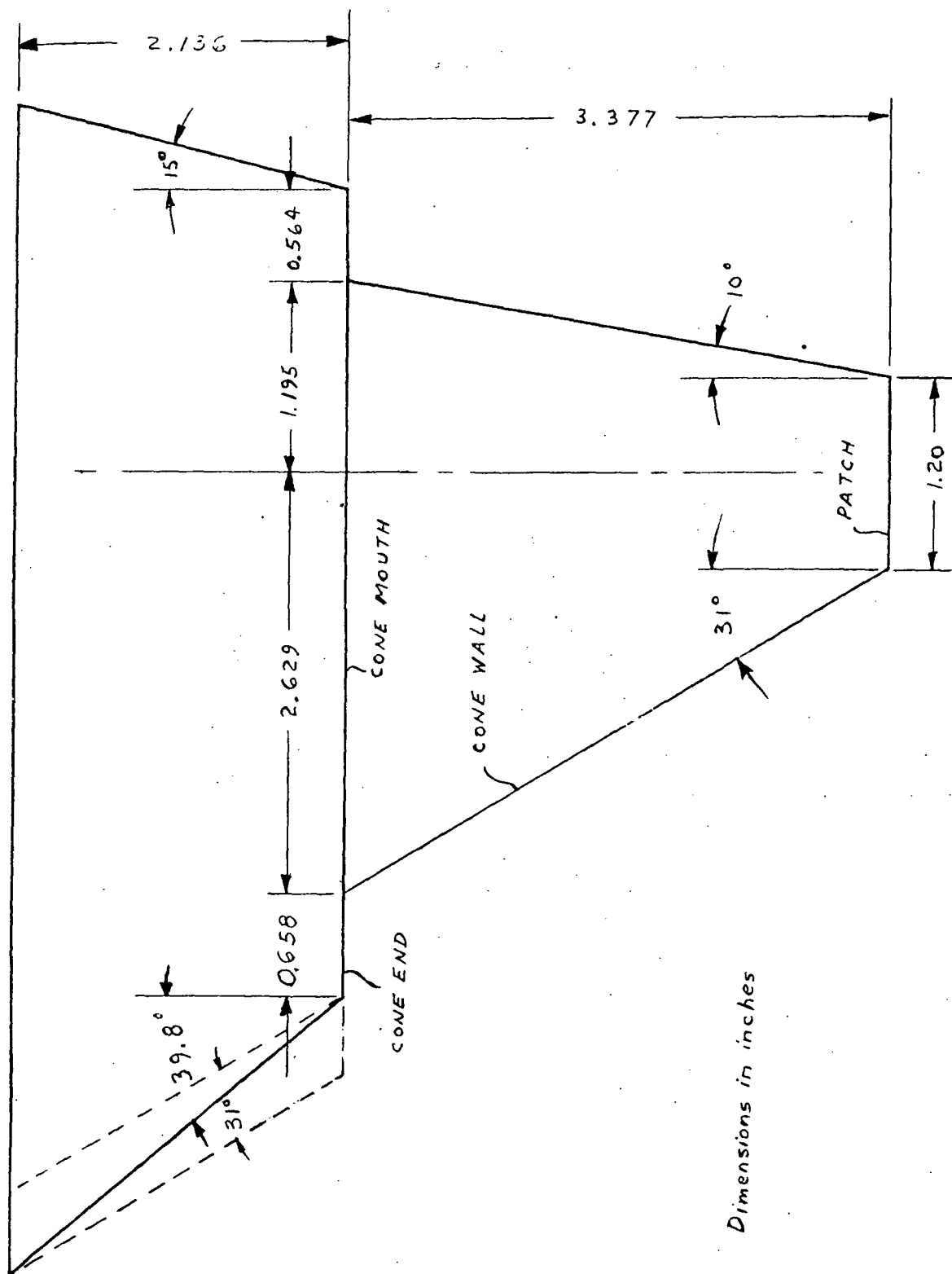
Figure 6.1-1 Vertical Plane of Design III B
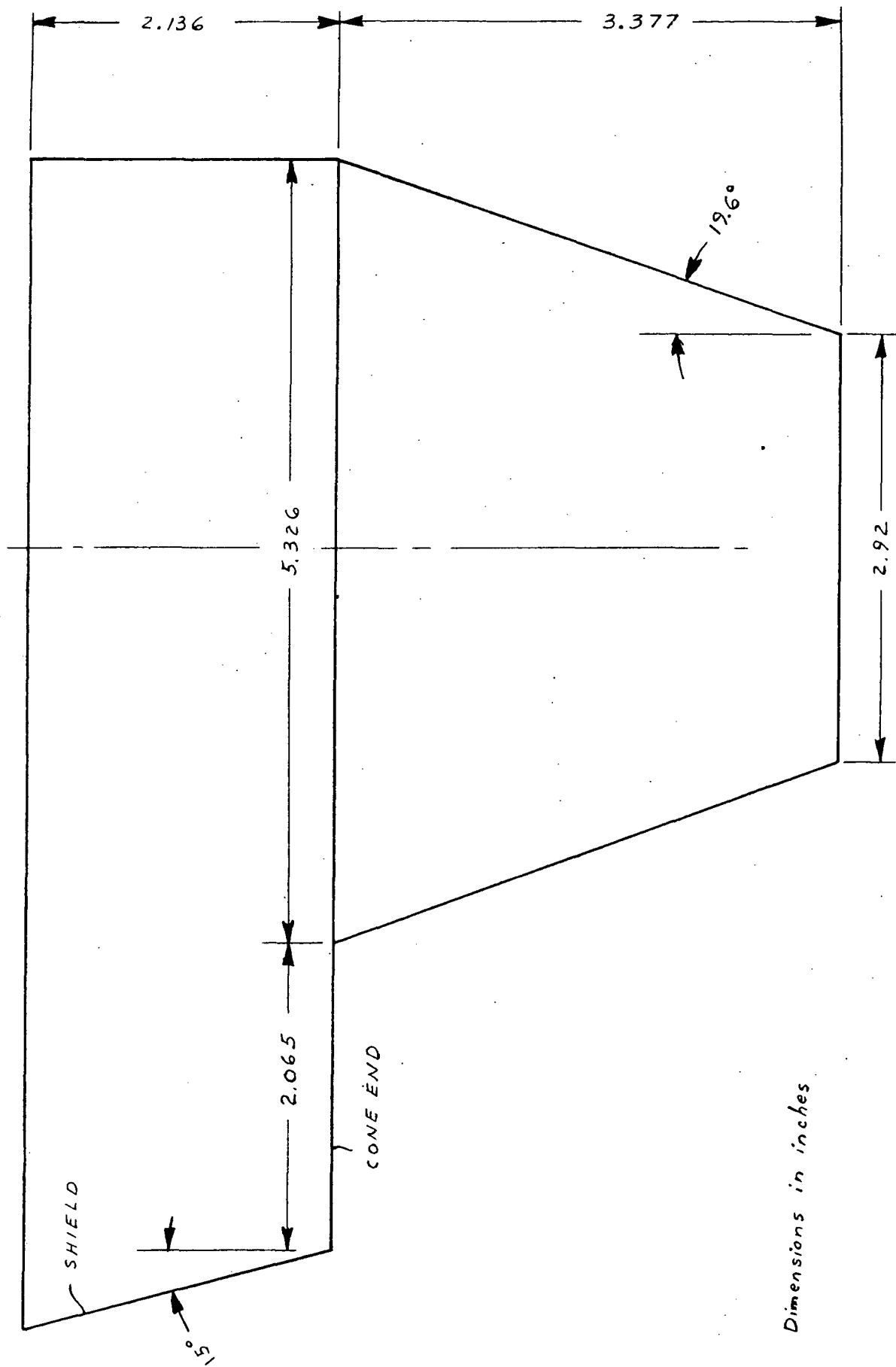
Figure 6.1-2  Horizontal Plane of Design III B
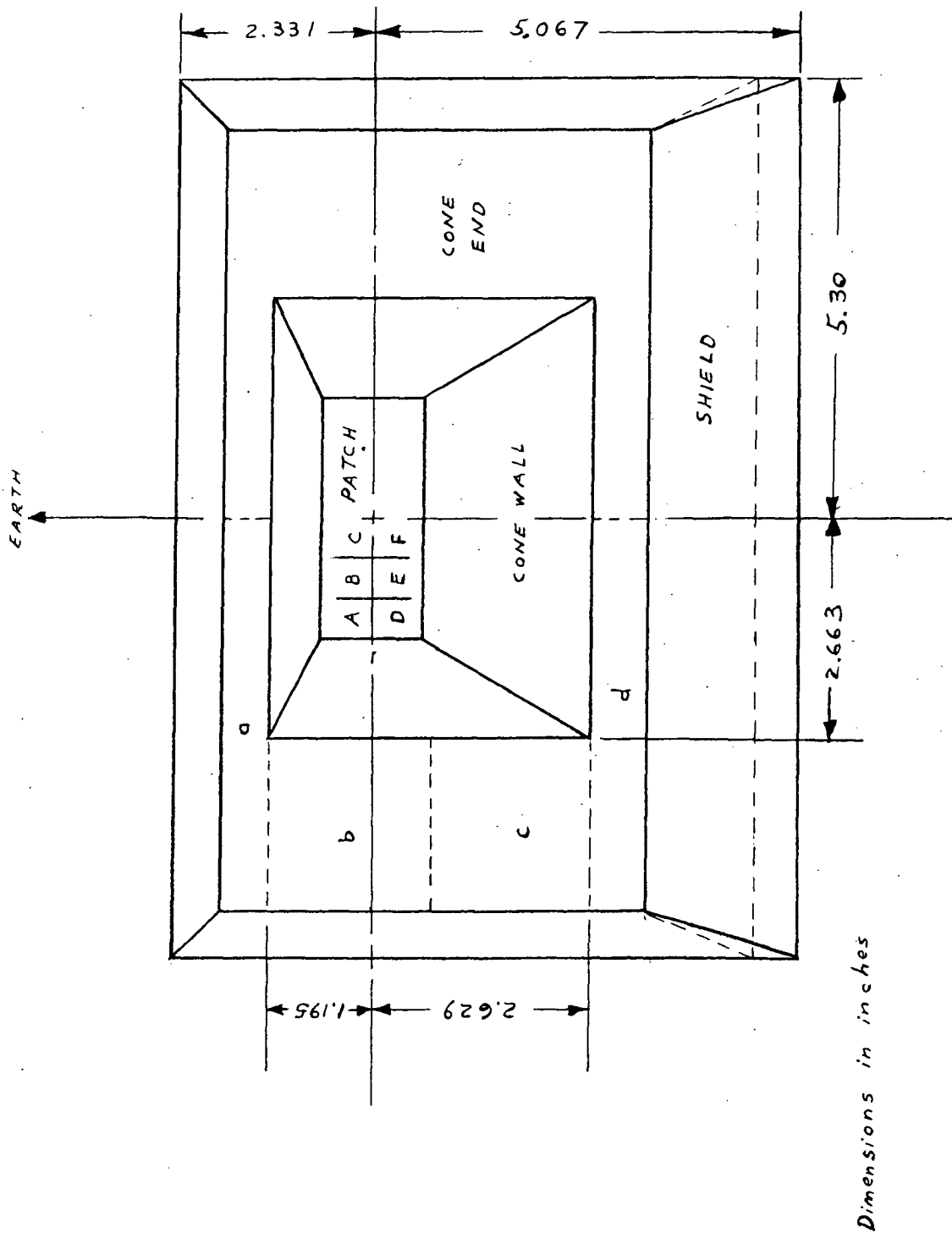
Figure 6.1-3  Top View of Design III B

maximum view angle to cold space away from earth in the vertical plane is then $48.8^\circ$. Because the constraints in the vertical plane are all angular in nature, all cone designs are the same in this plane except for a scale factor set by the selected patch width.

The wall angle in the horizontal plane was then determined by condition (4) that no more than one reflection be required for a horizontal patch ray to reach cold space

$$\tan \theta_H = \frac{-1 + \sqrt{3_a^2 + 1}}{3a} ,$$

where a is the ratio of cone length to patch length. The maximum cooler length (condition 6) and the requirement that the patch not see the shield then determine the height of the shield. The patch length and cone wall angle also determine the cone mouth dimension in the horizontal plane.

The position of the shield edges in the vertical plane are also set by the requirement that the patch not see the shield. The shield angle was set at $15^\circ$ in the horizontal plane and in the lower direction of the vertical plane. This reduces the influence of sunlight scattering off the shields at solar elevation angles (above the orbital plane) of $15^\circ$ and less. The shield angle in the upper vertical direction must be $31^\circ$ or greater to prevent the cone top from seeing the earth by reflection in the shield. The angle was set at $39.8^\circ$ in design IIIB. The values are $39.2^\circ$ and $40.3^\circ$ in designs IIA and IIIC, respectively. The larger than minimum shield wall angle reduces the radiative coupling between the shield and cone end and between the earth and cone end (assuming the cone end fills the space available for it). These reductions, however, are offset by a reduction in the size of the cone end area used to cool the cone. The prime reason for use of the larger angle is to provide clearance for the circuit boards mounted above the cooler.

## 6.2    Modifications to Design IIIB

Two modifications to the cone end and shield of design IIIB were studied, with the objective of improving thermal performance. In modification 1 (Figure 6.2-1), part of the cone end was tilted into the shield to reduce the radiative coupling to the earth. This change also eliminated solar exposure of the cone end at the $12^\circ$ elevation angle. The improvements, however, were offset by the increased radiative coupling to the shield and by the reduced cone end area (Section 6.3).

Figure 6.2-1 Modification 1 to Design III B

a & d, Flat elements of cone end

b & c, Tilted (15°) elements of cone end

As a result, modification 2 (Figure 6.2-2) was made. In this design, the shield on the earth side was extended to reduce the input from the earth, but the shield angle left unchanged to allow an increase in cone end area. The cooler length was maintained at 10.6 inches. This modification resulted in a significant improvement in thermal performance (Section 6.3) and will be incorporated into the final cooler design.

## 6.3    Thermal Analysis

The radiative transfer parameters calculated in Section 6.4 are applied below to the calculation of the cone and patch temperatures in the range of cooler designs described in Sections 6.1 and 6.2. The analysis is carried out for the anticipated ranges of housing temperature and sun angle. In addition, temperatures are determined for degraded values of thermal properties and for increased thermal loads on the patch.

For modification 2 of design IIIB, the cone temperature for no direct sunlight varies from 154.2K at a housing temperature of $0^\circ$C to 172.5K at $50^\circ$C. The corresponding patch temperatures ($T_p$) are 94.1K and 100.0K. Direct sunlight at the maximum expected elevation angle (above the orbital plane) of $12^\circ$ increase the cone temperature by only 0.5K ($\Delta T_p = 0.17K$). A degradation in the cone multilayer insulation by a factor of 0.8 increases the cone temperature by 3.9K. Combined with the same degradation in the patch insulation, the resultant increase in patch temperature is 1.7K. Doubling the solar absorptivity of the low $\alpha/\varepsilon$ cone end (to 0.30) increases the cone temperature by 1.1K ($\Delta T_p = 0.35K$). Increasing the infrared emissivity of the shield and cone wall from 0.05 to 0.07 increases the cone temperature by 3.9K and the patch temperature by 4.2K. The patch is heated not only by the warmer cone but also by the increased emission of the cone walls. If the input to the patch through the optical opening or by bias heating is increased by $1 \times 10^{-3}$W, the patch temperature increases by 2.1K.

Figure 6.2-2 Modification 2 to Design III B

### 6.3.1  Cone Temperature Range

The steady-state (equilibrium) thermal balance equation of the cone is:

$$\varepsilon_d \; \sigma T_c^{\,4} = \frac{1}{A_d} \; ( \; \Phi_e + \Phi_h + \Phi_s + \Phi_k + \Phi_i ),$$

where

$\varepsilon_d$ = emissivity of cone end

$A_d$ = area of cone end

$\Phi_e$ = input from earth

$\Phi_h$ = input from shield

$\Phi_s$ = input from direct sunlight

$\Phi_k$ = input through supports and leads

$\Phi_i$ = input through multilayer insulation

The radiative input from the earth is given by

$$H_e = \frac{\Phi e}{A_d} = ( \alpha_{me} W_r + \varepsilon_{me} W_e ) \frac{Am}{A_d} + ( \alpha_d W_r + \varepsilon_d W_e) \; Fde,$$

where

$\alpha_{me}$ = cone mouth absorptivity for earth reflected sunlight

$\varepsilon_{me}$ = cone mouth absorptivity for earth infrared

$W_r$ = average reflected sunlight exitance of earth

$W_e$ = average infrared exitance of earth

$A_m/A_d$ = ratio of cone mouth area to cone end area

$\alpha d$ = solar absorptivity of cone end

Fde = view factor from cone end to earth

The radiative input from the shield is given by

$$H_h = \frac{\Phi h}{A_d} = \varepsilon_d \; a_{dh} \; \sigma T_h^4$$

wnere $a_{dh}$ is the effective emissivity of the shield as seen from the cone end and $T_h$ the temperature of the shield ( instrument housing). The radiative input from direct sunlight is given by

$$Hs = \frac{\Phi_s}{A_d} = \alpha_d \; g_d \; S_o \sin \beta_s,$$

where

$g_d$ = average fraction of cone end area exposed to direct sunlight

$S_o$ = solar constant = $0.14$ W $cm^{-2}$

$\beta_s$ = elevation angle of sun above orbital plane

From Appendix I to the Final Report on Contract No. NAS5-10113 (Dec. 1967) we have

$$W_e = 2.1 \times 10^{-2} \; W \; cm^{-2}$$

$$W_r = \frac{1}{2\pi} \; S_o \; \cos \beta_s A \; \frac{\cos^2 \beta_e}{1 - \sin \beta_e},$$

Where A is the average solar reflection factor for the earth (0.4) and $\beta_e$ is the angle from the nadir to earth tangent line. At an altitude of 1100 km, $\beta_e$ is $58.5^{\circ}$, and

$$W_r = 1.65 \times 10^{-2} \; \cos \beta_s \; W \; cm^{-2}.$$

The coupling factors needed to complete the calculation of radiative inputs to the cone are given in Section 6.4.

The input from the instrument housing to the cone through mechanical supports and electrical leads is given by

$$K = K_c (T_h - T_c),$$

where $K_c$ is the thermal conductance between the housing and cone. $K_c$ is given by

$$K_c = \Sigma \frac{k_i A_i}{l_i}$$

where $k_i$ = thermal conductivity of connection i

$A_i$ = cross-sectional area of connection i

$l_i$ = length of connection i.

The supports and leads are listed in Table 6.3.1-1. The resultant thermal conductance is

$$K_c = 4.93 \times 10^{-4} \text{ W/K}.$$

Table 6.3.1-1

Cone Supports and Electrical Leads

| Length (inches) | Quantity to dia. (inch) | Material | k* |
|---|---|---|---|
| 3.50 | 2 supports ¼ X 3/16 | Synthane | $3.3 \times 10^{-3}$ |
| 1.50 | 2      "        " | " | " |
| 2.75 | 2      "        " | " | " |
| 2.75 | 4 Detectors $2 \times 10^{-3}$ | Ni | 0.78 |
| 2.75 | 2 C. Thermistor $3.3 \times 10^{-3}$ | Chromel | 0.13 |
| 2.75 | 2 P.    "        " | " | " |
| 3.50 | 2 C. Heater     " | " | " |
| 3.50 | 2 P.  "    $5.2 \times 10^{-3}$ | " | " |

* Thermal conductivity in W/cm. K

The input through the multilayer insulation may be considered entirely radiative (it is, in fact, a complex combination of radiative and conductive). The interchange between the housing and outer cone surface (wall and end) is reduced by the shielding factor $s_i$ of the insulation,

$$H_i = \frac{\Phi_i}{A_d} = \frac{\sigma A_i}{s_i A_d} (T_h^4 - T_c^4)$$

where $A_i$ is the area of the outer cone surface (Table 6.3.1-2).

<div align="center">

Table 6.3.1-2

Cone Surface Areas

</div>

| Design | $A_i$ | $A_d$ |
|--------|-------|-------|
| IIA | 100 | 25.40 |
| IIIB | 113 | 27.34 |
| IIIC | 111 | 26.03 |
| Mod. 1 IIIB | 110 | 24.41 |
| Mod. 2 IIIB | 120 | 34.48 |

<div align="center">

All in square inches

</div>

The cone temperatures of the various designs were first calculated for the following set of nominal radiative properties

$\varepsilon_h$ = infrared emissivity of shield = 0.05

$\varepsilon_c$ = infrared absorptivity of cone wall = 0.05

$\alpha_c$ = solar absorptivity of cone wall = 0.13 (Aluminum)

$\varepsilon_d$ = infrared emissivity of cone end = 0.85

$\alpha_d$ = solar absorptivity of cone end = 0.15

$s_i$ = shielding factor of cone insulation = 100*

The resultant cone temperatures are listed in Table 6.3.1-3 for no direct solar inputs and three values of housing temperature. The influence of direct sunlight at $12^o$ is shown in Table 6.3.1-4 for designs IIA, IIIB, and IIIC.

---

*In practice, a shielding factor of about 70 was realized. To obtain performance equivalent to a factor of 100, the cooler housing was thermally isolated from the main instrument structure and operated in the vicinity of $0^o$C.

## Table 6.3.1-3

### Cone Temperatures for Nominal Radiative Properties

|  | $T_c$ for $T_h$ equal to | | |
|---|---|---|---|
| Design | $0\,^\circ C$ | $25\,^\circ C$ | $50\,^\circ C$ |
| IIA | 166.7 | 174.3 | 182.6 |
| IIIB | 168.4 | 176.0 | 184.3 |
| IIIC | 169.6 | 177.2 | 185.5 |
| Mod. 1 IIIB | 170.0 | 178.2 | 187.4 |
| Mod. 2 IIIB | 154.2 | 163.1 | 172.5 |

Temperatures in kelvins; $\beta_s = 0^\circ$

## Table 6.3.1-4

### Cone Temperature for $12^\circ$ Sun Angle

| Design | $T_c$ | $\Delta T_c$ |
|---|---|---|
| IIA | 176.1 | 1.8 |
| IIIB | 176.5 | 0.5 |
| IIIC | 178.9 | 1.7 |

Temperatures in kelvins; $T_h = 25\,^\circ C$

The cone temperatures for degraded values of radiative properties are listed in Table 6.3.1-5 for design IIIB and its second modi-fication.  The increases listed are above the nominal values given in Table 6.3.1-3 at a housing temperature $T_h$ of $25\,^\circ C$.

## Table 6.3.1-5

### Cone Temperature For
### Degraded Thermal Properties

| Design | Insulation $s_i = 80$ | | Degraded Property Solar Absorptivity $\alpha_d = 0.30$ | | Infrared Absorptivity $\varepsilon_h = \varepsilon_c = 0.07$ | |
|---|---|---|---|---|---|---|
| | $T_c$ | $\Delta T_c$ | $T_c$ | $\Delta T_c$ | $T_c$ | $\Delta T_c$ |
| IIIB | 179.4 | 3.4 | 177.6 | 1.6 | 178.7 | 2.7 |
| Mod. 2 IIB | 167.0 | 3.9 | 164.2 | 1.1 | 167.0 | 3.9 |

Temperatures in kelvins; $T_h = 25^{\circ}C$ and $\beta_s = 0^{\circ}$.

## 6.3.2  Patch Temperature Range

The steady-state (equilibrium) thermal balance equation of the patch is

$$\Phi_p = \alpha A_p T_p^4 = \Phi_k + \Phi_r + \Phi_o + \Phi_j + \Phi_i,$$

where

$A_p$ = black radiating area of patch

$\Phi_k$ = input through supports, leads, and anti-frost enclosure

$\Phi_r$ = input from cone walls

$\Phi_o$ = input through optical opening

$\Phi_j$ = detector joule heating

$\Phi_i$ = input through multilayer insulation.

The mechanical supports and electrical leads are listed in Table 6.3.2-1.  They contribute an equivalent thermal conductance of

$$K_p = 4.62 \times 10^{-5} \text{ W/K}$$

when the effect of the support shields is included (HIRS for Nimbus F, Quarterly Report for July-Sept., 1972, NAS5-21651, Section 2.1.3.3).

### Table 6.3.2-1

### Conductive Couplings to the Patch

| Quantity | to | dia (inch) | Material |
|---|---|---|---|
| 2 | supports | 1/8 X 3/32 | Synthane |
| 4 | detectors | $2 \times 10^{-3}$ | Ni |
| 2 | p. thermistor | $3.3 \times 10^{-3}$ | Chromel |
| 2 | p. heater | $3.3 \times 10^{-3}$ | Chromel |

Supports and leads are all 4 inches long.

The radiative input from the low-emissivity cone walls above the black patch area is given by

$$\Phi_r = A_p \; \varepsilon_{pc} \; \sigma T_c^4$$

where $\varepsilon_{pc}$ is the effective patch-to-cone emissivity. The values of $\varepsilon_{pc}$ for the three cone designs and for two values of effective specular cone wall emissivity are given in Section 6.4.

The detector thermal input through the optical connection to the patch and the joule heating of the detectors is approximately

$$\Phi_o + \Phi_j = 2.8 \times 10^{-3} \text{ W}$$

The radiative input through the optical opening $(\Phi_o)$ is about $1.8 \times 10^{-3}$ W (Section 6.5). We have therefore allowed joule heating of $0.5 \times 10^{-3}$ W for each of the two detectors.

The multilayer insulation between the patch (back and side areas) has a nominal shielding factor of 200*. The areas covered are listed in Table 6.3.2-2 together with the black patch area $A_p$.

* Such a high value can be obtained only over very large areas. In fact the multilayer between the cone and patch was replaced by a gold-to-gold radiative decoupling to eliminate an outgassing source and to allow for the addition of $N_2$ gas purge. See Section 6.7.

## Table 6.3.2-2

### Patch Surface Areas

| Design | | $A_p$ | $A_{ip}$ |
|---|---|---|---|
| | IIA | 2.790 | 7.790 |
| | IIIB | 3.102 | 6.752 |
| | IIIC | 3.377 | 8.5895 |
| Mod. 1 | IIIB | 3.102 | 6.752 |
| Mod. 2 | IIIB | 3.102 | 6.752 |

All in square inches; the patches are 0.625 inch thick.

The patch temperatures of the various designs were first calculated for a nominal cone wall emissivity $\varepsilon_c$ of 0.05 and the above shielding factor for patch insulation. The results are listed in Table 6.3.2-3 for no direct sunlight on the cone and three values of housing temperature. The corresponding cone temperatures are given in Table 6.3.1-3.

## Table 6.3.2-3

### Patch Temperatures for Nominal Radiative Properties

| | Design | $0^o$ | $25^oC$ | $50^oC$ |
|---|---|---|---|---|
| | | | | |
| | IIA | 99.9 | 102.5 | 105.4 |
| | IIIB | 98.6 | 101.2 | 104.0 |
| | IIIC | 98.25 | 100.9 | 103.8 |
| Mod. 1 | IIIB | 99.2 | 101.9 | 105.1 |
| Mod. 2 | IIIB | 94.1 | 96.9 | 100.0 |

$T_p$ for $T_h$ equal to (column headers: $0^o$, $25^oC$, $50^oC$)

Temperature in kelvins; $\beta_s = 0^o$

The influence of direct sunlight at $12^o$ is shown in Table 6.3.2-4 for designs IIA, IIIB, and IIIC. The corresponding cone temperatures are listed in Table 6.3.1-4.

Table 6.3.2-4

### Patch Temperatures for $12^{\circ}$ Sun Angle

| Design | $T_p$ | $\Delta T_p$ |
|--------|-------|--------------|
| IIA | 103.1 | 0.6 |
| IIIB | 101.3 | 0.17 |
| IIIC | 101.5 | 0.6 |

Temperatures in kelvins; $T_h = 25^{\circ}C$.

The patch temperatures for degraded values of radiative properties are listed in Table 6.3.2-5 for design IIIB and its second modification. The corresponding cone temperatures are listed in Table 6.3.1-5.

Table 6.3.2-5

### Patch Temperatures for Degraded Thermal Properties

| Design | Insulation | Degraded Property Solar Absorptivity | Infrared Emissivity |
|--------|-----------|--------------------------------------|---------------------|
| | $S_i$ (Patch) = 160 | $\alpha_d = 0.30$ | $\varepsilon_h = \varepsilon_c = 0.07$ |
| | $S_i$ (Cone) = 80 | | |

| Design | $T_p$ | $\Delta T_p$ | $T_p$ | $\Delta T_p$ | $T_p$ | $\Delta T_p$ |
|--------|-------|--------------|-------|--------------|-------|--------------|
| IIIB | 102.9 | 1.7 | 101.7 | 0.5 | 105.5 | 4.3 |
| Mod. 2 IIIB | 98.6 | 1.7 | 97.25 | 0.35 | 101.1 | 4.2 |

Temperatures in kelvins; $T_h = 25^{\circ}C$ and $\beta_s = 0^{\circ}$

The patch temperatures for an increased bias heating (or increased rediative input through the optical opening) are given in Table 6.3.2-6. The increase of $1 \times 10^{-3}$ W would enable each detector to operate at a bias level of $1 \times 10^{-3}$ W.

## Table 6.3.2-6

### Patch Temperature for Increased Bias

| Design | $T_p$ | $\Delta T_p$ |
|---|---|---|
| IIIB | 103.05 | 1.85 |
| Mod. 2 IIIB | 99.00 | 2.1 |

$\Phi_o + \Phi_j = 3.8 \times 10^{-3}$ W; temperatures in kelvins.

In addition to thermal inputs considered above, the patch has a very small view of a solar panel. A representative situation is analyzed in Section 3.3 of Part I to the Final Report on Contract NAS5-11683 (8 April-31 Oct. 1969). The thermal input is shown to be approximately $0.3 \times 10^{-3}$ W and the increase in patch temperature, 0.6K.

## 6.4 Radiative Coupling Factors

The radiative coupling factors within the cooler and between the cooler and external sources were evaluated by means of the specular image array and contour integral techniques described in the Final Report on Contract No. NAS5-11603 (Part II 8 April-15 December 1969) and in Applied Optics for January 1970 (p. 185). First it is necessary to calculate several view factors (The fraction of power diffusely emitted from one area that directly strikes a second area is the view factor from the first area to the second). The view factors required for thermal analysis of the radiant cooler are:

a. $F_{p-m}(n)$ = view factor from the patch to the cone mouth images seen by n specular reflections in the cone walls.

b. $F_{d-h}(n)$ = view factor from the cone end to the shield mouth images seen by n specular reflections in the shield wall.

c. $F_{d-e}$ = view factor from the cone end to the visible region of the earth.

d. $F_{m-e}(n)$ = view factor from the cone mouth to the visible region of the earth whose radiation is reflected n times in the cone walls.

The view factors (a) are used to determine the patch-cone radiative coupling factor or effective patch-to-cone emissivity. (Final Report on Contract NAS5-10113, December 1967, Section 1.3).

$$\varepsilon_{pc} = 1 - \Sigma_n \, F_{p-m}(n) \, (1 - \varepsilon_c)^n,$$

where $\varepsilon_c$ is the emissivity of the cone walls and the patch is black (emissivity of one).

The view factors (b) are used to determine the effective emissivity of the shield as seen from the cone end (equal to the effective absorptivity of the shield for cone end radiation),

$$a_{dh} = \Sigma_n \quad a_n \, F_{d-h(n)},$$

where $a_n$ is the emissivity (absorptivity) produced by n shield wall reflections. For infrared radiation, $a_n = 1 - (1 - \varepsilon_h)^n$, where $\varepsilon_h$ is the infrared absorptivity (emissivity) of the shield walls. Using the conservation condition

$$\Sigma F_{d-h(n)} = 1,$$

the above may also be written as

$$a_{dh} = 1 - \Sigma F_{d-h(n)} \, (1 - \varepsilon_h)^n.$$

The cone end-shield radiative coupling factor or effective emissivity is obtained by multiplying $a_{dh}$ by the emissivity $\varepsilon_d$ of the cone end. This is the case because radiation leaving the cone end by emission or reflection never returns when the shield walls are specularly reflecting and outward sloping (a condition which also holds between the patch and cone walls).

The view factors (c) and (d) are used to determine the absorptivity of the cone end and cone mouth, respectively, for radiation from the earth. In the case of the cone mouth, multiple reflections at the cone walls must be taken into account. The effective absorptivity for earth radiation is then

$$a_{me} = \Sigma a_n \, F_{m-e}(n),$$

wher $a_n$ is the absorptivity produced by n cone wall reflections. For infrared from the earth, $a_n = 1 - (1 - \varepsilon_c)^n$ and for reflected sunlight, $a_n = 1 - (1 - \alpha_c)^n$, where $\varepsilon_c$ and $\alpha_c$ are the infrared absorptivity (emissivity) and solar absorptivity, respectively.

The radiative view factors and radiative coupling factors are listed in Tables 6.4-1 through 6.4-3 for cooler designs IIA, IIIB, and IIIC, including the modifications to IIIB. For purposes of calculating the view factors, the patch was divided into 12 equal elements, and the cone end (bib) into 8 unequal elements. By symmetry, there are 6 different view factors from the patch elements and 4 different view factors from the cone end elements (See Figure 6.1-3). Values of $\varepsilon_{pc}$ are shown for two values of effective specular cone wall emissivity $\varepsilon_c$, 0.07 and 0.05. Values of $a_{dh}$ and $\varepsilon_{me}$ (infrared value of $a_{me}$) are shown for a cone wall

6-20

and shield wall infrared absorptivity of 0.05. Values of $\alpha_{me}$ (reflected sunlight value of $a_{me}$) are shown for cone wall solar absorptivities of 0.22 (gold) and 0.13 (aluminum). Coupling factors to the earth are from the nominal altitude of 1100 km.

<div align="center">Table 6.4-1</div>

<div align="center">Cone-Patch Coupling Factors*</div>

| Design | $F_{p-m}(o)$ | $F_{p-m}(1)$ | $F_{p-m}(2)$ | $\epsilon_{pc}$ (0.07) | $(\epsilon_c)$ (0.05) |
|--------|------------|------------|------------|---------|---------|
| IIA | 0.3196 | 0.5083 | 0.1721 | 0.0588 | 0.0422 |
| IIIB | 0.3231 | 0.5078 | 0.1691 | 0.0584 | 0.0419 |
| IIIC | 0.3271 | 0.5050 | 0.1679 | 0.0580 | 0.0416 |

<div align="center">* Results neglect very small $F_{p-m}(3)$</div>

<div align="center">Table 6.4-2</div>

<div align="center">Cone-End (Bib) Coupling Factors</div>

| Design | $F_{de}$ | $a_{dh}$ (0.05) | $A_d/A_m$* |
|--------|---------|---------|---------|
| IIA | 0.0779 | 0.0161 | 1.61 |
| IIIB | 0.0787 | 0.0167 | 1.34 |
| IIIC | 0.0809 | 0.0162 | 1.24 |
| Mod. 1 IIIB | 0.0587 | 0.0219 | 1.20 |
| Mod. 2 IIIB | 0.0403 | 0.0189 | 1.69 |

<div align="center">* Ratio of cone end to cone mouth area</div>

## Table 6.4-3

### Cone Mouth Coupling Factors

| Design | $\varepsilon_{me}$ (0.05) | $\alpha_{me}$ (0.22) | $\alpha_{me}$ (0.13) | $F_{me}$* |
|---|---|---|---|---|
| IIA | $8.40 \times 10^{-3}$ | $3.38 \times 10^{-2}$ | $2.09 \times 10^{-2}$ | 0.0935 |
| IIIB | $9.28 \times 10^{-3}$ | $3.71 \times 10^{-2}$ | $2.31 \times 10^{-2}$ | 0.1014 |
| IIIC | $9.19 \times 10^{-3}$ | $3.71 \times 10^{-2}$ | $2.30 \times 10^{-2}$ | 0.1063 |
| Mod. 1 IIIB | $9.28 \times 10^{-3}$ | $3.71 \times 10^{-2}$ | $2.31 \times 10^{-2}$ | 0.1014 |
| Mod. 2 IIIB | $4.43 \times 10^{-3}$ | $1.725 \times 10^{-2}$ | $1.09 \times 10^{-2}$ | 0.0403 |

*From cone mouth center

An example of the specular image array technique used to determine view factors is shown in Figure 6.4-1. The boundaries of the shield and cone mouth images (formed by reflection in the cone walls) are projected onto the equivalent earth disk (H.C. Hottel and A.F. Sarofim, Radiative Transfer, McGraw-Hill, 1967, p. 65). The view is from the center of the cone mouth in Design IIIB. The projections divide the earth into regions whose radiation requires from 1 to 3 cone wall reflections to leave the cone or whose radiation is blocked by the shield.

The radiant cooler will also be exposed to direct sunlight during part of the year. The shield is designed to shade the cone mouth up to the maximum expected solar elevation angle of $12^{o}$ above the orbital plane. As a result, we need to consider only the direct solar irradiance of the low $\alpha/\varepsilon$ cone end. Because of the large thermal time constant of the cone structure, the influence of direct sunlight is averaged over an orbital period. The average fraction of cone end area exposed over an orbit (the solar exposure factor) is given by

$$g_d = \frac{1}{\pi} \int_o^\pi g_d (\varphi_s) \, d\varphi_s,$$

where $g_d (\varphi_s)$ is the fraction of exposed area at a solar azimuth angle $\varphi_s$.

The variations of $g_d (\varphi_s)$ with $\varphi_s$ are given in Figures 6.4-2 through 6.4-4, for designs IIA, IIIB, and IIIC, respectively. The $\varphi_s = 0^{o}$ point is when the spacecraft, earth, and sun are in line in that order. The earth shades the spacecraft from direct sunlight from $0^{o}$ to $58.5^{o}$. It is seen that the maximum exposure at the $12^{o}$ solar elevation angle is less than 9% of the end area for design IIIB.

(N) = number of cone wall reflections

Images and shield edge projected as to plane of earth disk
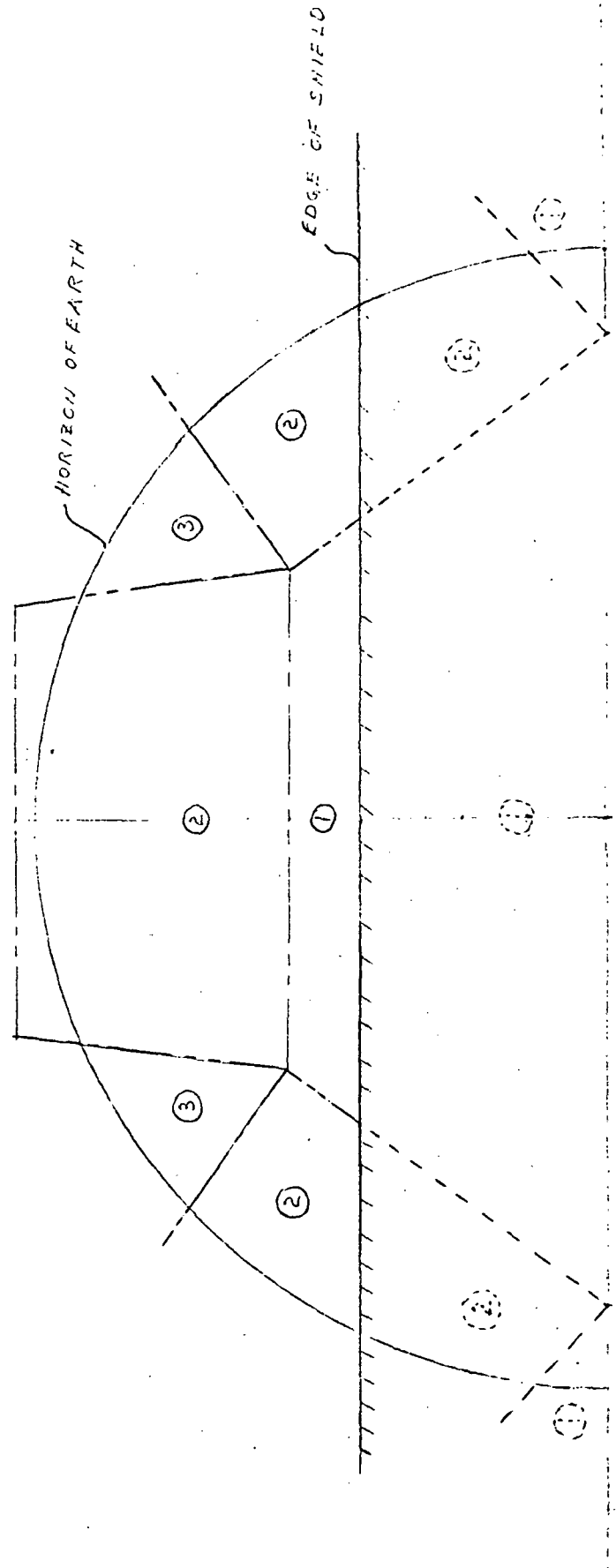
Figure 6.4-1 Equivalent Earth for Cone Wall Absorption
as seen from Cone Mouth Center (Design III B)

6-23

Figure 6.4-2

Figure 6.4-3

SOLAR ELEVATION = 12°

$g(\varphi_s)$

$\varphi_s$

IN SHADOW
OF EARTH

6-25

Figure 6.4-4

SOLAR ELEVATION = 12°

IN SHADOW
OF EARTH

$g(\varphi_s)$

$\varphi_s$

6-26
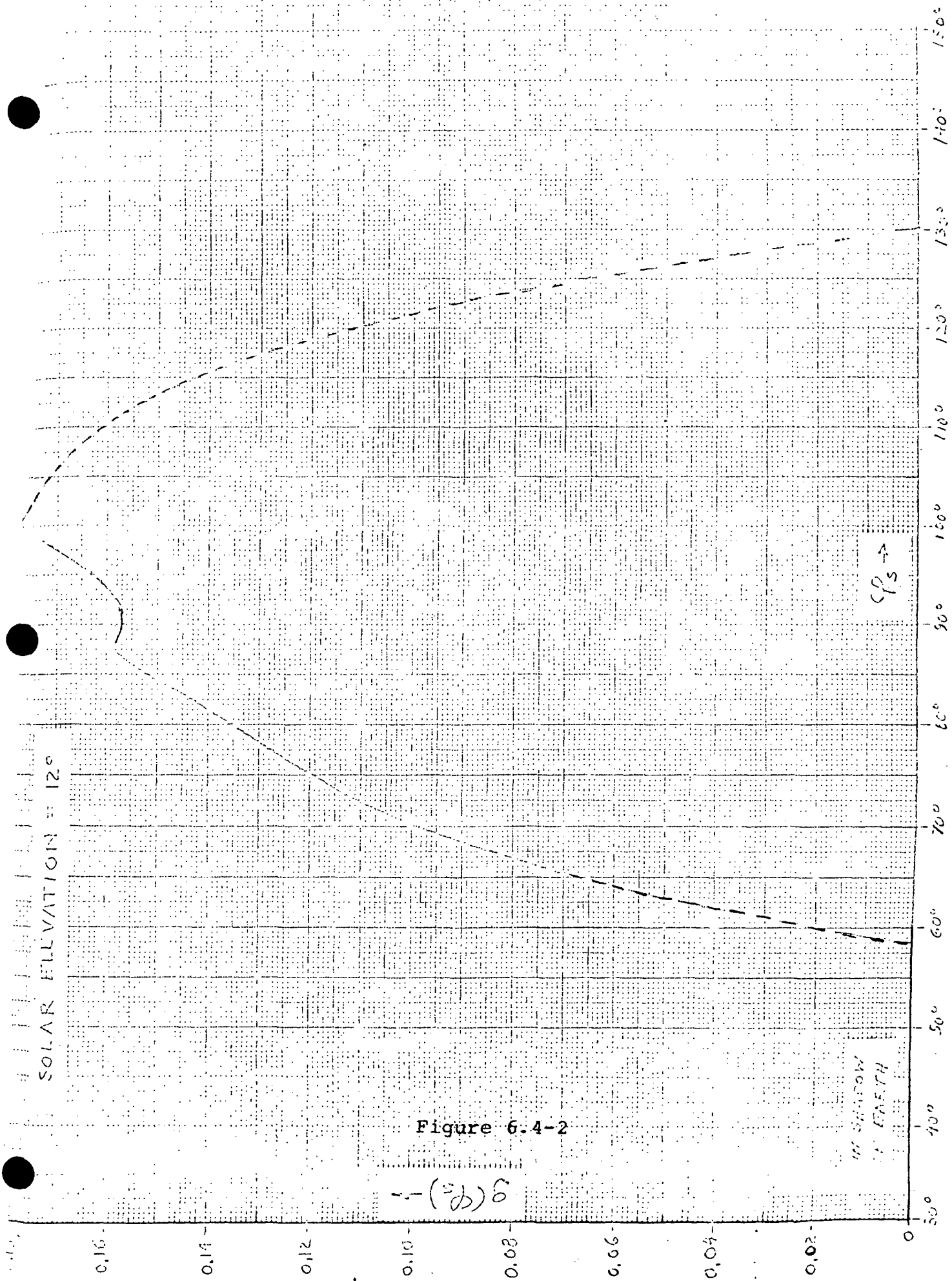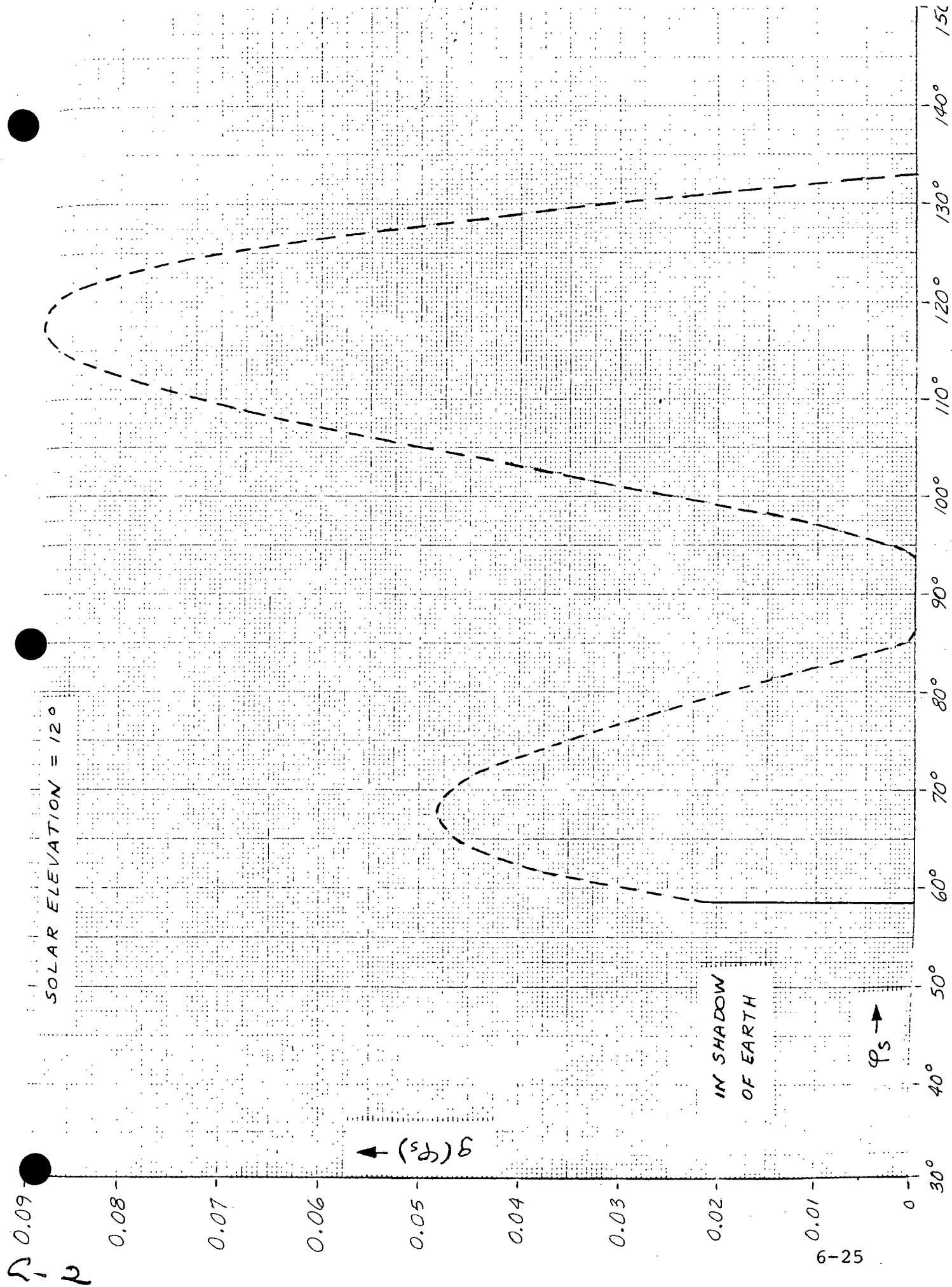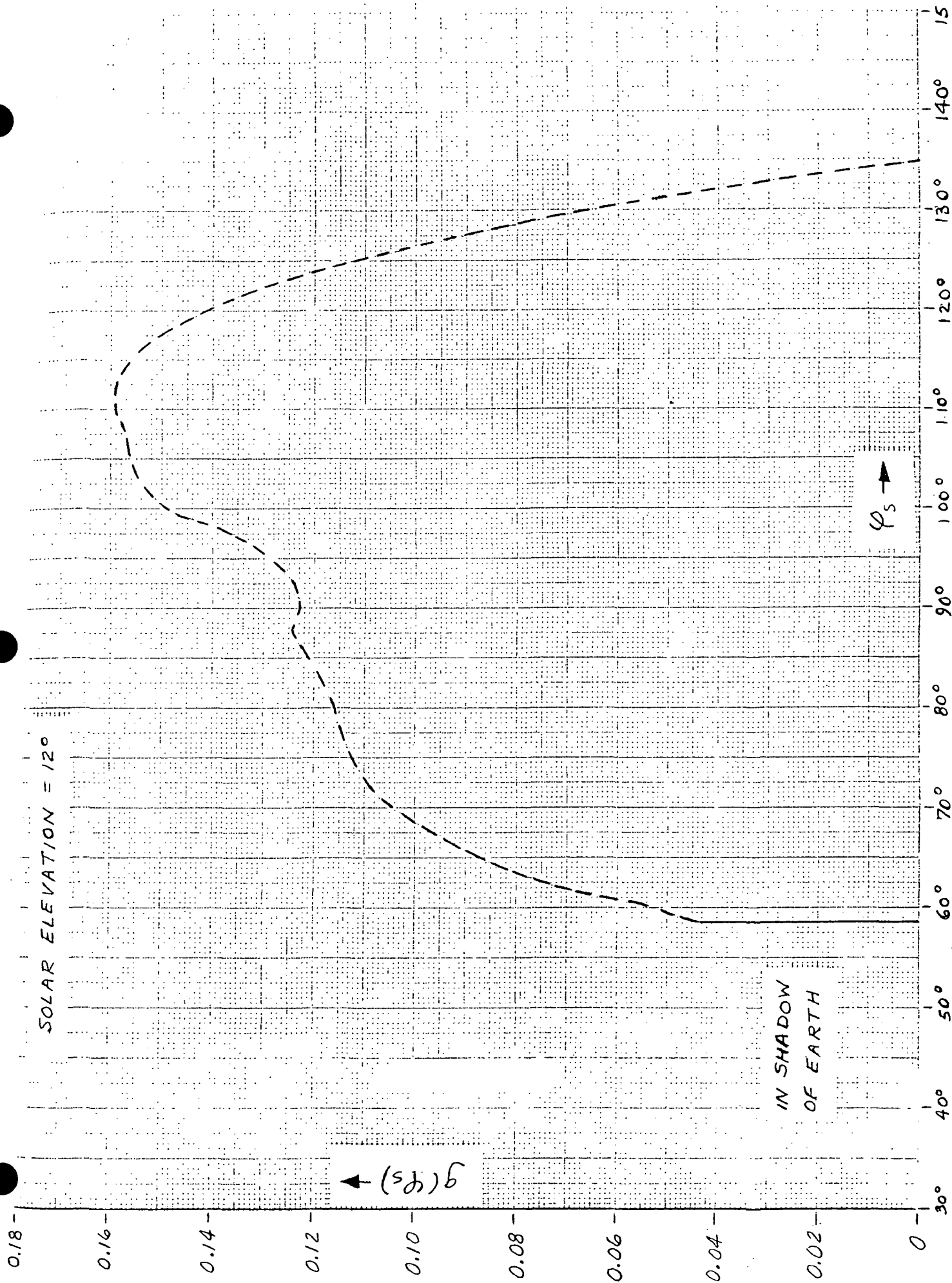
Integration of the curves yields the solar exposure factors
listed in Table 6.4-4.

Table 6.4-4

Solar Exposure Factor at 12$^{\circ}$ Sun Angle
(Cone End)

| Design | $g_d$ |
|--------|-------|
| IIA | $4.89 \times 10^{-2}$ |
| IIIB | $1.66 \times 10^{-2}$ |
| IIIC | $4.98 \times 10^{-2}$ |

6.5    Radiative Input through Optical Openings to Patch

The magnitude of the radiative input ($\Phi_O$) to the patch
through the optical openings depends on the optical and mechanical
design of the instrument.  To maintain accurate positioning of
the detector with respect to the optics, the last lens is mounted
in the patch with the detector element.  Use of an aplantic lens
in this position allows an increase in the speed of the optical
beam by a factor equal to the refractive index of the lens material
(4 in the case of germanium).  The speed of the beam striking the
aplanatic element is then relatively low and allows the placement
of the spectral filter on the patch in front of the element with-
out significantly changing the filter's characteristics (as a
result of variations in incidence angle).  In this position, the
interference filter reduces $\Phi_O$ by reflecting part of the incident
radiation.

In addition, the optical opening is designed so that it does
not pass through the cone wall area seen by the black top of the
patch.  The first structure seen from the patch is then the space
between the patch and cone rather than that between the cone and
housing.  As a result, the source closest to the optical opening
on the patch is at a lower temperature.

Finally, the Irtran 2 window on the cone wall serves to
block radiation from components beyond it in the direction of the
instrument housing.  Irtran 2 absorbs or reflects wavelengths of
15 µm and greater (D.E. McCarthy, Appl. Opt. 2, 591, 1963).  In
combination with the reflective properties of the spectral filter
at wavelengths below 15 µm, the window essentially eliminates
radiative coupling between the patch and objects beyond the window.
The window also serves two other purposes.  It provides a cone
enclosure seal to permit evacuation during bench cooling of the
detector and to prevent outgassing of the instrument through the
cooler.

The value of $\Phi_O$ may be estimated by assuming that an area $A_O$ of each of two spectral filters at the edge of the patch views a black window at the cone temperature and a black space between the patch and cone. We then have

$$\Phi_O = 2\,\sigma A_O\,(E_A F_{PA} T_A{}^4 + E_c\,F_{pc}\,T_c{}^4)$$

where $E_j$ = fraction of blackbody radiation at a temperature $T_j$ that is transmitted by the filter (the remainder being relected)

$F_{pj}$ = view factor from $A_O$ to area j

$A$ = multilayer between patch and cone

$C$ = window on cone structure

The insulation is assumed to be at a temperature given by

$$T_A{}^4 = \tfrac{1}{2}\,(T_C{}^4 + T_p{}^4) \cong \tfrac{1}{2}\,T_C{}^4.$$

The cone window is about 0.9 inch from the patch edge and has a diameter of approximately 0.55 inch. The opening ($A_O$) at the edge of the patch is a circle whose diameter is about 0.30 inch. The two openings are therefore circles with a common central normal. The view factors between them may therefore be calculated from the formula given by M. Jakob (Heat Transfer, Vol. II, John Wiley and Sons, 1957, p. 14). If $F_{pc}$ is the view factor from $A_O$ to the window, the other view factor is given by

$$F_{pA} = 1 - F_{pc}$$

For the geometry described above, the results are

$$F_{pc} = 0.084$$

$$F_pA = 0.916$$

We will neglect the small fraction of radiation passed by the narrow spectral band to which a channel is sensitive. Instead, we will assume that all wavelengths greater than 18 μm (where the detector is insensitive) are transmitted by the filter. For $T_c = 170$ K and $T_A = 140$ K, we then have the approximate values

$$E_A = 0.8$$

$$E_c = 0.7$$

Finally, the radiative input through two optical channels is approximately

$$\Phi_O = 1.8 \times 10^{-3} \text{ W}.$$

## 6.6    Final Radiant Cooler Design for SCMR

The final radiant cooler design for the SCMR is close to that of Modification 2 to design IIIB described in Section 6.2.  The only difference  is in the shield design, as shown in Figures 6.6-1 and 6.6-2.  The shield wall on the earth side of the cooler is longer but not as wide to permit its use as a deployable cone mouth cover.  The cone temperature of the final design was calculated for the nominal set of conditions and radiative properties. It was found to be identical to that of Modification 2 to design IIIB (Table 6.3.1-3).  Addition of a solar input to the cone end at a solar elevation of $12^{\circ}$ increases the cone temperature by about 0.9K.

The cone end and cone mouth view factors for the final design are (See Section 6.4).

$$F_{de} = 4.085 \times 10^{-2}$$

| | $F_{m-e(n)}$ | $F_{d-h(n)}$ |
|---|---|---|
| 0 | - | 0.6515 |
| 1 | 0 | 0.3147 |
| 2 | 0.0289 | 0.0338 |
| 3 | 0.0072 | - |

And the radiative coupling factors for the nominal property values are

$$\varepsilon_{me}(0.05) = 3.84 \times 10^{-3}$$

$$\alpha_{me}(0.22) = 1.39 \times 10^{-2}$$

$$a_{dh}(0.05) = 1.90 \times 10^{-3}.$$
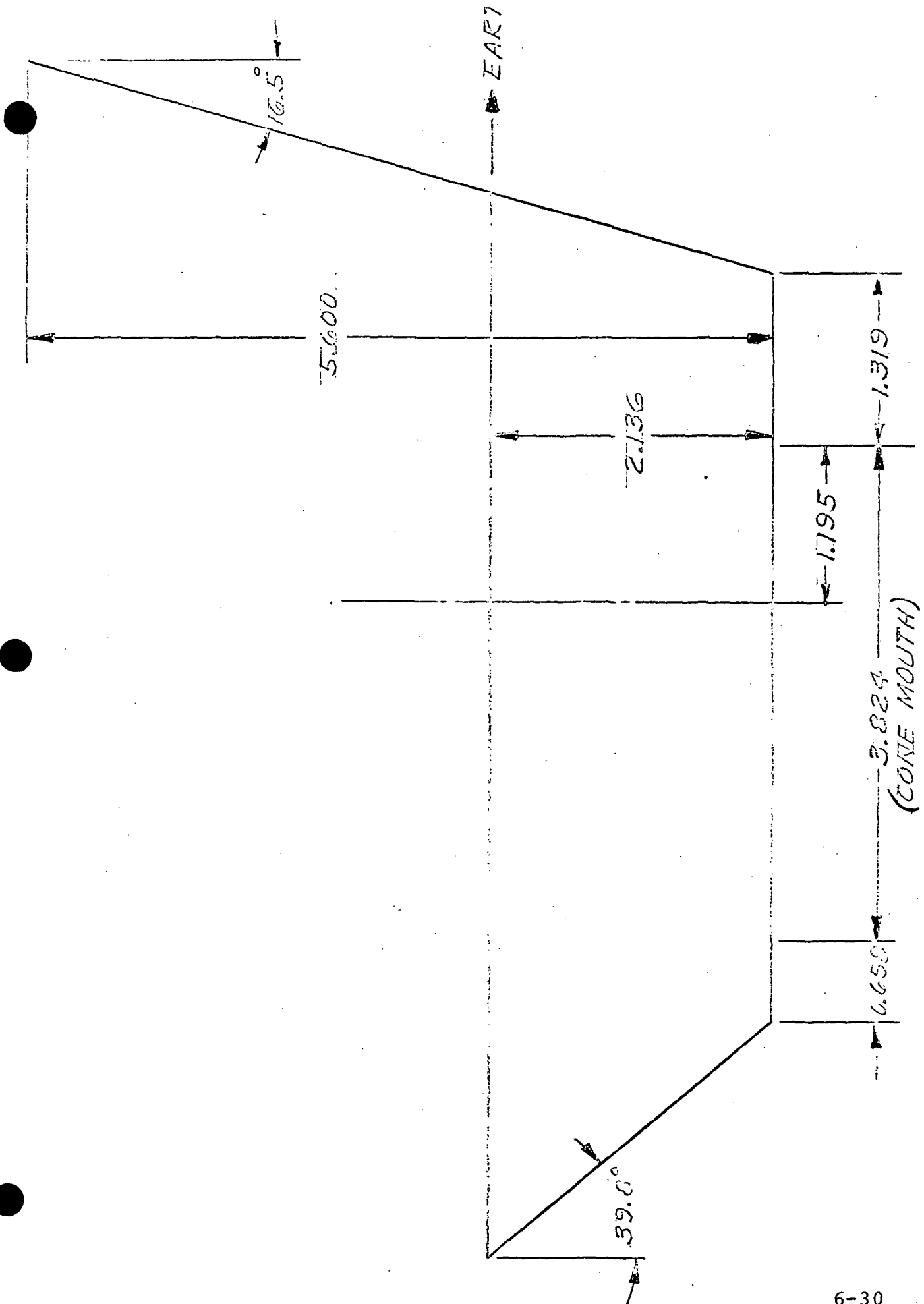
Figure 6.6-1  Shield Vertical Plane, Final SCMR Cooler Design
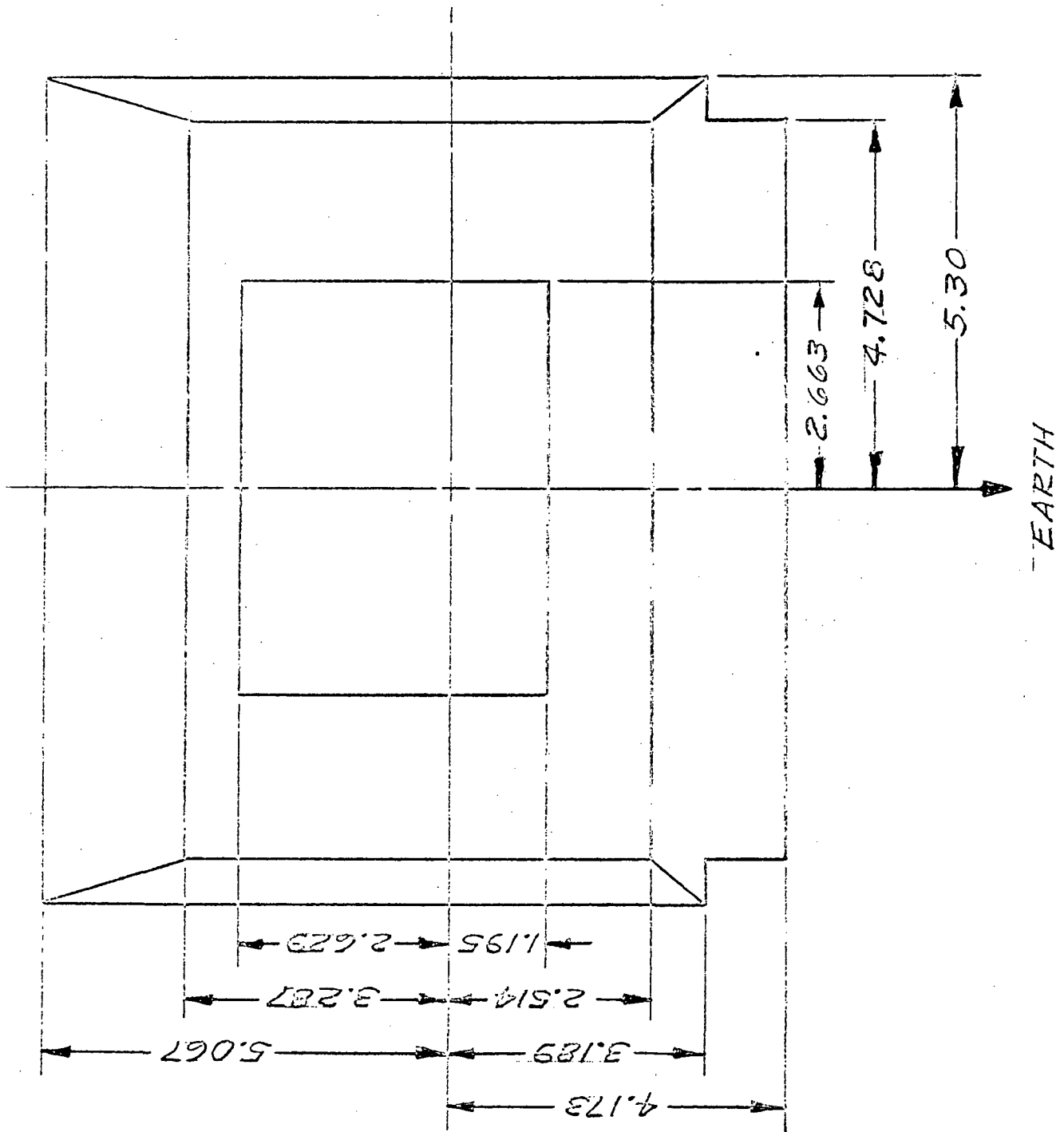
Figure 6.6-2 Top View of Shield & Cone End, Final SCMR Design

The fraction $g_d$ $(\varphi_s)$ of cone end area in the final design exposed to sunlight is shown in Figure 6.6-3 as a function of solar azimuth $\varphi_s$ at a solar elevation of $12^{\circ}$. The average value over an orbit is

$$g_d = 2.06 \times 10^{-2}.$$

At a housing temperature $T_h$ of $25^{\circ}C$ and a solar elevation of $0^{\circ}$, the thermal balance equation of the cone in the final design yields

$$5.015 \times 10^{-12} T_c^4 + 2.2 \times 10^{-6} T_c = 3.910 \times 10^{-3} \text{ W cm}^{-2}$$

for the nominal radiative properties. The solution is

$$T_c = 163.1 \text{ K.}$$

This is identical to the cone temperature of modification 2 to design IIIB under the same conditions. At a solar elevation of $12^{\circ}$, the right side of the above equation is increased to 3.995 $\times 10^{-3}$ W cm$^{-2}$ and the equilibrium cone temperature to 164.0 K.

The distribution of thermal inputs to the cone at a temperature of 163.1 K is

| Source | Watts | Percentage |
|---|---|---|
| Earth | 0.216 | 28.5% |
| Shield | 0.161 | 21.2 |
| Supports and Leads | 0.067 | 8.8 |
| Multilayer Insulation | 0.315 | 41.5 |

Of the earth load, 0.185 W or about 85% is absorbed in the white cone end and the remainder in the cone walls.
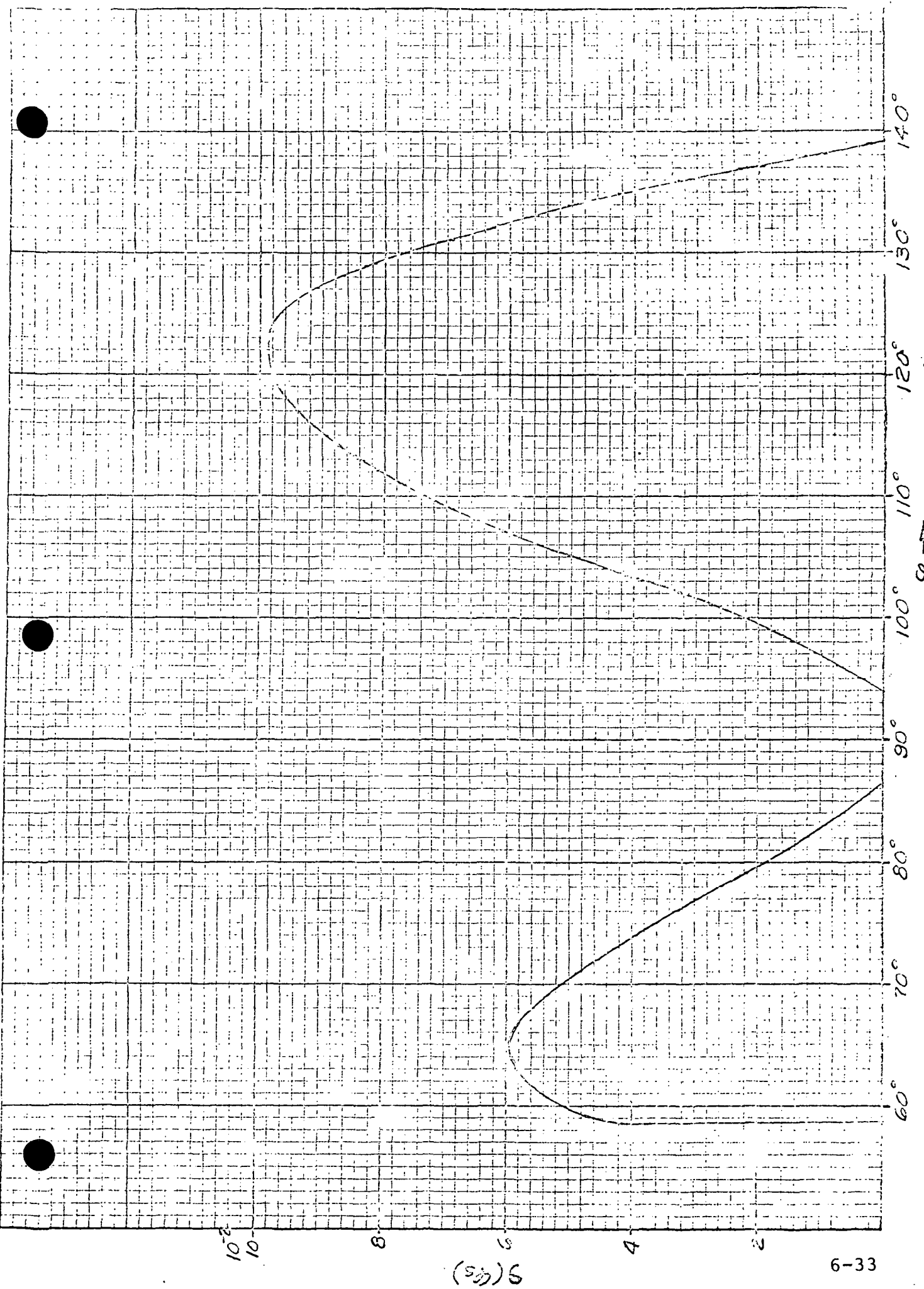
Figure 6.6-3  Cone End Exposure Factor at $\beta_s = 12^\circ$;
Final SCMR Design

6-33

## 6.7    Analysis of Tests on the Prototype Radiant Cooler

The measurements on the SCMR prototype cooler at the ends of the 48 hour hot and cold cycles in the thermal-vacuum test are listed in Table 6.7-1.

### Table 6.7-1

### Results of SCMR Prototype Tests

|  | Hot | Cold |
|---|---|---|
| Nominal baseplate | $40^{\circ}C$ | $-5^{\circ}C$ |
| Cooler housing | 270.7K | 259.4K |
| Cone | 162K | 157K |
| Patch | 115.6K | 115.6K |
| Patch control heat | $2.50 \times 10^{-3}W$ | $4.90 \times 10^{-3}W$ |
| Detector joule heat | $1.2 \times 10^{-3}W$ | $1.2 \times 10^{-3}W$ |

The analysis shows that the thermal performance of the cone was very good. For an assumed white paint emissivity $\varepsilon_d$ of 0.85, the insulation factor of the multilayer blanket between the cone and cooler housing was 72 at the end of the hot cycle and 83.5 at the end of the cold. If $\varepsilon_d$ is 0.87 instead, the respective insulation factors are 69 and 78.5. On the other hand, the analysis shows that the thermal performance of the patch is severely limited by the poor insulation factor between the sides and rear of the patch and the gold box. This insulation factor was only about 18, which corresponds to an average surface emissivity of 0.10.

However, an analysis of the orbital performance shows that the heat input to the patch was reduced by 3.95 milliwatts. This is attributed to the absence of reflecitons from cold space. In the chamber, a very small fraction of the radiant emission from the cone is reflected from the space target to the patch (see Construction and Test of a Dual Patch Multielement Radiant Cooler, NAS5-21132, June 1971, Section 2.3.3). The actual insulation factor was therefore about 32 rather than 18.

The patch operated in orbit with nearly the same temperature and control heat (i.e., cooling margin) realized during chamber testing on the ground. The absence of space reflections was compensated in orbit by a higher cone temperature (171 K). Based on the model described below, the SCMR cooler had an in-orbit cone to housing insulation factor of about 46. The reduction from the chamber value of about 71 is apparently the result of little or no outgassing of the insulation blanket in the vicinity of the cooler housing. This housing quickly reached $0^{\circ}C$ and remained there; no provision was made for in-orbit heating of the housing.

## Cone

The thermal balance equation of the cone is:

$$\Phi_d = \varepsilon_d A_d \sigma T_c^4 = \Phi_e + \Phi_s + \Phi_h + \Phi_k + \Phi_i$$

where   d  = cone end, e = earth, s = direct sunlight

   h  = shield, k = conduction, i = insulation

   $\varepsilon$  = emissivity

   A  = area

   T  = Temperature

   $\Phi_h = A_d \varepsilon_d a_{dh} \sigma T_h^4$

   $a_{dh}$ = effective shield emissivity

   $\Phi_k = K_c (T_h - T_c)$,   $K_c$ = thermal conductance

   $\Phi_i = \dfrac{A_i \sigma}{S_i} (T_h^4 - T_c^4)$,   $S_i$ = insulation factor

For a cone end emissivity of 0.85 and solar absorptivity of 0.20, the calculated value of $\Phi_e + \Phi_s$ at a $12^\circ$ sun angle is 0.248W. The tests were run with a $\Phi_e + \Phi_s$ value (heater) of 0.296W including an estimated 0.016W from lead wire dissipation. Based on published data, experiments conducted on the dual patch cooler (Contract NAS5-21132), and calculations in Section 6.3, we assumed the following values:

   $\varepsilon_d$ = 0.85

   $\varepsilon_h$ = 0.04, so that $a_{dh}$ = 0.01524

   $A_d$ = 33.0 $in^2$

   $A_i$ = 120 $in^2$

   $K_c$ = 4.93 x $10^{-4}$ W/K

The insulation factor $S_i$ is then determined by the thermal balance equation. For the hot cycle, the result is:

   $S_i$ = 71.6

If we assume $\varepsilon_d$ is 0.87 instead of 0.85, $S_i$ is reduced to 69.2. In either case, the insulation factor is comparable to the values obtained in the dual patch cooler and in separate insulation tests (See Construction and Test of a Dual Patch, Multi-Element Radiant Cooler, NAS5-21132, June 1971, Sections 2.2.1 and 2.2.4).

The thermal inputs to the cone during the cold cycle are listed in Table 6.7-2. We see that the cone temperature is largely determined by the fixed inputs from the earth and sun and by the input from the cooler housing through the insulation blanket.

<div align="center">

### Table 6.7-2

Cone Thermal Inputs During Cold Cycle ($\varepsilon_d$ = 0.85)

</div>

| Source | Watts | % |
|---|---|---|
| Earth and Sun | 0.296 | 48 |
| Shield | 0.0708 | 11 |
| Conduction | 0.0505 | 8 |
| Insulation | 0.2061 | 33 |

Using the temperatures recorded at the end of the cold cycle (Table 6.7-1), we find that $S_i$ has increased to 83.5 (78.5) for $\varepsilon_d$ equal to 0.85 (0.87). In general, the effectiveness of the insulation blanket increases with a reduction in the temperature of the warm boundary (Thermal Insulation Systems, NASA SP-5027, 1967).

## Patch

The thermal balance equation of the patch is:

$$\Phi_p = \varepsilon_p \sigma A_p T_p^4 = \Phi_r + \Phi_o + \Phi_j + \Phi_k + \Phi_i$$

where   p = patch, r = cone walls

o = optical ports, j = joule heat

$\Phi_r = \varepsilon_p \varepsilon_{pe} \sigma A_p T_c^4$, $\varepsilon_{pc}$ = effective emissivity of cone walls as seen from patch

$$\Phi_o = 2\sigma(\varepsilon_o A_o + \pi d_o \delta)(T_c^4 - T_p^4)$$

$\varepsilon_o$ = absorptance of patch optical port

$d_o$ = diameter of optical port

$\delta$ = thickness of black ring around port

The joule heat is the sum of the detector dissipation ($1.2 \times 10^{-3}$W) and the control heat. The following values were used:

$\varepsilon_p = 0.93$

$A_p = 3.50 \text{ in}^2$

$\varepsilon_{pc} = 0.03357$ ($\varepsilon_c = 0.04$, See SCMR Design Study Report)

$\varepsilon_\delta = 0.6$ (germanium substrate)

$d_o = 0.40$ inch

$\delta = 0.015$ inch

$K_p = 4.62 \times 10^{-5}$ W/K

$A_i = 8.89 \text{ in}^2$

For the hot cycle (Table 6.7-1), we then obtain

$S_i = 18.1.$

The average surface emissivity $\varepsilon_i$ of the insulated patch area $A_i$ and the facing gold box area $A_o$ can be calculated from:

$$S_i = \frac{1}{\varepsilon_i} + \left( \frac{1}{\varepsilon_i} - 1 \right) \frac{A_i}{A_o} .$$

The value of $A_o$ is 10.105 $\text{in}^2$, so that

$\varepsilon_i = 0.10.$

The emissivity of the gold surfaces has obviously been severely degraded by areas of high emissivity, such as the support openings and vibration bumpers. For the cold cycle, the calculated insulation values are:

$S_i = 17.7$

$\varepsilon_i = 0.10$ .

This shows that the thermal model of the cooler yields consistent results.

The distribution of heat inputs to the patch is shown in Table 6.7-3 for the hot cycle. Again, the poor quality of the insulation is brought out.

Table 6.7-3

Patch Thermal Inputs During Hot Cycle

| Source | Milliwatts | % |
|---|---|---|
| Cone Walls | 2.76 | 13 |
| Optic Ports | 3.52 | 16 |
| Detector Bias | 1.20 | 6 |
| Control Heat | 2.50 | 12 |
| Conduction | 2.14 | 10 |
| Insulation | 9.17 | 43 |

## 6.8    Radiant Cooler Configuration SCMR Flight Model

The radiant cooler configuration can best be seen by examination of the Radiant Cooler Assembly drawing, ITT Drawing No. 8116040.  This drawing is not included in this report but is available in the drawing sets supplied to GSFC by ITT.

Figure 6.8-1 shows schematically the mechanical configuration of the cooler from the patch to the optical focus lens.

## 6.9    SCMR Flight Model Radiant Cooler Performance

Data was taken with stable baseplate during thermal vacuum test conducted on Flight Model instrument Oct. 15 through Oct. 27, 1972.  The following tabulation shows Flight Model performance.

| | | |
|---|---|---|
| Baseplate Temperature | $+40^\circ$C | $0^\circ$C |
| Cone Wall Temperature | $160^\circ$K | $157.0^\circ$K |
| Patch Temperature | $114.9^\circ$K | $114.9^\circ$K |
| Cone Housing Temperature | $-8.5^\circ$C | $-16.5^\circ$C |
| Patch Control Heat | 1.8 mw | 5 mw |
| Patch Heat Margin | | $1.8^\circ$K/mw |

VACUUM HOUSING
GOLD BOX
PATCH
DETECTOR
APLANAT
FILTER
IRTRAN WINDOW
COOLER OUTER HOUSING
MULTILAYER INSULATION
FOCUS LENS
EARTH
CONE
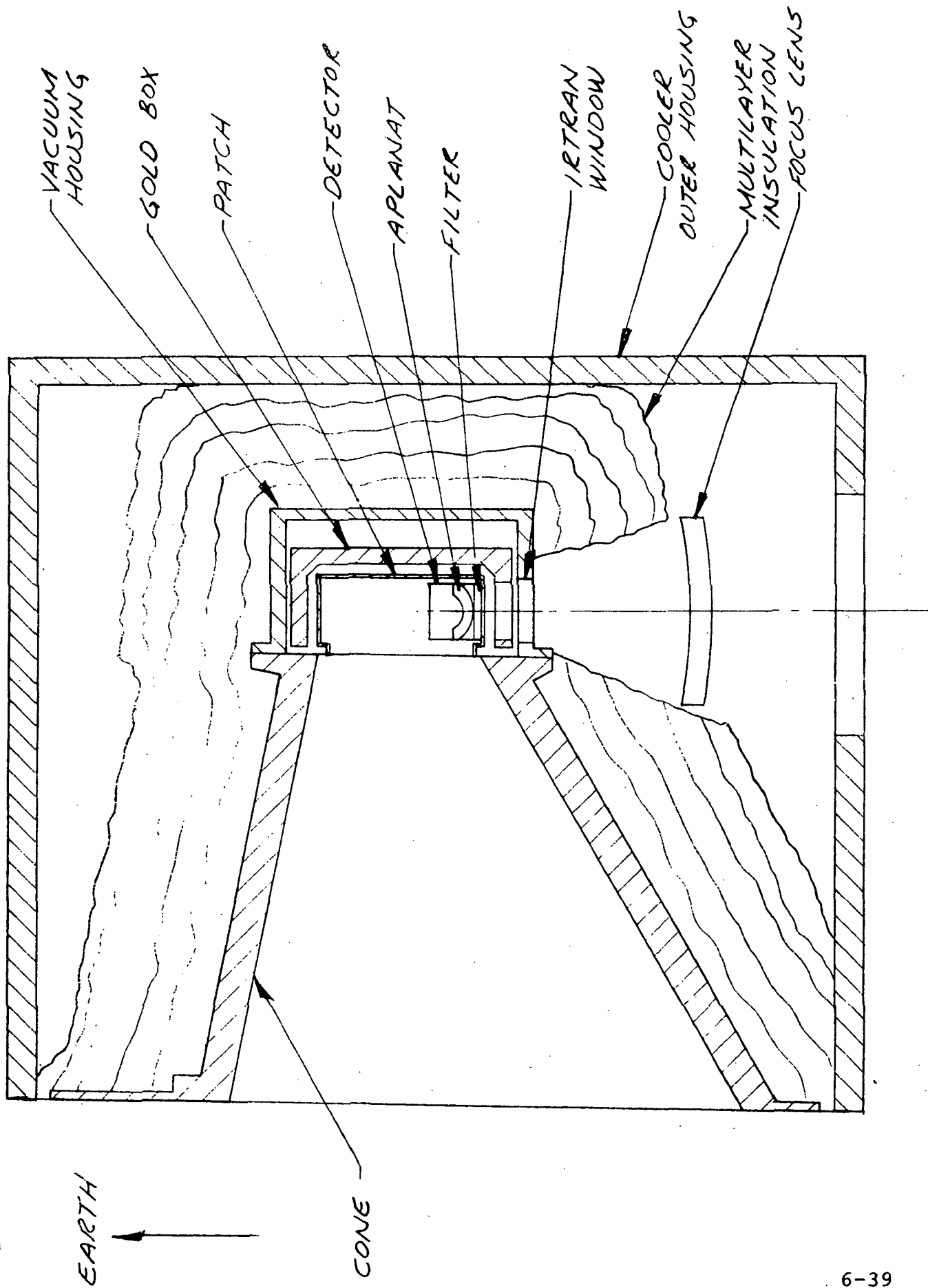
SCHEMATIC OF COOLER CONFIGURATION

Figure 6.8-1

## 7.0   SCMR ELECTRICAL SYSTEM

A simplified Block Diagram of the SCMR Electronics is shown in Figure 7.0-1. The SCMR Electronics has the basic function to transmit to the spacecraft two channels of video data synchronized with the spacecraft clock and the rotation of the SCMR scan Mirror. The input signals to the SCMR are the spacecraft -24.5 VDC bus, clock signals of 50 KHz, 10 KHz and 400 Hz 2-phase, and spacecraft commands to the SCMR to implement the available modes of operation. The SCMR electronics provides the power conversion, timing and control, signal generation, digital and analog telemetry for verification of operation, and signal amplification for required operation.

The basic blocks of the SCMR are:

1. IR Data Amplifiers

2. Visible Data Amplifiers

3. Power Converter

4. Voltage Regulators

5. Timing and Control Circuits

6. Calibration signal generation circuits

7. Analog TM circuits

8. Command and Digital TM circuits

These functions are individually described in the following sections. Schematics referenced in the following text are located in tne Appendix of this report.

## 7.1   Video Output

A representation of the video output for one scan line is shown in Figure 7.1-1. An angular representation of one scan is shown in Figure 7.1-2. Both diagrams are referenced to the occurrence of the sync pulse which occurs at the start of the interval when the scan mirror views space just prior to the view of the earth.

## 7.2   Commands and Digital TM

Commands are received by the SCMR from the spacecraft as pulses of 40 millisecond duration on two isolated lines for each command. The command is stored by means of latching relays and digital command verification telemetry is outputted.
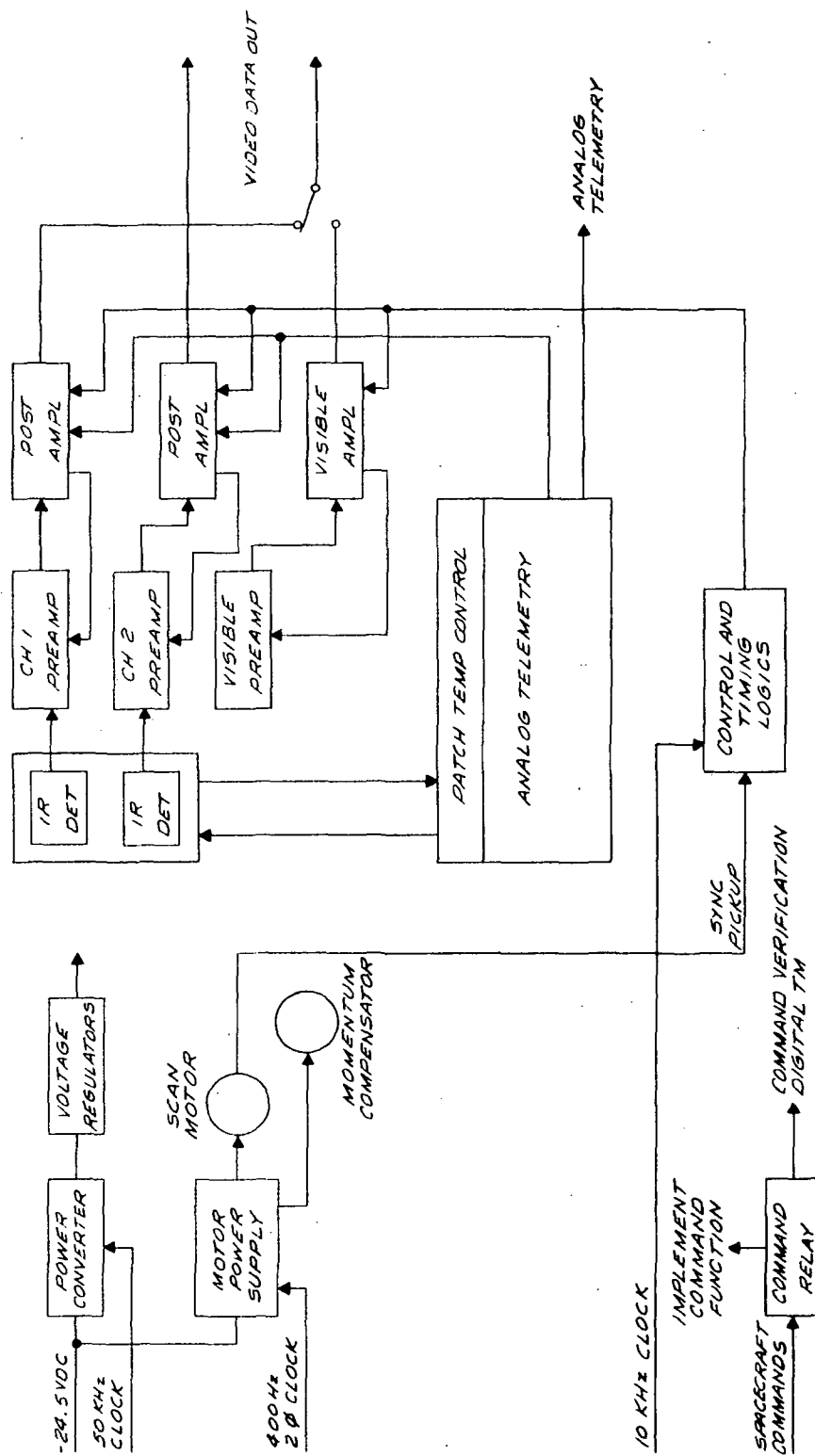
SCMR ELECTRONICS
SIMPLIFIED BLOCK DIAGRAM

Figure 7.0-1
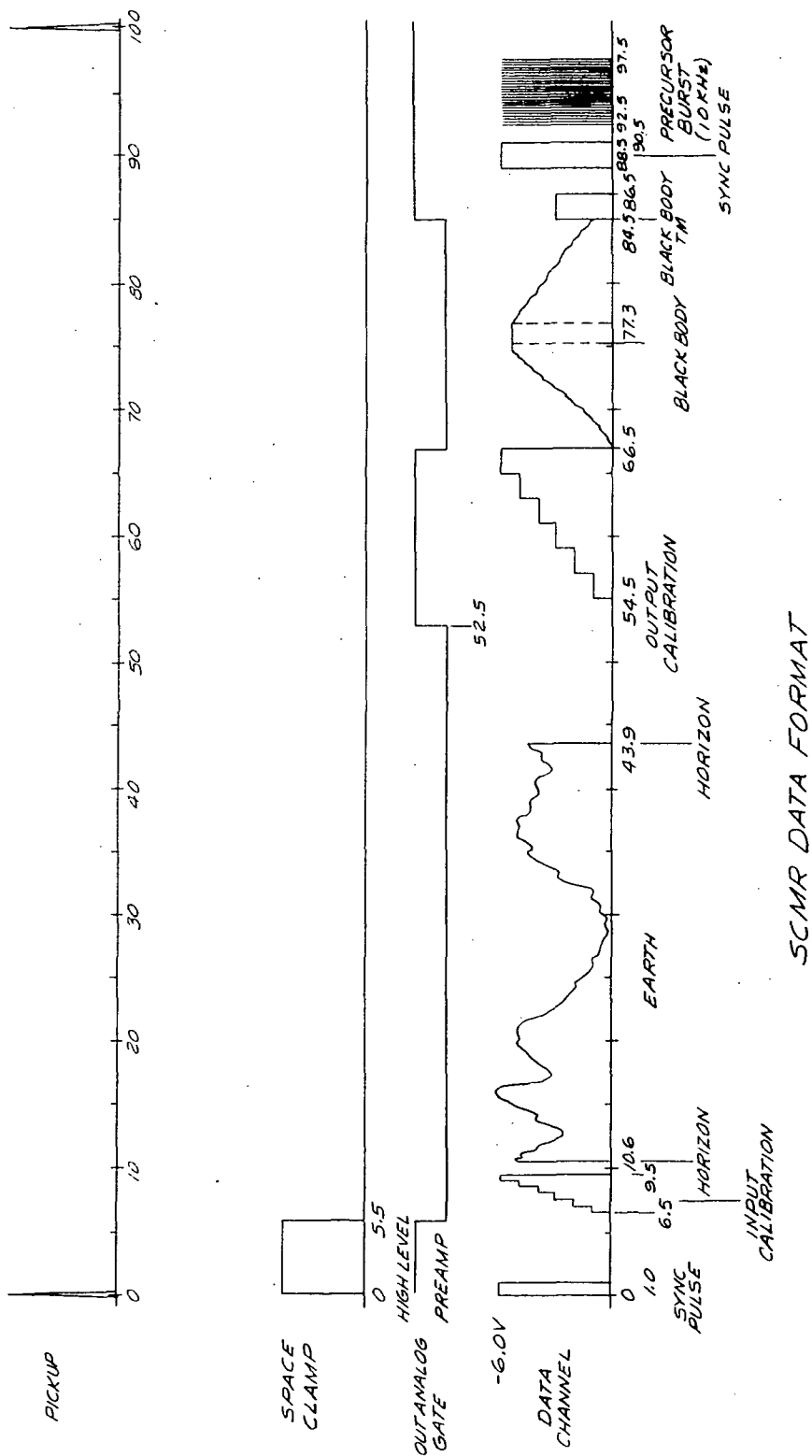
SCMR DATA FORMAT
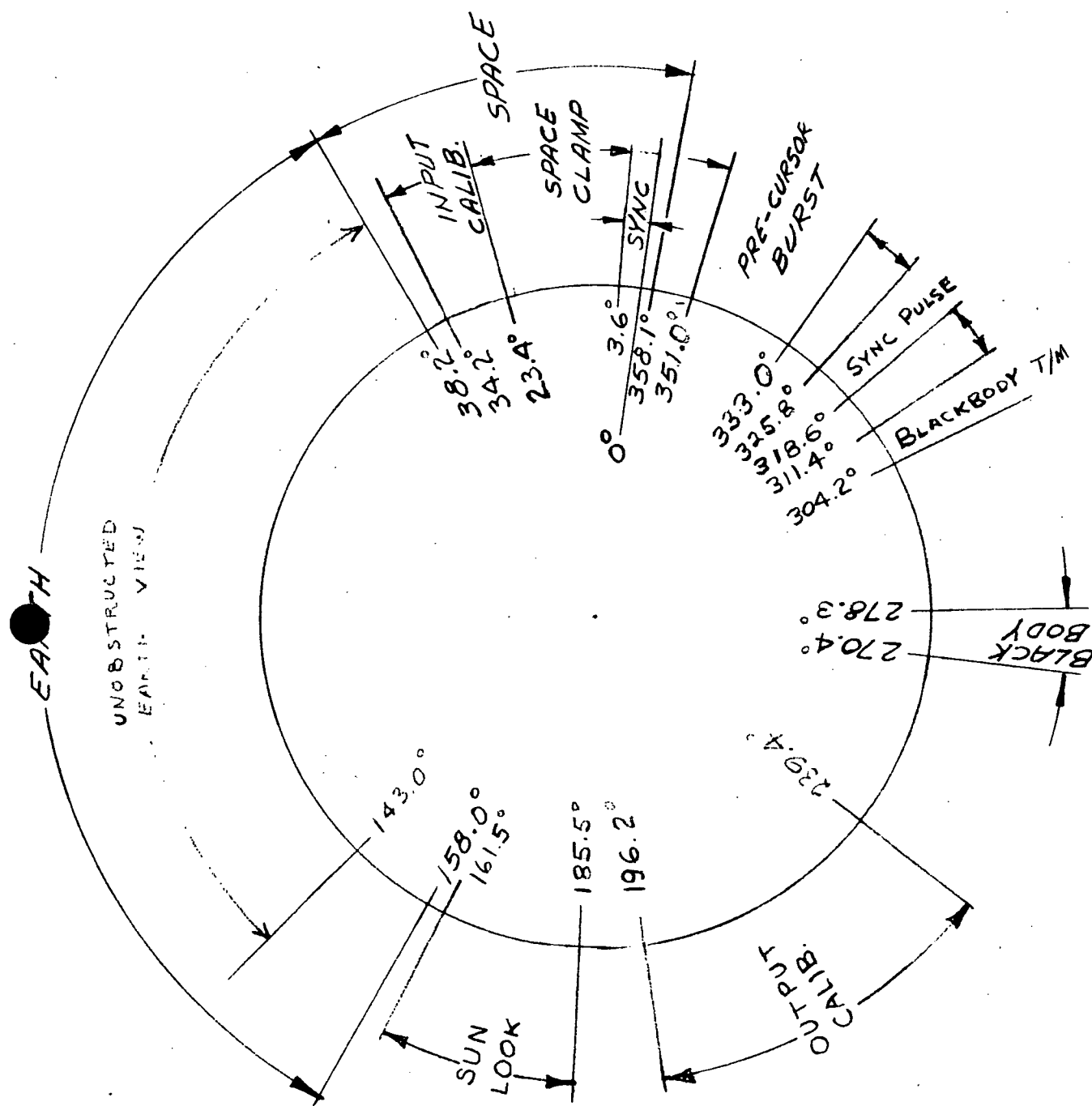
Figure 7.1-1

Figure 7.1-2  SCMR ANGULAR DATA FORMAT

The schematics of the command system of the SCMR are shown on drawings 8116466 and 8116462.

The commands, their functions, and the telemetry response are as follow:

Motor ON/OFF - Applies DC power to the scan motor and momentum compensator. Turns on analog telemetry through the power converter. Motor ON is Logic 1.

Motor High/Low Power Mode - High power mode applies -24.5 VDC to Scan Motor P.S. Low Power Mode applies -15 VDC to Scan Motor P.S. through a switching regulator. Motor Low Power Mode is Logic 1.

Electronics ON/OFF - Applies power to theSCMR Electronics through the power converter. Also turns on the analog telemetry through the Power Converter. Electronics ON is Logic 1.

Purge ON/OFF - Applies -24.5 VDC to the SCMR purge system to release a flow of dry nitrogen gas around the patch. Purge ON is Logic 1.

Cone Heater ON/OFF - Applies -24.5 VDC to the heater on the cooler cone walls. Cone Heater ON is Logic 1.

Patch Heater ON/OFF - Applies -24.5 VDC to the patch heater. Patch Heat ON is Logic 1.

Visible Video/IR Video - Connects to output of the designated amplifier to the video interface connector. Visible Video is Logic 1.

Cone Cover Deploy/Store 1 & 2 - Duplicate Pair of commands. Both must be in the same state to cause operation. Applies -24.5 VDC to cone cover circuits to operate cooler door in commanded direction. Circuit removes -24.5 VDC load at completion of operation. Cone Cover Deploy is Logic 1.

## 7.3   Power Conversion Circuits

DC power for the SCMR Electronics is obtained by the Power Converter shown in Schematic 8115674. The clock signal for the converter is derived by AMP 1 operating as an oscillator. The 100 KHz oscillator is normally synchronized to the spacecraft 50 KHz clock. Two separate converter circuits are separately powered. One is used for the electronic circuits, the other is used for the Analog Telemetry circuits.

Linear regulator circuits for the DC power are shown in schematic 8116516. Plus 15 volts, minus 15 volts, and plus 5 volts are provided for the Electronics. Plus and minus 15 volts are provided for telemetry circuits.

## 7.4 SCMR Clock Signals

The SCMR normally operates with a 50 KHz and 10 KHz spacecraft clock signals. The 50 KHz clock is used to synchronize a 100 KHz oscillator in the power converter for power conversion. The 10 KHz clock is used for the logic timing function.

In the event of the loss of the 10 KHz clock from the spacecraft, a clock detector circuit on the logic No. 2 board switches in a 10 KHz clock which is counted down from the 100 KHz power converter clock. This provides a 10 KHz clock timing signal which is synchronous to the spacecraft 10 KHz clock but not necessarily coherent to it.

In the event of the loss of the 50 KHz clock line, the power converter oscillator will continue to operate at a frequency near 100 KHz. The logic timer clock will continue to operate from the spacecraft 10 KHz clock line as long as it is present.

With the loss of both clock lines the SCMR will continue to operate but internal timing will be a function of the internal oscillator. The scan period, however, will be maintained as long as the 400 Hz clock to the scan motor is maintained.

## 7.5 Logic Clock

The timing anc control functions of the SCMR are shown on Schematics for Logics No. 1, drawing 8116450, and Logic No. 2, drawing 8116502.

The 10 KHz spacecraft clock enters at pins 40 and 41 of the Logic No. 2 board. AMP 1 functions as a receiver and a shaping circuit. Positive feedback supplied by R2 and R3 provide controlled hysteresis of this circuit to provide immunity from the noise occurring during the transition causing multiple triggering. Transistor Q1 and associated components provide an AC coupled detection circuit. A positive voltage across R26 provides a logic 1 input at pin 5 of 12 which gates in the clock output of AMP 1. The absence of this signal gates in the output of the divide by 10 counters comprised of U7 through U10. The selected clock appears at the output of the OR gate at U12, pin 3. The gating of the U1 and the status of FFU2 determine the phase of the clock which appears at pin 37 for use by the scan counter.

The negative going transition of the clock at pin 37 triggers the monostable U4. The transition of the pick-up signal to initiate scan timing triggers monostable U5. If these transitions occur within 10 microseconds of each other, the combined signal will reverse the state of Flip-Flop U2, causing the opposite phase of the 10 KHz clock to be present at pin 32. This is done to prevent the clock edge which advances the scan counter to occur near the sync pulse so that scan motor jitter will not come a continuous 100 microsecond jitter in the timed calibration signals.

7-6

## 7.6    Logic Timing & Control

The logics for controlling the gating signals for the SCMR scan timing are shown on 8116450 - Schematic Logics No. 1.

The time base for the scan count is the 10 KHz clock from the Logic No. 2 board which is under normal operation the spacecraft 10 KHz clock signal. Flip-Flop 1, 2 and 3 are a divide by five counter to give a 2 KHz time base (500 μsecond interval) for decoding. Flip-Flops 4 through 11 are connected as a conventional binary ripple counter. The counter is preset to a 11.5 millisecond count to allow proper sequence of counter operation for the staircase input and output calibration signals at the required times. Weighted input calibration signals are obtained from Flip-Flops 4 through 7 while output calibration is derived from Flip Flops 6 through 8.

The counter string is held in a reset condition by the toggle composed of NAND 1 and NAND 2. The reset is removed by a negative going pick-up pulse signal at NAND 16 thtough NAND 47. The count continues for 97.5 milliseconds when the reset is again applied.

The gating outputs from the logics are the five signals:

1.   Space Clamp

2.   Data Amp Logic

3.   Black Body Logic

4.   Analog Gate

5.   Visible Bias Gate

Space Clamp causes a sample of the Video Amplifier output to be taken for zero reference correction. Data Amp logic causes the output of the Video Amplifier for each stage to be connected to the output driver. Blackbody logic gates the Blackbody TM signals to output driver in the IR Channels. The Analog Gate signal gates the D to A output to the output Driver. The Visible Bias Gate gates in a 3 volt offset during input calibration time on the Visible channel since the output calibration signals are set up to normally operate in the IR channels which are offset by 3 volts. A zero logic level on these outputs is the level which causes the stated operation.

Four logic Levels which are the inputs to the D to A converter are also generated. Table 7.6-1 shows the signal source and time intervals for these signals.

The timing for the gating and calibration signals are shown in Figures 7.6-1 and 7.6-2.
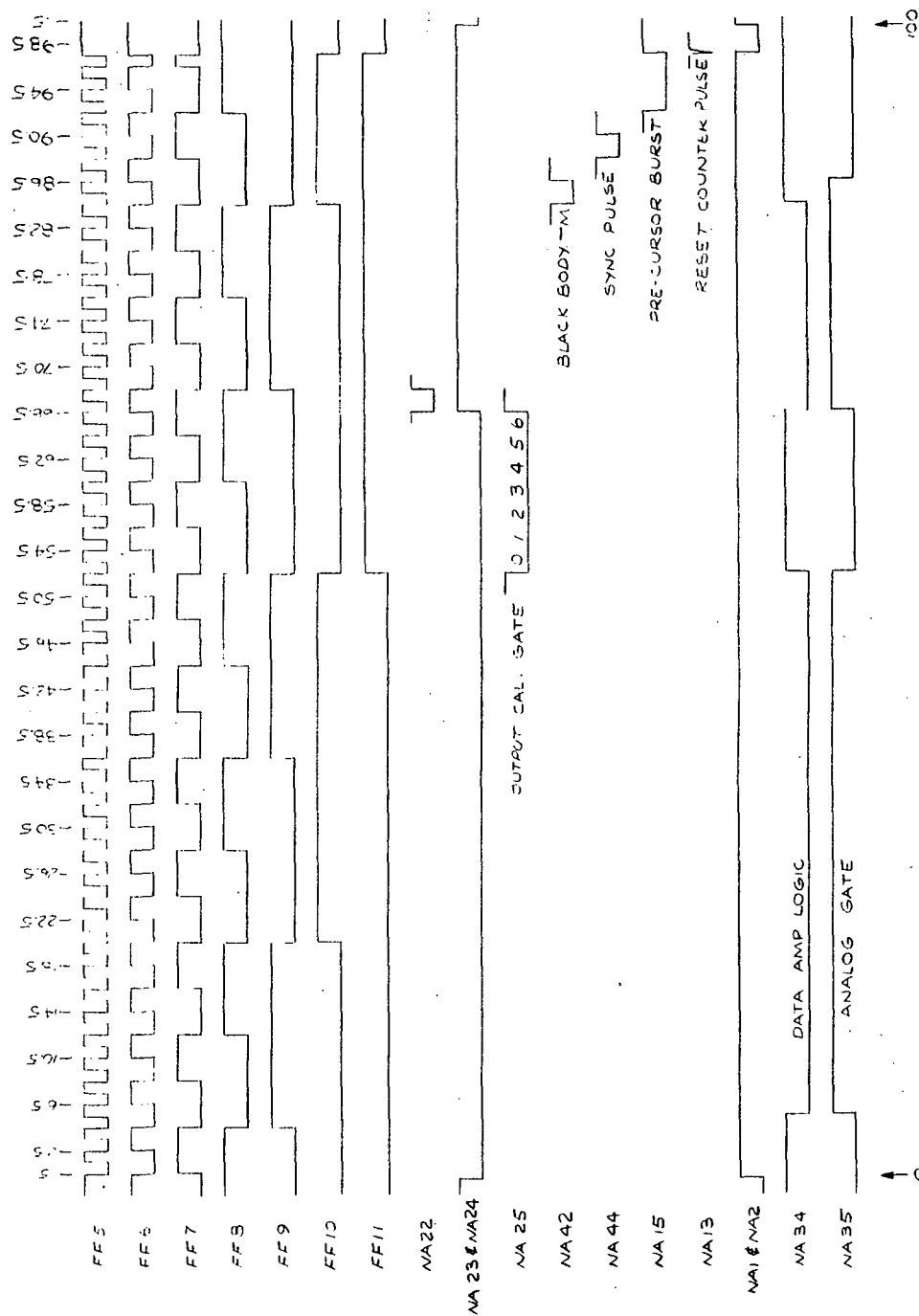
SCMR LOGIC TIMING

Figure 7.6-1
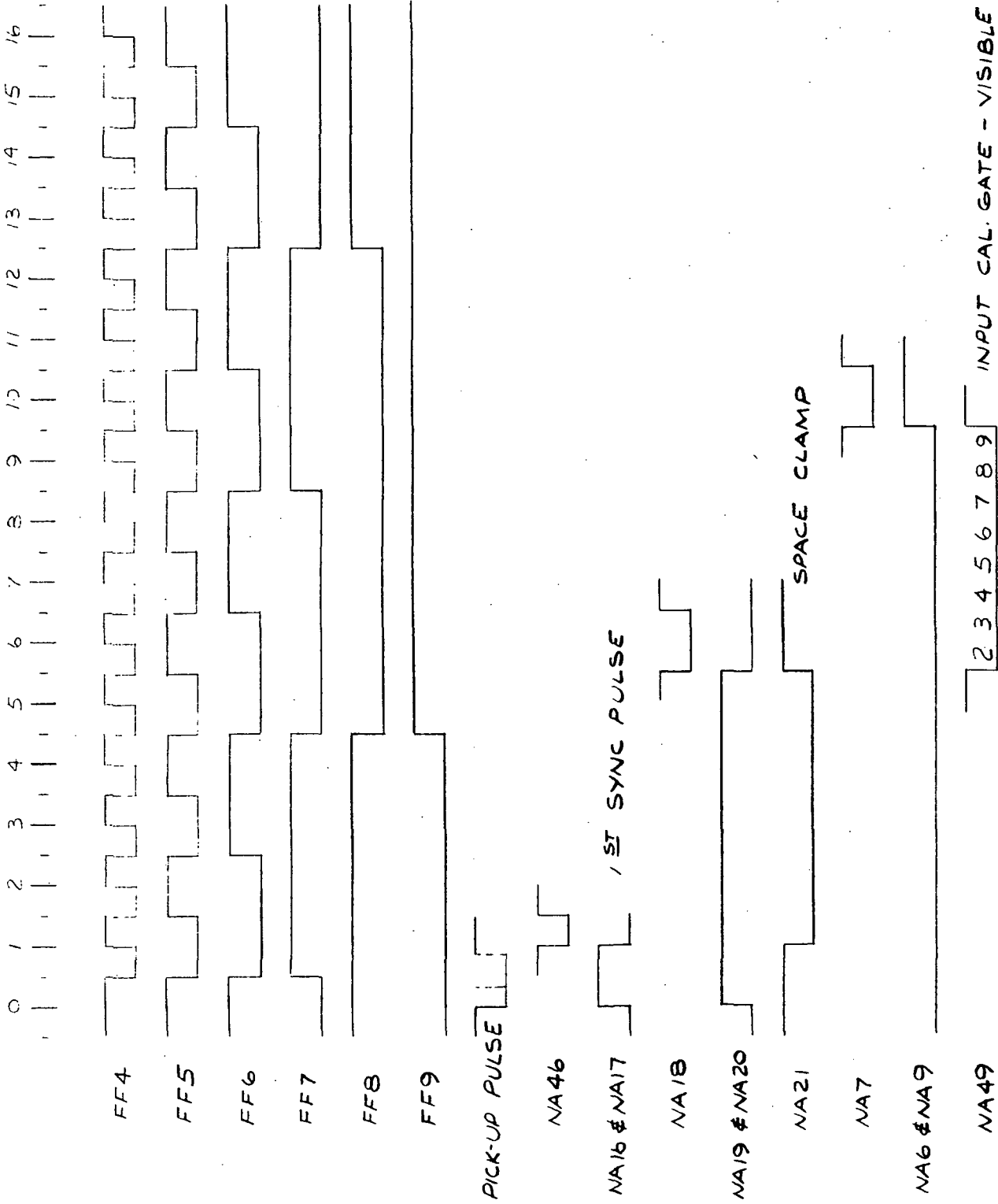
SCMR LOGIC TIMING

Figure 7.6-2

## Table 7.6-1

### D to A Logic Control Signals

| Name | Time | Signal | Signal | Path | Binary Weight |
|---|---|---|---|---|---|
| Sync | 0 - 1 msec | 6 V | FF(NA16 & NA17)-NA45-NA28-NA36 | | $2_2^1$ |
| | | | FF(NA16 & NA17)-NA45-NA29-NA38 | | $2$ |
| Input Cal. | 5.5 to 9.5 msec | 2V to 9V | FF4 - NA - NA37 | | $2^0$ |
| | | | FF5 - NA9 - NA36 | | $2^1$ |
| | | | FF6 - NA11 - NA38 | | $2^2$ |
| | | | FF7 - NA48 - NA12 - NA39 | | $2^3$ |
| Output Cal. | 52.5 to 66.5 msec | 0 V to 6 V | FF6 - NA30 - NA37 | | $2^0$ |
| | | | FF7 - NA48 - NA32 - NA36 | | $2^1$ |
| | | | FF8 - NA33 - NA38 | | $2^2$ |
| Sync. | 88.5 to 90.5 millsec | 6 V | NA44 - NA45 - NA28 - NA36 | | $2_2^1$ |
| | | | NA44 - NA45 - NA24 - NA38 | | $2$ |
| Pre-cursor | 92.5 to 97.5 msec | 6 V modulated by 10 Kh | NA4 - NA27 - NA45 - NA28 - NA36 | | $2_2^1$ |
| | | | NA4 - NA27 - NA45 - NA29 - NA38 | | $2$ |

## 7.7 IR Data Amplifiers

The IR data amplifiers are physically divided into two sections; the IR preamplifiers which are individually packaged, and mounted to the cooler housing, and the Post Amplifiers, two of which are on the same printed circuit card in the Electronics Box. The data amplifiers for each channel are identical except for tailoring to its own detector.

### 7.7.1 IR Preamplifier

The schematic for the IR Preamplifier is shown on drawing 8116495. Each preamplifier has its own plus and minus 12 volt regulators to provide isolation from the SCMR plus and minus 15 volt Electronics supplies. In addition, the -12 volt supply is compensated to maintain a constant voltage over the ambient temperature range. The temperature varying voltage drop of diode CR6 is divided down by R33 and R34. The voltage drop across R34 modifies the voltage at pin 1 of the LM104 regulator to compensate for its voltage variation with temperature. The circuit is tailored and tested to maintain a voltage which will vary less than $\pm$ 0.1% over greater than the expected ambient temperature conditions.

The detector bias is determined by the value of the R15 and the -12 volt supply. The fact that detector responsivity is almost a linear function of the bias is the reason for the care taken for the stability of the -12 volt power source. Resistor R15 is a stable resistor with a temperature coefficient of 2 ppm.

The input circuit for the IR preamplifier is a differential pair. Transistor Q2 provides a constant current source for Q3 and Q4. The detector is the only signal input at the base of Q3. Feedback from the output of amplifier AMP 1 which is a portion of the first amplifier stage, feedback from space look for DC stabilization from amplifier AMP 3, and input calibration signals are summed at R7 at the base of Q4. A DC bias through resistor R17 is also summed at this point. The value of R17 is chosen to allow amplifier AMP3 to operate at approximately 0 volt output to allow for maximum space look correction margin and to set operation at minimum output offset.

Amplifier AMP2 is a conventional inverting amplifier stage with a gain of approximately 5.

Capacitor C11 stores the output of the data amplifier prior to the 3 volt offset at the time the scan mirror views space. Amplifier AMP 4 is a unity gain non-inverting stage with high input impedance for buffering to the following stage. Amplifier AMP 3 is a low pass filter stage with a very low high frequency cut-off as determined by C9 and R27 and a DC gain of 220. R28 and C10 comprise a lead network for stability to prevent over-correction for scan to scan sample differences.

The individual amplifier stages provide essentially flat response to 50 KHz so that the frequency response is determined by the filter network in the Post Amplifier.

The input calibration signal at terminal E6 is attenuated by the network comprised of R20, R21, R22 and R23. These values are tailored after the amplifier gain is determined to provide the 1 Volt input calibration steps.

### 7.7.2   IR Post Amplifier

The schematic of the post amplifiers for the two IR channels is shown on drawing 8116446. The two amplifiers are identical in function and the designators for channel 1 will be used in the following discussion but apply equally to channel 2.

Amplifier AMP 1 is a conventional inverting amplifier with a gain of approximately 5. R5, L1, C4, L2, C5, and R6 comprise a linear phase filter for noise attenuation. Amplifier AMP 2 is a non-inverting stage with a gain of 5. The output of AMP 2 is the full value output of the channel prior to the insertion of the 3 volt offset and as such has a full scale output of +9 volts.

The output of this stage is sampled through R10 across CR1 and CR2 at the time the scan mirror is viewing space. CR1 and CR2 are used to limit the feedback signal at turn on before the amplivier chain stabilizes. Limiting the signal in this manner allows better response in the space look feedback loop during normal operation. U1 and U2 are dual FET switches assemblies with logic compatible drivers. One section of U2 (pins 12 and 13) gates the output to the preamplifier.

Amplifiers AMP3 and AMP are a driver stage with an inverting gain of unity and a non-inverting gain of two. Amp 3 is a voltage amplifier and Amp 4 is a unity gain current driver provided to drive the output line capacitance. One section of U1 gates the output of AMP 2 (Video) to the inverting input of AMP 3 (pins 12 and 13). A DC offset signal through R12 and R13 provide a signal to offset the video output by -3 volts. The offset voltage at pin 7 and the values of R12 and R13 are tailored to provide a current to the summing point equal to the current of a 3 volt signal through feedback resistor R17. Diode CR4 blocks all positive going signals. Diode CR3 provides a low impedance feedback path for positive signals to prevent amplifier input saturation. This clipping action with the current bias provides a 0 Volt to -6 Volt output for signals which correspond to the +3 volt to +9 volt signals at the output of AMP 2.

Output calibration signals are switched in through U2 (pins 10 and 9). Blackbody TM signals are switched in through U1 (pins 10 and 9). Each is attenuated by a factor of 2 due to the gain of 2 of the output stages operating in the non-inverting mode. The two sync pulses and the 10 KHz pre-cursor boost are 6 volt levels from the D to A on the Output Calibration line and are switched in at the appropriate times under logic control.

The flight model operates with a 7 ma bias on the channel 1 detector and a combined preamplifier and Post Amplifier gain of 20,700. Channel 2 has a 5 ma bias and a gain of 24,000.

7.7.3    Visible Amplifier

The schematic for the visible channel preamplifier is shown in Figure 7.7-1. The Visible Post Amplifier is shown on schematic 8116530. The silicon photodiode is operated with reverse bias as a current source to inverting input of the operational amplifier buffered by the FET input stage.

The Post Amplifier for the Visible Channel is identical in operation to the IR Post Amplifier. The zero reference feedback circuits utilizing a sample of amplifier output while viewing space are identical to the equivalent circuits in the IR Preamplifier.

④ +15V

R1
2M
1%

⑨ +15V

R2
10K
5%

R3
10K
5%

3 AR1
μA740
2 7
6 OUTPUT ②
4

-15V

⑥

CR1
EG&G
CUSTOM
PHOTODIODE

Q1

Q2

(2)
NPD 0123C
2N 5196

-15V

⑤

8 SPACE LOOK

Q3
NPD 122C

-15V

⑥
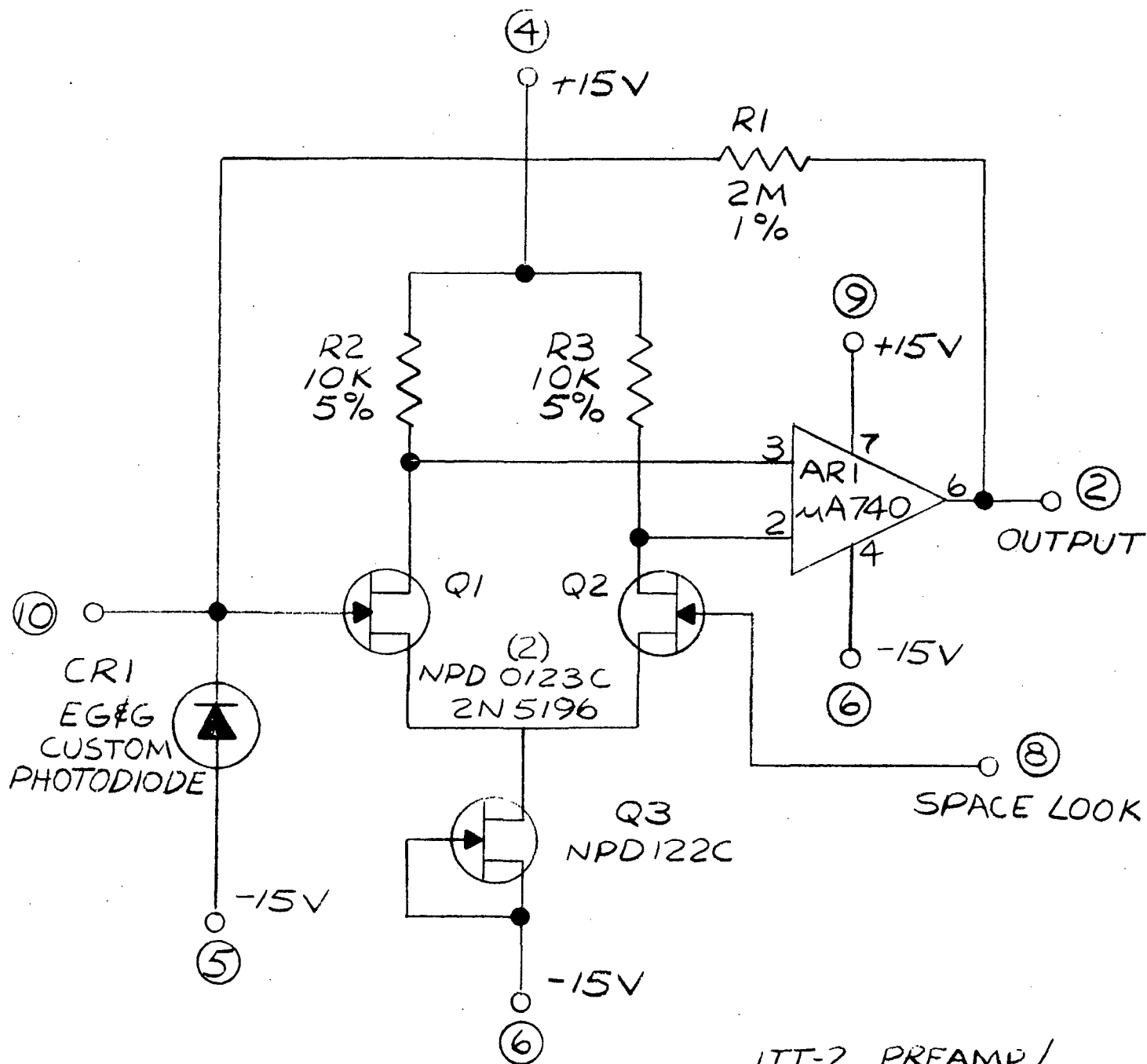
ITT-2 PREAMP/
PHOTODIODE
SCHEMATIC
DIAGRAM

Figure 7.7-1

TOP VIEW
-15V

③ -15V          +15V ②
    6  5  4
NC 7        30 NC
④ +IN 08      20 OUTPUT ①
    9  10  1
+15V        NC
        NC

PIN DIAGRAM

7-13
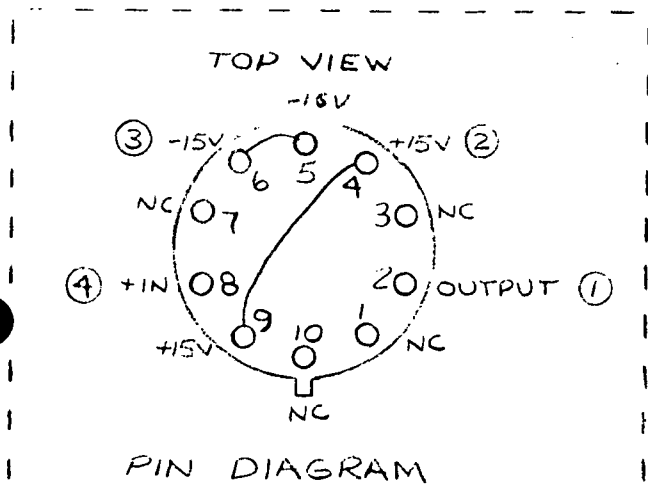
### 7.7.4  Motor Power Supply

The Power Supply for the SCMR Scan and Momentum Compensator motors is a conventional bridge switching amplifier. The circuit for the Momentum Compensator is powered from the -24 Volt bus. The circuits for the scan motor can be powered directly from the bus or from the switching regulator which supplies -15 VDC. Base drive for the switching transistors is derived from the spacecraft 400 Hz 2 phase clock through an isolation transformer.

### 7.8  Analog Telemetry

The SCMR Analog Telemetry signals together with location of associated are:

| Signal | Circuit Location |
|---|---|
| Electronics Temperature | Temp Tel and Control |
| Baseplate Temperature | Temp Tel and Control |
| Blackbody No. 1 Temperature | Temp Tel and Control |
| Blackbody No. 2 Temperature | Temp Tel and Control |
| Cone Wall Temperature | Temp Tel and Control |
| Patch Temperature | Temp Tel and Control |
| Patch Heat | Temp Tel and Control |
| Motor Current | Temp Tel and Control |
| Cone Cover Position | Temp Tel and Control |
| Electronics Current | Telemetry No. 2 |
| Purge Pressure | Telemetry No. 2 |
| Cone Wall Housing | Telemetry No. 2 |
| Motor Housing Temperature | Telemetry No. 2 |
| Momentum Compensator Speed | Motor Speed TM |
| Scan Motor Speed | Motor Speed TM |
| +15 Volt Electronics Supply | Voltage Regulator |
| -15 Volt Electronics Supply | Voltage Regulator |
| +5 Volt Electronics Supply | Voltage Regulator |
| -15 Volt TM Supply | Voltage Regulator |
| Detector Bias No. 1 | Ch. 1 Preamplifier |
| Detector Bias No. 2 | Ch. 2 Preamplifier |
| Offset Bias Voltage | Logic No. 2 |

Calibration curves for the Flight Model Analog TM signals are given in Volume 1 of the Flight Model Instruction Manual. Table 7.8-1 is a summary of the analog telemetry points.

### 7.9  Calibration Signals

The input and output calibration signals are generated by the Digital to Analog Converter V6 on the Logic No. 2 Board. This device is one-half of a basic 8 bit device with an accuracy of $\pm$ ½ LSB. The reference voltage for the D to A is supplied by negative voltage regulator REG 1. This device is temperature compensated to a stability of $\pm$ 0.1% in the same manner as those in the IR

Preamplifiers. This stabilized regulator is also used as the source voltage for the 3 volt offset in the data amplifiers. Separate amplifiers are provided for input and output calibration outputs. Tailoring resistors for output calibration for each channel are provided on the Logic No. 2 board.

TABLE 7.8-1

SCMR FLIGHT MODEL
ANALOG TELEMETRY SUMMARY

1. ELECTRONICS TEMPERATURE T/M

   FUNCTION      MEASURES THE TEMPERATURE OF THE ELECTRONICS MODULE
                 STRUCTURE

   RANGE         -2 TO +60°C

   RESOLUTION    103 MV/DEGREE CENTIGRADE

2. CONE TEMPERATURE T/M

   FUNCTION      MEASURES THE TEMPERATURE OF THE CONE WALL STRUCTURE

   RANGE         144 TO 297°K

   RESOLUTION    42 MV/DEGREE KELVIN

3. BASEPLATE TEMPERATURE T/M

   FUNCTION      MEASURES THE TEMPERATURE OF THE BASEPLATE AT ONE OF
                 THE MOUNTING FEET IN THERMAL CONTACT WITH THE
                 SPACECRAFT.

   RANGE         -2 TO +60° CENTIGRADE

   RESOLUTION    103MV/DEGREE CENTIGRADE

4. BLACKBODY #1 TEMPERATURE T/M

   FUNCTION      MEASURES THE TEMPERATURE OF THE BACK-SCAN BLACKBODY
                 TARGET FOR IN-FLIGHT CALIBRATION CHECK.

   RANGE         -2 TO +60° CENTIGRADE

   RESOLUTION    103MV/DEGREE CENTIGRADE

5. BLACKBODY #2 TEMPERATURE T/M

   FUNCTION      MEASURES THE TEMPERATURE OF THE BACK-SCAN BLACKBODY
                 TARGET FOR IN-FLIGHT CALIBRATION CHECK.

   RANGE         -2 TO +60° CENTIGRADE

   RESOLUTION    103 MV/DEGREE CENTIGRADE

6. PATCH TEMPERATURE T/M

    FUNCTION     MEASURES THE TEMPERATURE OF THE RADIANT COOLER
                   DETECTOR MOUNTING STRUCTURE.

    RANGE         85 TO 127$^O$K

    RESOLUTION   152MV/DEGREE KELVIN

7. MOTOR DRIVE CURRENT T/M

    FUNCTION     MEASURES CURRENT TO THE MOTOR POWER SUPPLY FOR
                   THE COMPENSATION AND MIRROR DRIVE MOTORS.

    RANGE         0 TO 354 MA

    RESOLUTION   18MV/MA

8. +15 VOLT T/M

    FUNCTION     MONITORS THE OUTPUT VOLTAGE OF THE ELECTRONICS
                   +15V REGULATOR

    RANGE         +1.8 TO +30 V

    RESOLUTION   1MV/4.2 MV

9. -15 VOLT T/M

    FUNCTION     MONITORS THE OUTPUT VOLTAGE OF THE ELECTRONICS
                   -15V REGULATOR

    RANGE         0 TO -19.1V

    RESOLUTION   1 MV/3 MV

10. +5 VOLT T/M

    FUNCTION     MONITORS THE OUTPUT VOLTAGE OF THE ELECTRONICS
                   +5V REGULATOR

    RANGE         0 TO +15 V

    RESOLUTION   1 MV/2.35 MV

11. DETECTOR #1 BIAS SUPPLY T/M

    FUNCTION     MONITORS THE OUTPUT VOLTAGE OF THE -12V REGULATOR
                   ON THE PRE-AMPLIFIER #1 BOARD.

    RANGE         0 TO -12.75V

    RESOLUTION   0.5V/VOLT

12. DETECTOR #2 BIAS SUPPLY T/M

   FUNCTION        MONITORS THE OUTPUT VOLTAGE OF THE -12V REGULATOR
                   ON THE PRE-AMPLIFIER #2 BOARD

   RANGE           0 TO -12.75V

   RESOLUTION      0.5V/VOLT

13. TELEMETRY POWER T/M

   FUNCTION        MONITORS THE OUTPUT VOLTAGE OF THE TELEMETRY -15V
                   REGULATOR

   RANGE           0 TO -19V

   RESOLUTION      1 MV/3 MV

14. CONE COVER POSITION T/M

   FUNCTION        MONITORS POSITION OF THE RADIANT COOLER COVER

   RANGE           0 TO 150 DEGREES

   RESOLUTION      41.7 MV/DEGREE

15. PATCH POWER T/M

   FUNCTION        MONITORS THE OUTPUT VOLTAGE OF THE PATCH TEMPERA-
                   TURE CONTROL CIRCUIT

   RANGE           0 TO 6 MW

   RESOLUTION      > .57 V/MW

16. CONE WALL HOUSING TEMPERATURE T/M

   FUNCTION        MONITORS THE TEMPERATURE OF THE CONE WALL HOUSING
                   STRUCTURE

   RANGE           +60 TO -25°C

   RESOLUTION      >60MV/DEGREE CENTIGRADE

17. ELECTRONICS CURRENT

   FUNCTION        MEASURES CURRENT TO THE ELECTRONICS CIRCUITRY.

   RANGE           0 TO 625 MA

   RESOLUTION      10MV/MA

18. PURGE PRESSURE

    FUNCTION     MEASURES THE PRESSURE OF THE PATCH DECONTAMINATION PURGE SUPPLY

    RANGE        0-100 PSIΔ

    RESOLUTION  63MV/PSI

19. OFFSET BIAS VOLTAGE

    FUNCTION     MEASURES OFFSET BIAS REGULATOR SUPPLY VOLTAGE.

    RANGE        -0.25 TO -7.9V

    RESOLUTION  .833V/VOLT.

20. MOTOR HOUSING TEMPERATURE

    FUNCTION     MEASURES THE TEMP. OF THE SCANNER MOTOR HOUSING.

    RANGE        -5 TO +50$^{\circ}$C

    RESOLUTION  116MV/DEGREE CENTIGRADE

21. SCAN MOTOR SPEED

    FUNCTION     MONITORS SPEED OF THE SCAN MOTOR

    RANGE        0-640 RPM

    RESOLUTION  10MV/RPM

22. MOMENTUM COMPENSATOR SPEED

    FUNCTION     MONITORS SPEED OF THE MOMENTUM COMPENSATOR MOTOR.

    RANGE        1400 - 5000 RPM

    RESOLUTION  1.77MV/RPM

## 8.0    INSTRUMENT TEST SUMMARY/FINAL CALIBRATION

Complete test procedures and data are available in the flight model, "Instruction Manual for the Surface Composition Mapping Radiometer Vol. II."   Table 8.0-1 is a summary extracted from the manual.

8.1    Final calibration curves for the 3 data channels of the flight model are shown in Figures 8.1-1 thru 8.0-7.

8.2    Figure 8.2-1 is a thermal profile generated from telemetry readings taken during the final vacuum thermal cycle.

The data indicates that for a $40^{\circ}C$ $\Delta T$ at the instrument baseplate[1]:

$$
\begin{array}{lll}
\text{ELECTRONICS} & \Delta T = & 30^{\circ}C \\
\text{CONE HOUSING} & \Delta T = & 8.8^{\circ}C \\
\text{CONE WALL} & \Delta T = & 4.5^{\circ}C \\
\text{UNCONTROLLED PATCH [2]} & \Delta T = & 5.4^{\circ}C \\
\end{array}
$$

The Radiant cooler margin to maintain control at nominal instrument temperature $(+15^{\circ}C)$ = 4.0 milliwatts x $1.8^{\circ}$ = 7.2 DEGREES KELVIN.

---

1.    At the flight level of the thermal vacuum temperature cycle.

2.    Patch margin = $1.8^{\circ}K$/Milliwatt

FIELD OF VIEW

|                              | CH 1(SWL) | CH2(LWL) |
|------------------------------|-----------|----------|
| NORMAL TO SCAN AXIS          | .84 mr    | .6 mr    |
| PARALLEL TO SCAN AXIX        | .74 mr    | .69 mr   |

REGISTRATION

| LWL/SWL NORMAL TO SCAN AXIS   | .072 mr |
|-------------------------------|---------|
| LWL/VIS. NORMAL TO SCAN AXIS  | .078 mr |
| LWL/SWL PARALLEL TO SCAN AXIS | .20 mr  |
| LWL/VIS PARALLEL TO SCAN AXIS | .06 mr  |

DETECTOR OPERATING TEMP.                    $116^{O}$ KELVIN

| | CH 1 | CH2 |
|---|---|---|
| DETECTOR RESPONSIVITY ($110^{O}$K) | $42\times10^{3}$V/WATT (7MA) | $63\times10^{3}$V/WATT (5 MA) |
| DETECTOR D* ($110^{O}$K) | $3.38\times10^{10}$CM HZ$^{\frac{1}{2}}$ W$^{-1}$ | $2.36\times10^{10}$CM HZ$^{\frac{1}{2}}$ W$^{-1}$ |
| NE $\Delta$T | $0.31^{O}$K | $0.8^{O}$K |

NOISE (RMS MV

SLOPE (MV/$^{O}$K) @ $280^{O}$K

| SINGLE ELEMENT RESOLUTION | 47% | 57% |
|---|---|---|

VISIBLE DETECTOR

    RESPONSIVITY            0.356AMPS/WATT(.9µ)

    DARK CURRENT            0.430NA.

MOTOR JITTER

| LOW POWER MODE LINE/LINE AVG. | 5µSEC.(.3mr.)  |
|-------------------------------|----------------|
| HI POWER MODE LINE/LINE AVG.  | 2µSEC.(.12 mr) |

TABLE 8.0-1
TEST SUMMARY

NEAR IR CHANNEL
FINAL CALIBRATION
FLIGHT MODEL

% ALBEDO

OUTPUT VOLTS

FIGURE 8.1-1

8-3
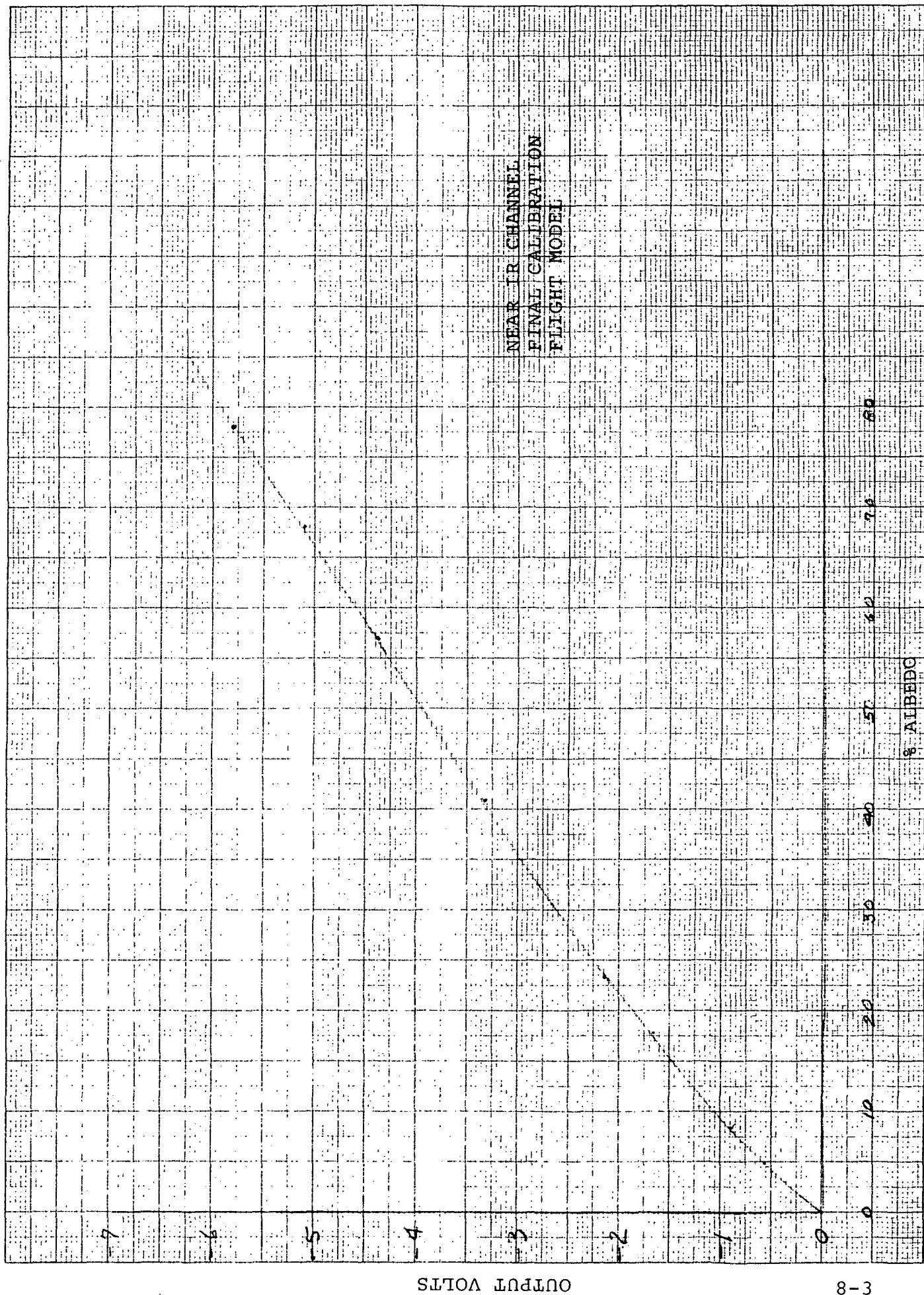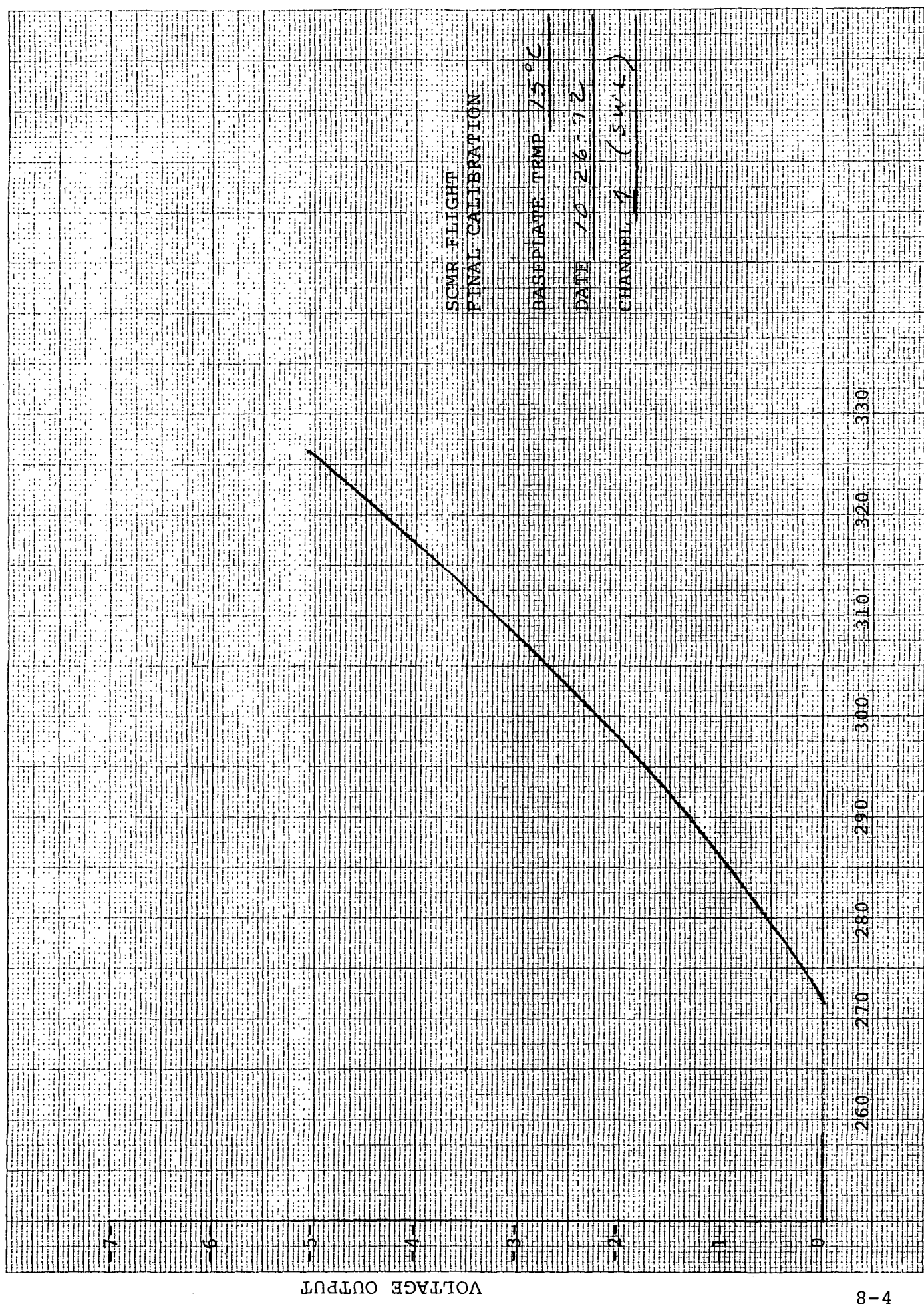
SCMR FLIGHT
FINAL CALIBRATION

BASEPLATE TEMP  15°C

DATE  10-26-72

CHANNEL  1  (Sw-1)
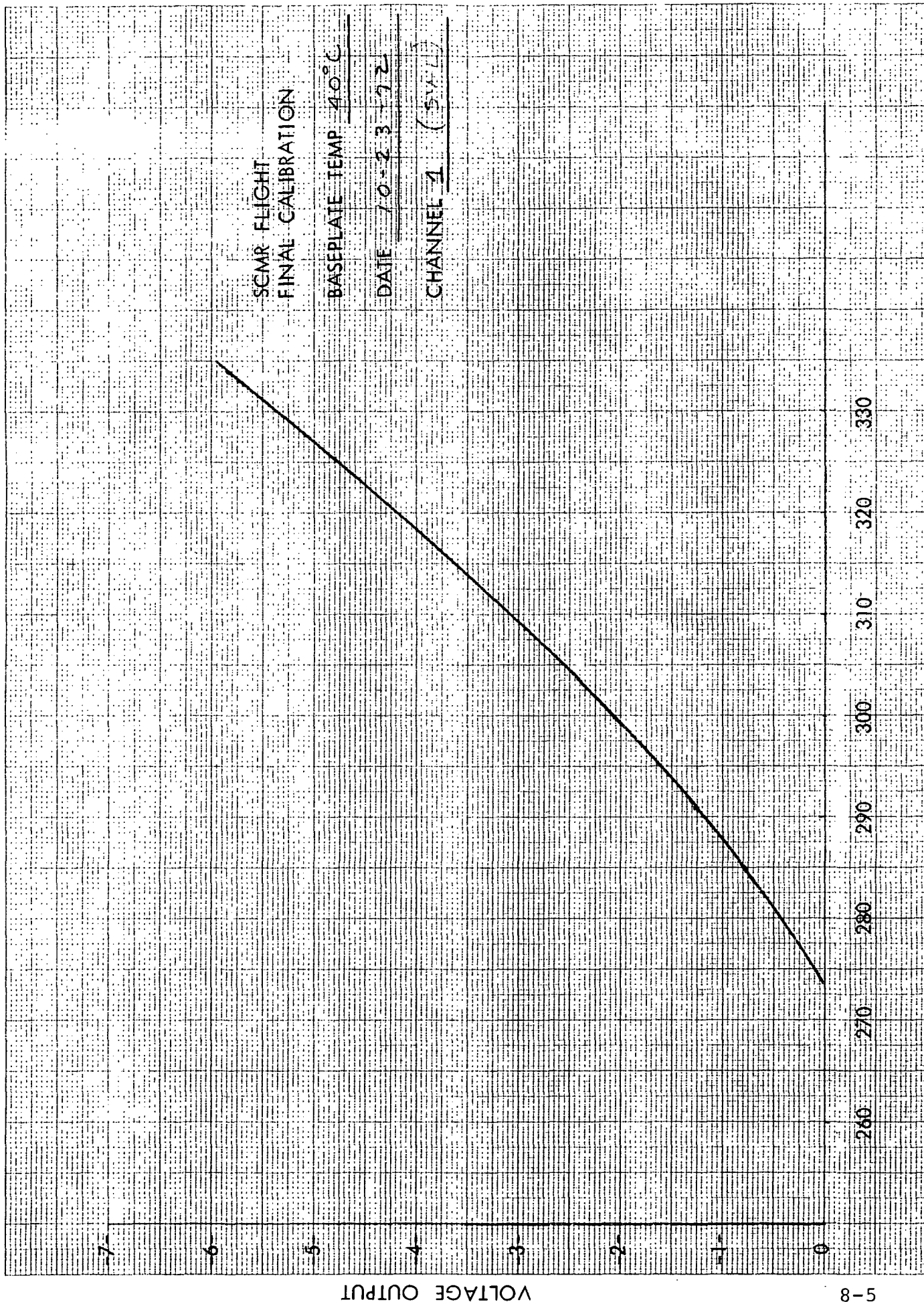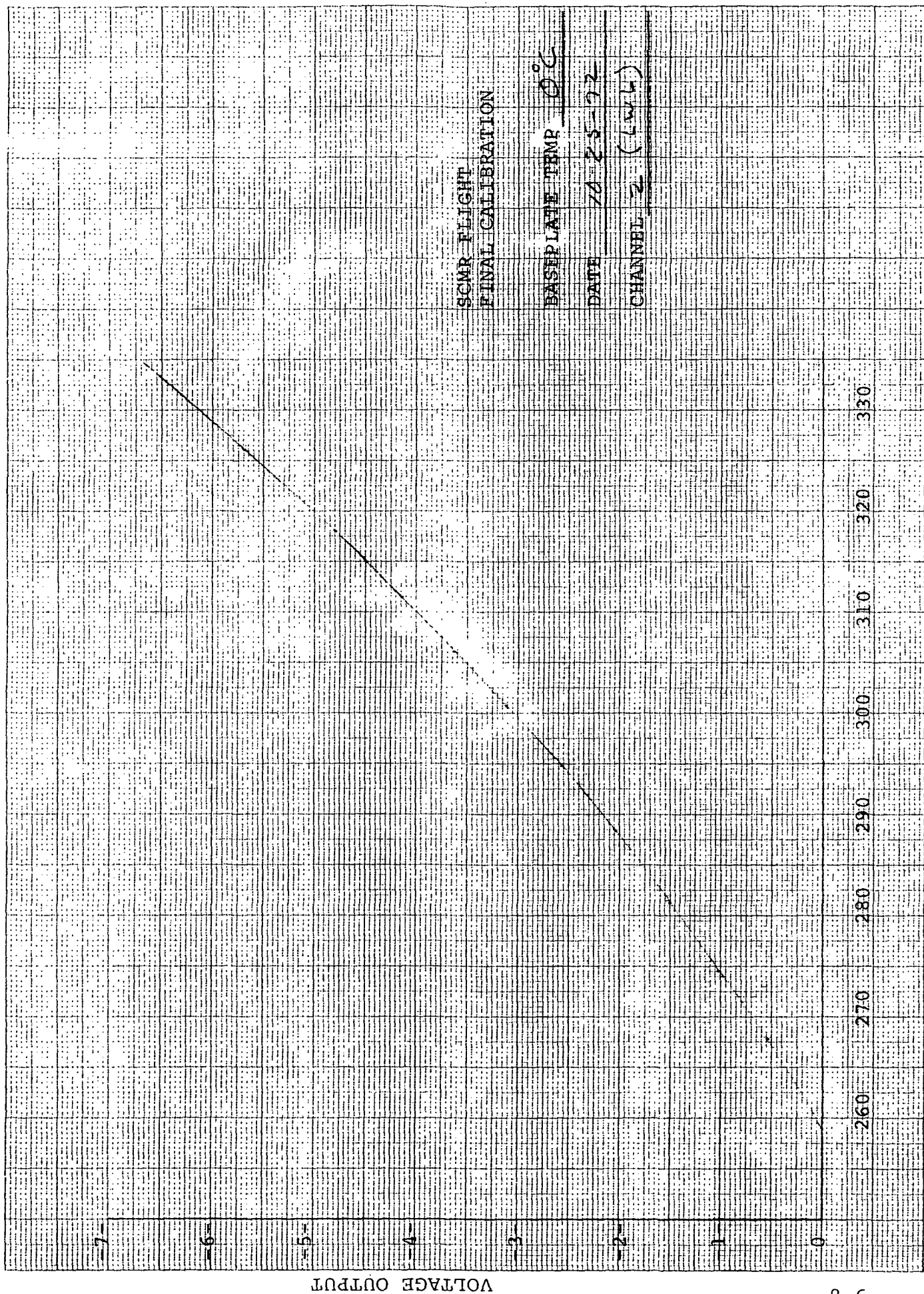
VOLTAGE OUTPUT

TEMPERATURE/DEGREES KELVIN

FIGURE 8.1-2

8-4

SCMR FLIGHT
FINAL CALIBRATION

BASEPLATE TEMP. 40° C

DATE 10-23-71

CHANNEL 1 (5.4.L)

VOLTAGE OUTPUT

TEMPERATURE/DEGREES KELVIN

FIGURE 8.1-3

SCMR FLIGHT
FINAL CALIBRATION

BASEPLATE TEMP __0°C__

DATE __10-25-72__

CHANNEL __2 (LWL)__

TEMPERATURE/DEGREES KELVIN

VOLTAGE OUTPUT

FIGURE 8.1-4

8-6

FIGURE 8.1-5

SCMR FLIGHT
FINAL CALIBRATION

BASEPLATE TEMP 15°C

DATE 10-24-72

CHANNEL 2 (LWL)

VOLTAGE OUTPUT

TEMPERATURE/DEGREES KELVIN

8-7

SCMR FLIGHT
FINAL CALIBRATION

BASEPLATE TEMP 4C°C

DATE 10-23-72

CHANNEL 2 (LWL)
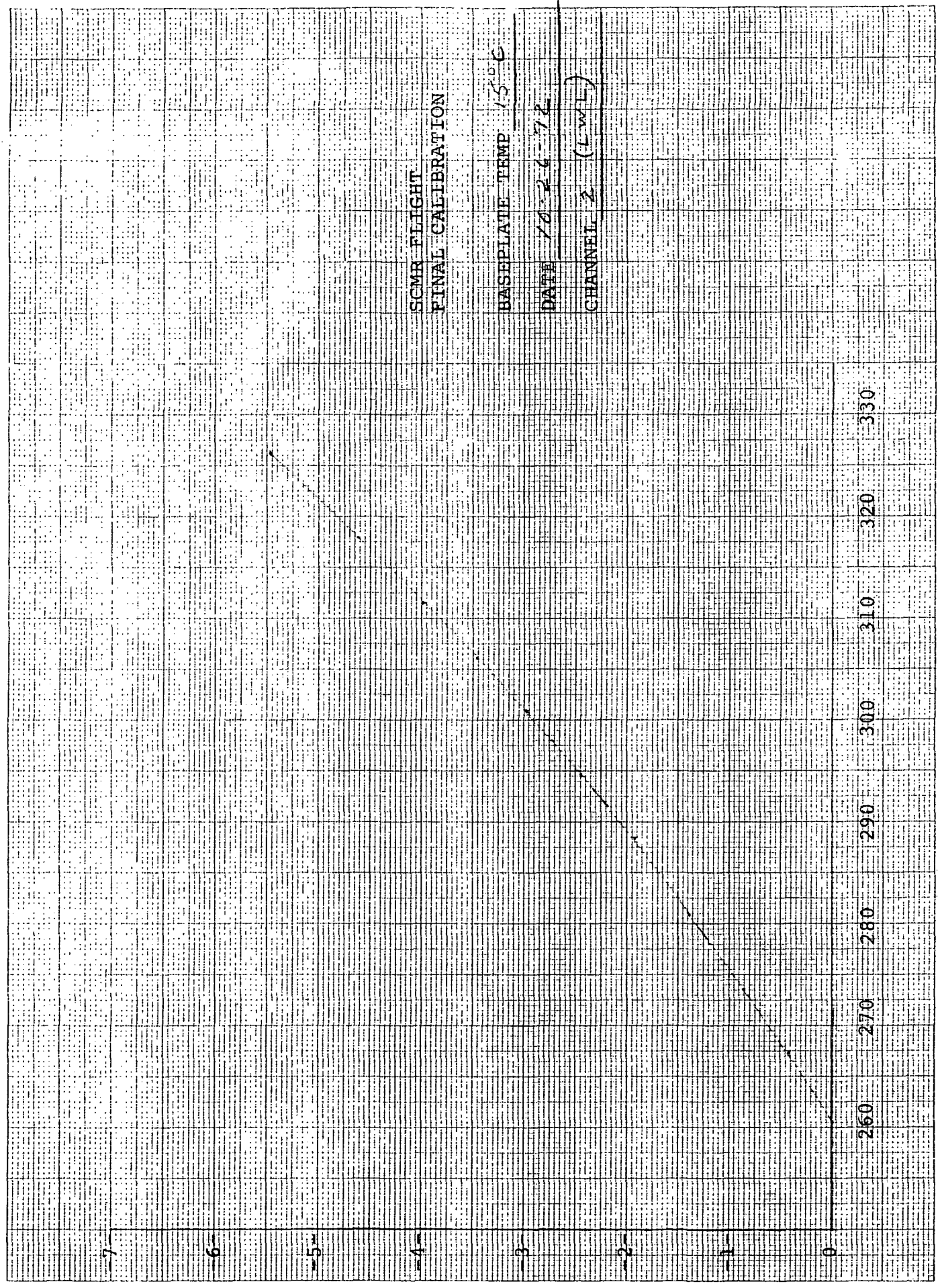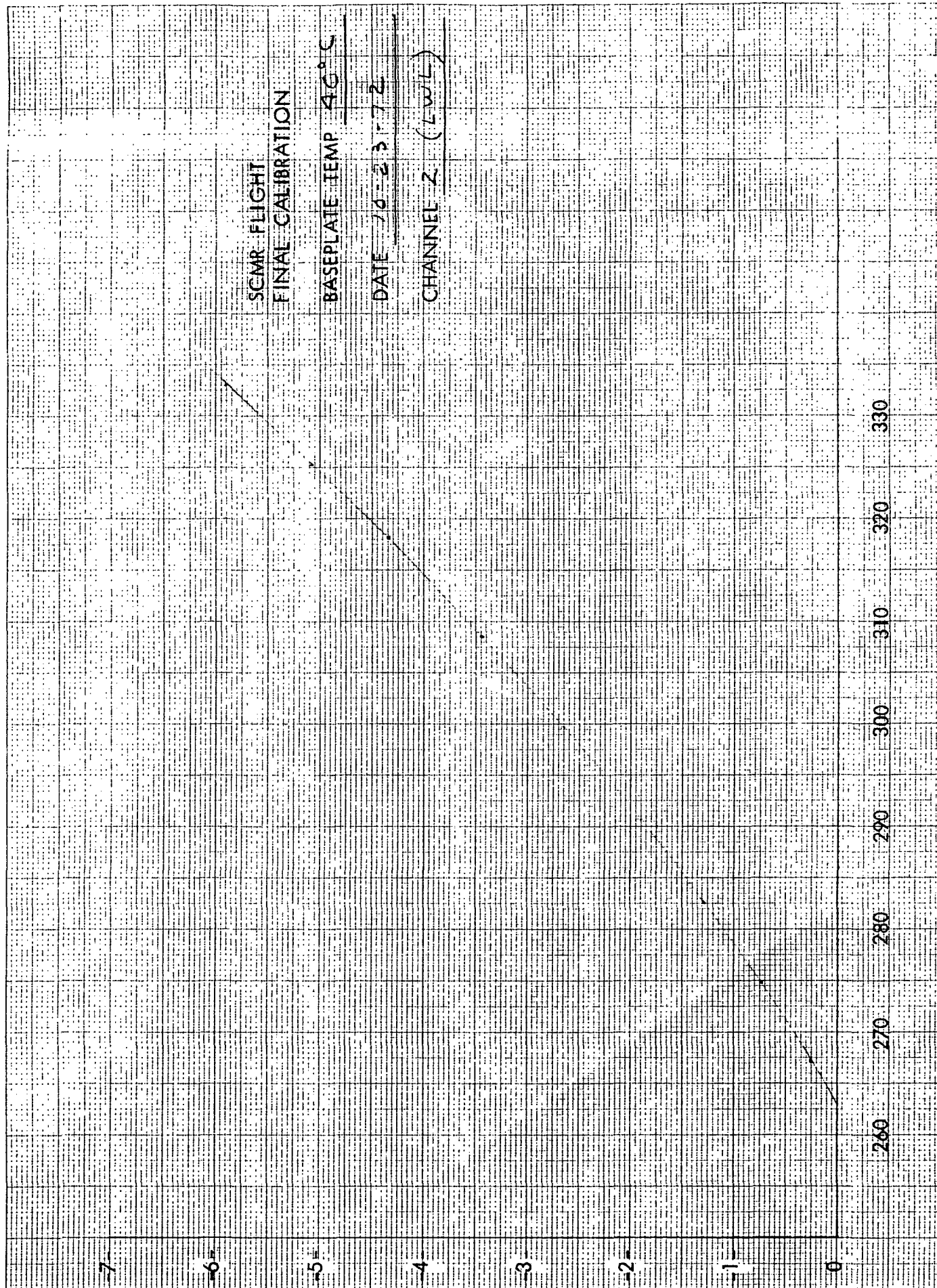
FIGURE 8.1-6    TEMPERATURE/DEGREES KELVIN

VOLTAGE OUTPUT

SCMR FLIGHT
FINAL CALIBRATION

BASEPLATE TEMP  0°C
DATE  10-25-72
CHANNEL  4  (SW-L)

TEMPERATURE/DEGREES KELVIN

OUTPUT VOLTAGE

FIGURE 8.1-7

8-9
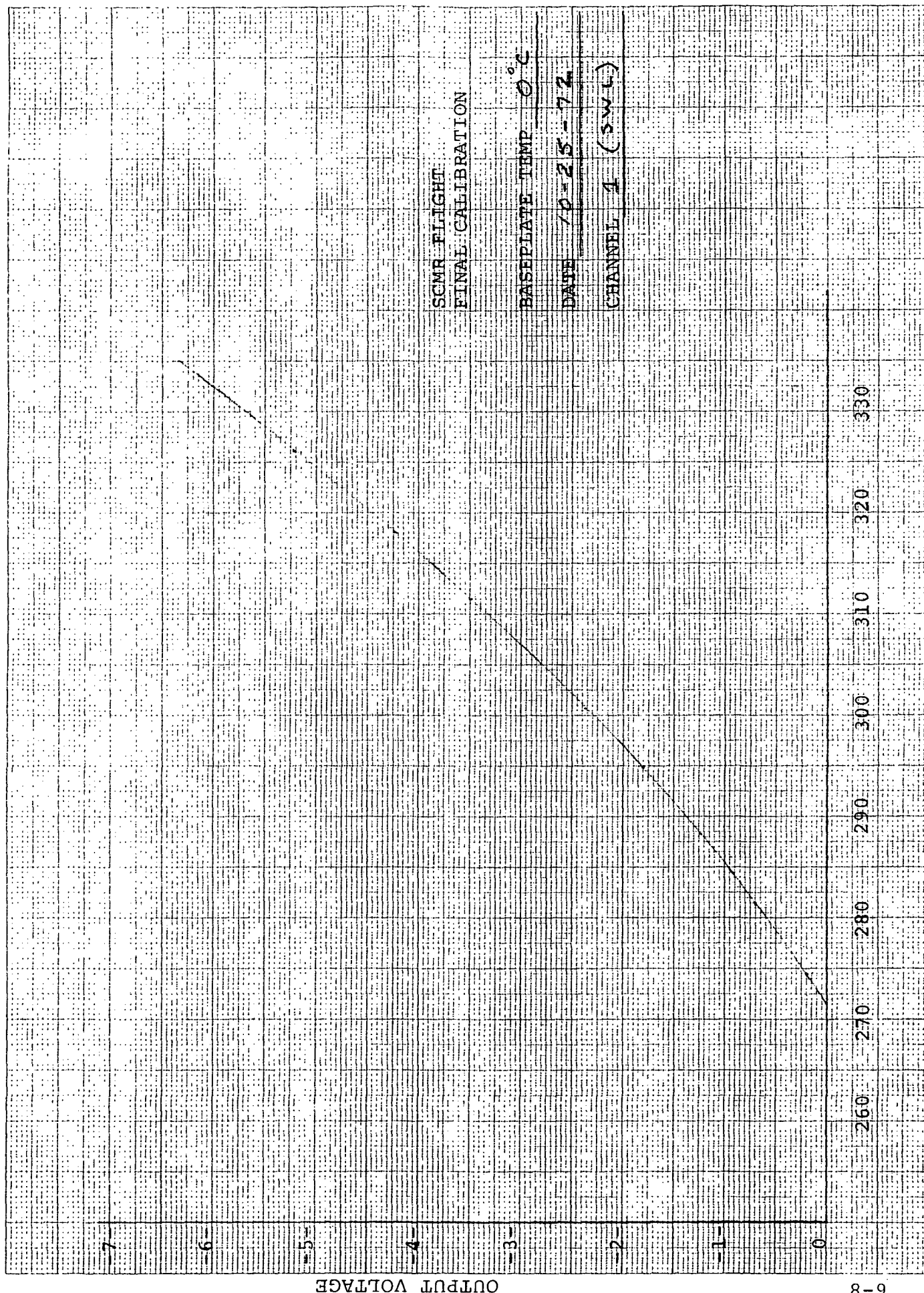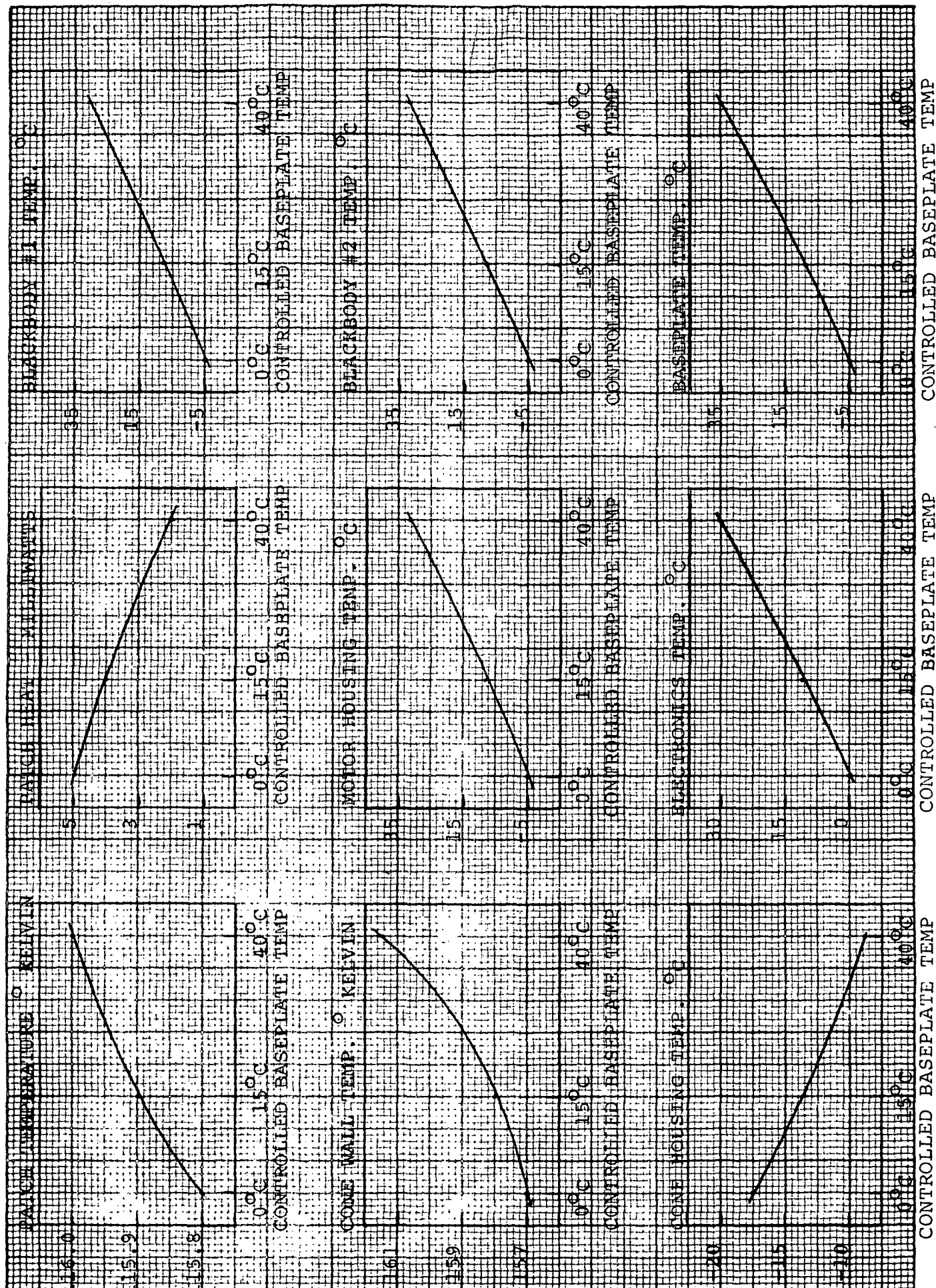
FIGURE 8.2-1   THERMAL PROFILE

# APPENDIX

## CONTENTS

| | |
|---|---|
| 8116466 | SCHEMATIC, COMMAND RELAY #1 |
| 8116462 | SCHEMATIC, COMMAND RELAY #2 |
| 8116458 | SCHEMATIC, AMPL CONE COVER |
| 8116544 | SCHEMATIC, TELEMETRY #2 |
| 8116446 | SCHEMATIC, POST AMP |
| 8115674 | SCHEMATIC, POWER CONVERTER |
| 8116495 | SCHEMATIC, PRE AMP |
| 8116524 | SCHEMATIC, TEMP T/M AND CONTROL |
| 8116516 | SCHEMATIC, VOLTAGE REGULATORS |
| 8116530 | SCHEMATIC, VISIBLE CHANNEL |
| 8116454 | SCHEMATIC, MOTOR POWER SUPPLY |
| 8116450 | SCHEMATIC, LOGIC #1 |
| 8116502 | SCHEMATIC, LOGIC #2 |

REVISIONS

| ZONE | LTR | DESCRIPTION | DATE | APPROVED |
|---|---|---|---|---|

LAST NOS USED
R19   CR14
K6    C6

NOS NOT USED
K4    CR1  R10  R11  CR5
C4    CR7  R12

REFERENCE DESIGNATORS ARE
ABBREVIATED. PREFIX THE DES-
IGNATION WITH THE PREFIX OR
ASSEMBLY DESIGNATION CR BOTH.

UNLESS OTHERWISE SPECIFIED:
ALL RESISTOR VALUES ARE IN
OHMS, ¼ W.
ALL CAPACITANCE VALUES ARE IN
MICROFARADS, ±10% JOT.

**ITT AEROSPACE/OPTICAL DIVISION**
FORT WAYNE, INDIANA, U.S.A.
INTERNATIONAL TELEPHONE AND TELEGRAPH CORPORATION

NOMENCLATURE OR DESCRIPTION

SCHEMATIC -
COMMAND RELAY #1

| SIZE | CODE IDENT NO. | | |
|---|---|---|---|
| D | 31550 | 8116466 | |

Labels (pin assignments):

- T/M SELECT POWER
- CONE HEATER ON COMMAND
- CONE HEATER ON RETURN
- CONE HEATER OFF COMMAND
- CONE HEATER OFF RETURN
- PATCH HEATER ON COMMAND
- PATCH HEATER ON RETURN
- PATCH HEATER OFF COMMAND
- PATCH HEATER OFF RETURN
- VIDEO OUT
- VISIBLE VIDEO COMMAND
- VISIBLE VIDEO RETURN
- IR VIDEO COMMAND
- IR VIDEO RETURN
- CONE COVER LOGIC
- CONE COVER DEPLOY #1 COMMAND
- CONE COVER DEPLOY #1 RETURN
- CONE COVER CLOSE #1 COMMAND
- CONE COVER CLOSE #1 RETURN
- CONE COVER DEPLOY #2 COMMAND
- CONE COVER DEPLOY #2 RETURN
- CONE COVER CLOSE #2 COMMAND
- CONE COVER CLOSE #2 RETURN

- CONE HEATER T/M
- PATCH HEATER T/M
- I.R. VIDEO
- VISIBLE VIDEO
- VISIBLE VIDEO T/M
- CONE COVER POWER
- CLOSE LIMIT SW
- OPEN LIMIT SW
- CONE COVER DEPLOY #1 T/M
- OPEN LIMIT SW
- CLOSE LIMIT SW
- CONE COVER DEPLOY T/M
- -24.5 V RETURN

SCHEMATIC-AMPL
CONE COVER

ITT AEROSPACE/OPTICAL DIVISION
FORT WAYNE, INDIANA, U.S.A.
INTERNATIONAL TELEPHONE AND TELEGRAPH CORPORATION

D | 31550 | 8116458

DIAGRAM, SCHEMATIC-
TELEMETRY NO.2

ITT Aerospace/Optical Division
FORT WAYNE, INDIANA, U.S.A.

D 31550 8116544

Schematic — Post Amp

ITT Aerospace/Optical Division
D 31550 8116446

A-8

SCHEMATIC -
VOLTAGE REGULATORS

ITT AEROSPACE/OPTICAL DIVISION
FORT WAYNE, INDIANA, U.S.A.

D | 31550 | 8116516

A-11

SCHEMATIC - MOTOR POWER SUPPLY

ITT AEROSPACE/OPTICAL DIVISION
FORT WAYNE, INDIANA, U.S.A.
INTERNATIONAL TELEPHONE AND TELEGRAPH CORPORATION

D 31550 8116454

SCHEMATIC-
LOGIC NO. 1

8116450

D 31550

+5V

VISIBLE BIAS GATE

TO ALL PIN 14'S

TO ALL PIN 7'S

LOGIC GRD

ANALOG GATE

BLACK BODY LOGIC

DATA AMP LOGIC

SPACE CLAMP

PICKUP F.F.

PICKUP PULSE

SCHEMATIC - LOGIC NO.2

D 31550 8116502

A-14